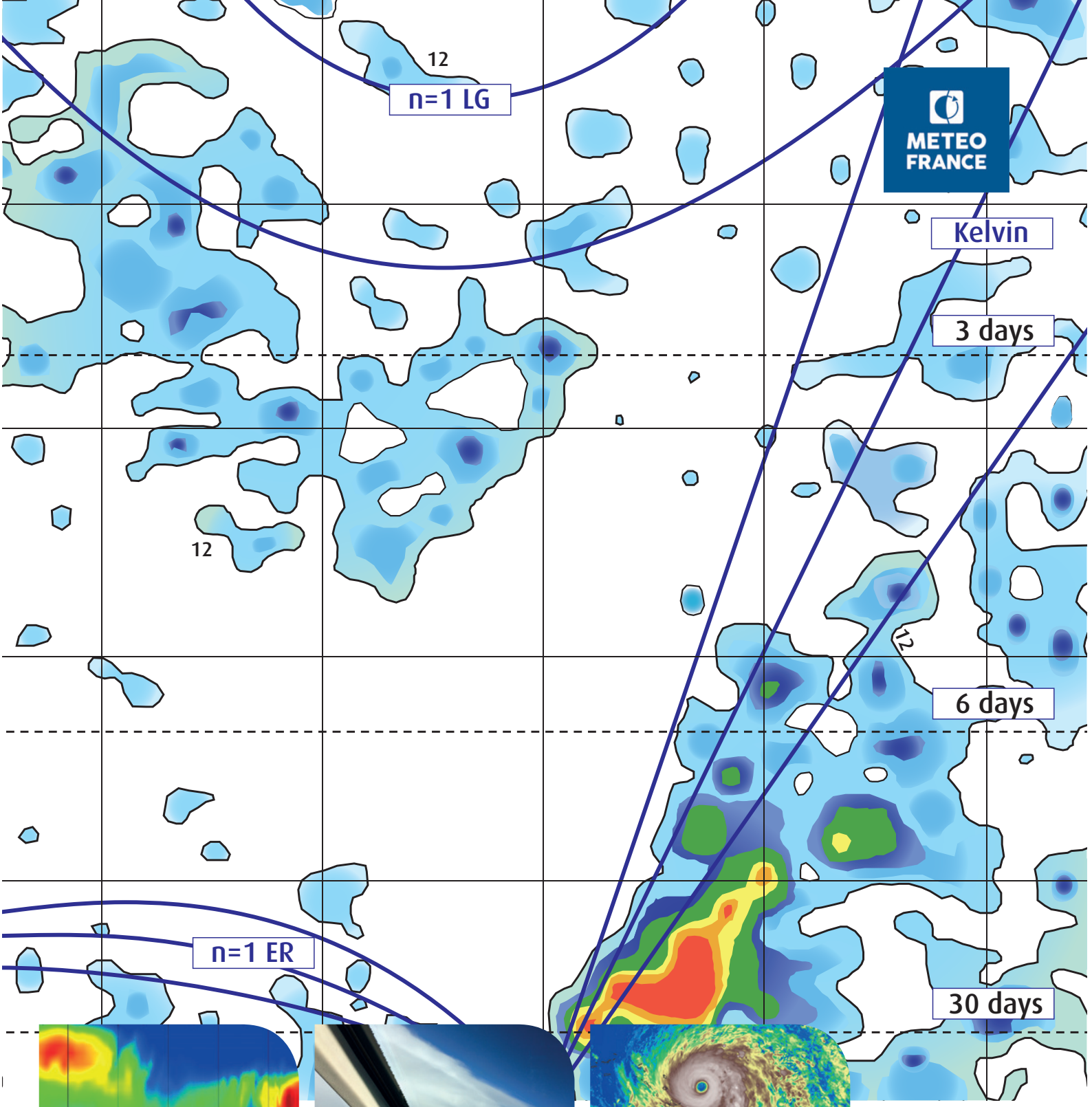

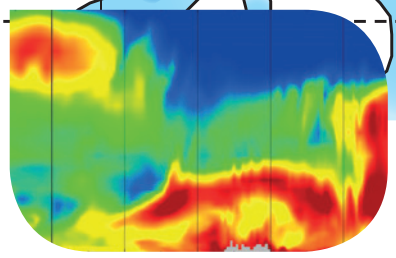

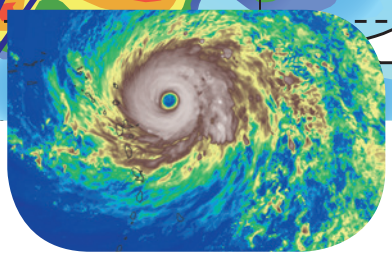

Research **Report**

2018

Research Report 2018

Table of contents

Numerical weather prediction and data assimilations ● page 5

Process studies ● page 14

Climate ● page 22
Diagnostic, study and climate modelling, from season to century
Impacts and adaptation

Chemistry, aerosols and air quality ● page 34

Snow ● page 38

Oceanography ● page 41

Engineering, campaigns and observation products ● page 46
Observation engineering and products
Campaigns

Research and aeronautics ● page 54

Appendix ● page 59

Numerical weather prediction and data assimilations

Meteo-France operates several state-of-the-art operational numerical weather prediction systems: a global one called ARPEGE and a convection-permitting one called AROME. AROME is run on many limited areas around the Globe, the instance covering mainland France (AROME-F) further benefits from a 3D variational data assimilation and it also provides ensemble forecasts. ARPEGE is run from 4D variational assimilations and also has both an ensemble of data assimilation as well as an ensemble forecast. Some of the most significant operational achievements of 2018 are the following ones:

- The forecast range of AROME-F has been extended so as to cover the current day and the next one and the ensemble version is run 4 times/day instead of 2. This prepares for extending the « vigilance » or public warning procedure from one to two days.
- Forecasts from the overseas AROME areas all have a length of +42h. Significantly, they can be extended up to +78h if the situation requires it, which is when a tropical cyclone is threatening that area.
- An ensemble of 25 3D variational data assimilation, with a 3 hourly cycle, has been introduced into the operational suite. It covers the AROME-F domain with a 3.25km horizontal resolution. At the moment, it provides perturbation fields that dramatically improve the performances of the AROME ensemble forecast at short ranges.
- The global ARPEGE ensemble is now also run 4 times per day.

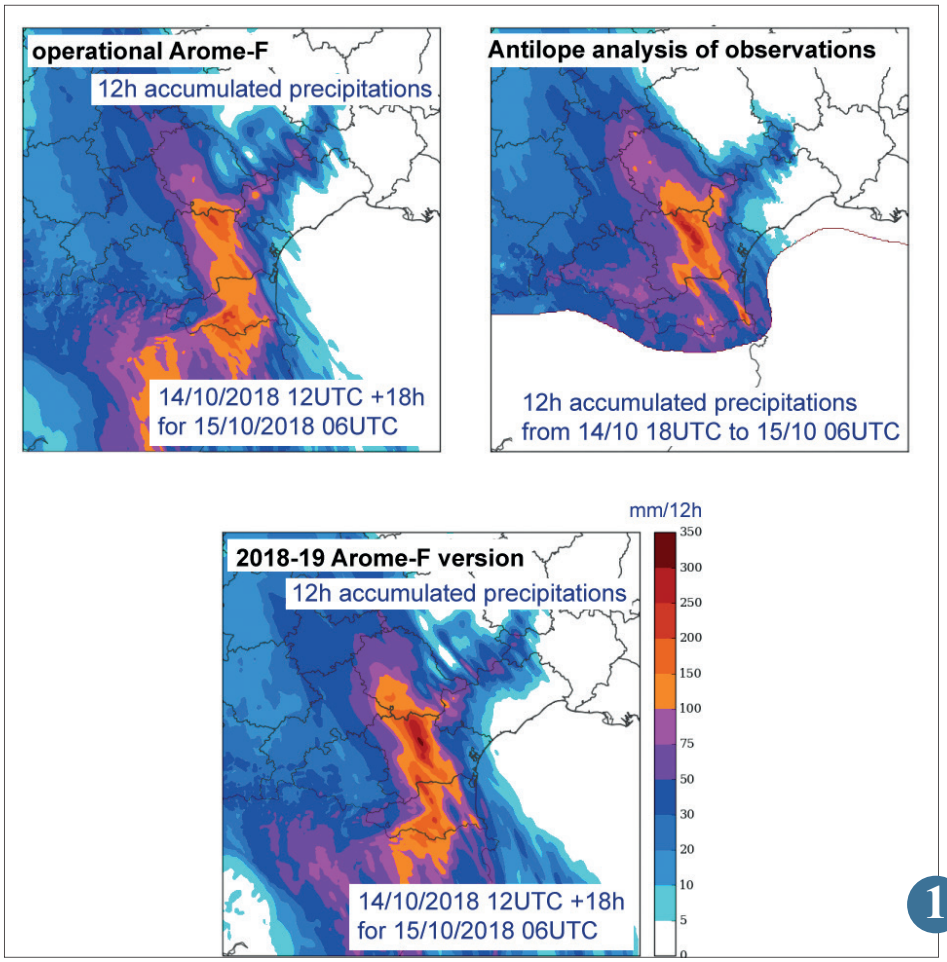

1

◀ 12h accumulated precipitations forecast by the AROME-F operational version (left) and the future version under trial (right), the latter driven by the global model ARPEGE future version as well. The middle panel is the accumulated precipitation given by the Antilope analysis from DSO. The case is that of devastating sudden floods in the Aude County, 14th to 15th of October 2018. The new version shows improved realisticness in the area where the extreme precipitations took place, a most noticeable improvement, yet not all deficiencies are corrected, such as the too large amounts over the Pyrenees mountains themselves.

A number of exciting developments are aiming to help Meteo-France deeply revising the organization of the production of end-user forecasts. They take the form of new quantities diagnosed from model state, such as a quite rich description of the kind of precipitation. On some cases, probabilistic versions are also derived from ensemble output. Perhaps the most novel approach is the ability to represent fields not as values on a grid but as objects or areas with a blurred boundary representing uncertainty on their shapes or locations. The construction of the objects can be accelerated by using multilayer neural networks.

A major work has been to prepare a full trial suite of new versions of all the NWP applications, based on a recent version of the common NWP code shared with ECMWF and 25 other hydro-meteorological national services. The main highlights are improved horizontal resolutions of the global systems and all changes consistent with this. A remarkable dedicated task has been to adjust the behaviour of the deep precipitating convection parameterization scheme so that it can operate with reasonable results at resolutions between 10 and 5km. The research study has concentrated on the conditions that lead to activate the scheme. In the AROME systems, the main change to be tested is a fully new version of the microphysics scheme that describes how precipitations form and grow within cloud regions. These new versions have been tested intensively and encouragingly improve forecast quality. They should become operational in 2019.

In the area of remote sensing, one should point out the ongoing research work on the benefits of taking into account the actual specific content of a given absorber trace gas, such as ozone or carbon dioxide when assimilating infra-red radiances. Another area of progress is the extensive testing of the two stage approach to using cloud or rain-affected micro-wave radiances. A new source of in-situ observations is beginning to be tested, the use of wind derived from the short messages exchanged between commercial aircrafts and air traffic control. Ensemble variational data assimilation or EnVar, as they are called, is the medium term target for renewing the data assimilation algorithms, has also made significant progress. From two sets of experiments performed with AROME, on different periods, it is now clear that, EnVar has an actual potential to improve the quality of AROME forecasts. Several reanalysis projects have either come to an end, as is the case of the HyMeX reanalysis, or starting anew, as the future Copernicus high resolution European surface reanalysis project. A scientist from the NWP group has found a way to solve a new set of equations describing atmospheric motions, the so-called quasi-elastic equation system, within a single semi-implicit problem. A side result is a sounder reformulation of the lower boundary condition of the current AROME numerical scheme that improves its stability. The following pages will provide short accounts of these and other research work, such as on tropical cyclones, floods and further topics. Among these, a particularly bold extreme experiment has been to successfully run the Meteo-France global ARPEGE model activating the non-hydrostatic dynamical core (the same one as AROME is using) with a 2.5km grid over an extended period, without major numerical trouble.

1

Simulations at kilometric scale with the global model ARPEGE

The global model ARPEGE uses large time steps due to the so called “semi-implicit and semi-lagrangian” character of its dynamical core, leading to a great computational efficiency but at the cost of spectral transforms performed at each step. Those spectral transforms have the reputation to adapt poorly to the modern super-computers. Hence there is the necessity to test ARPEGE with a domain size that might be used in the future and also to assess the quality of ARPEGE at kilometric scale.

In this context we took part to the DYAMOND project those goal was to compare models on the whole earth working at a scale allowing explicit representation of clouds and convection (<5km). We had to perform a fifty days long simulation in climatological mode with a horizontal resolution of 2.5km (using non-hydrostatic dynamics). It has been observed that the forecast produced relevant results especially concerning the explicit convection with computational costs of the same order of magnitude than the best models of the DYAMOND project. This enables us to conclude that ARPEGE’s core will still be efficient enough in an operational context for at least fifteen years

2

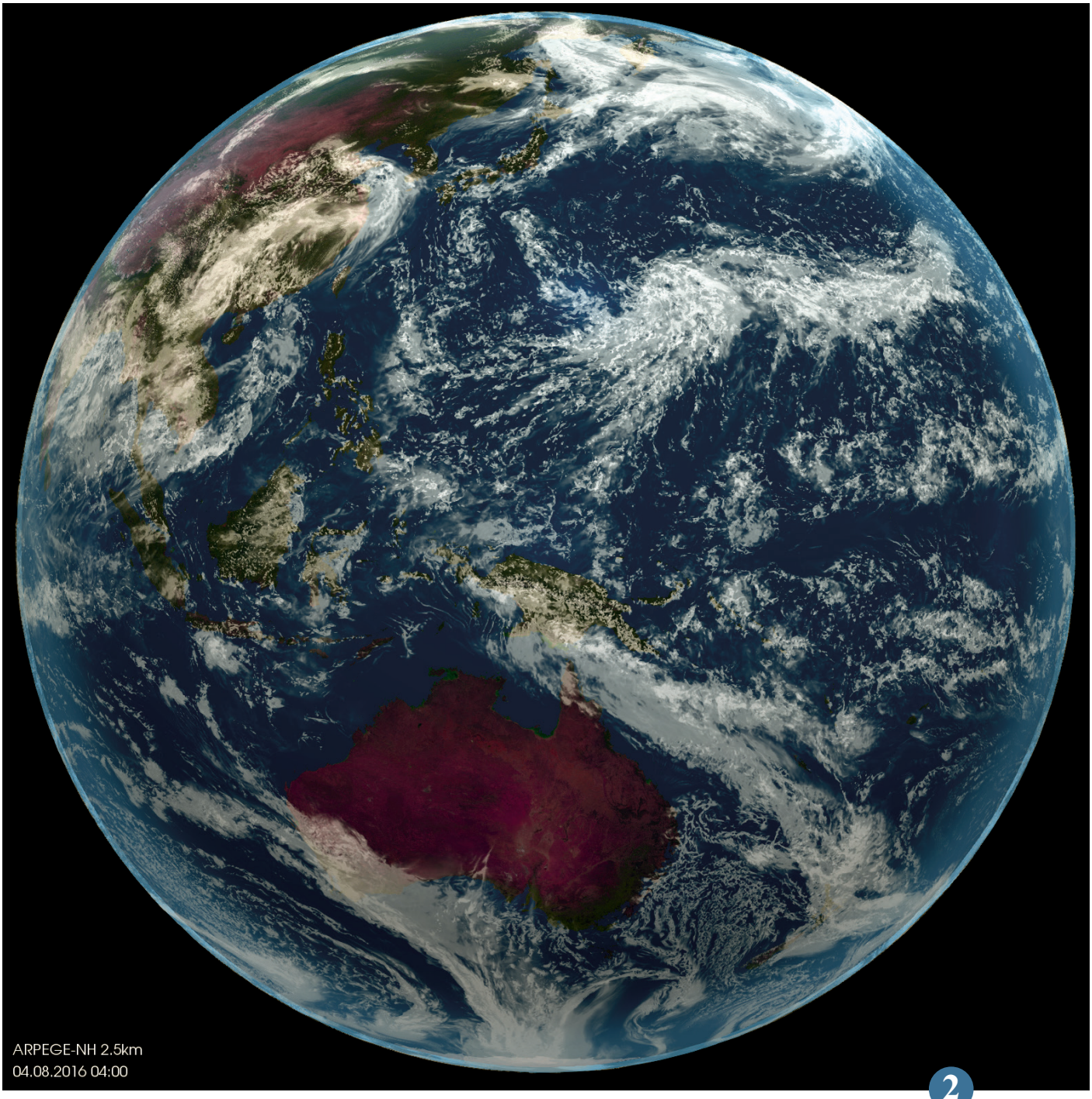

▲ Nebulosity forecast from ARPEGE model at 2.5km resolution (courtesy of Niklas Röber and the DRKZ).

Deep Learning methods for the detection of precipitating objects in AROME and AROME-PE forecasts

The utilization of precipitation forecasts could be improved with an appropriate processing of model fields. An innovative and promising approach consists in extracting from the forecast fields information at a larger, and thus more predictable, scale than the model grid, under the form of "stochastic precipitating objects". These objects are defined by fuzzy contours within which the distribution of rainfall, in terms of intensity and/or spatial variability (also known as texture), is homogeneous. Automatically detecting these objects is however complicated and different approaches are possible. A first heuristic solution has been developed in order to detect intensity-based objects from a similarity measure between the local precipitation distribution and reference distributions.

A novel detection method, based on the use of a convolutional neural network initially developed for the segmentation of medical images, has been evaluated. The network is trained on the outputs of the existing algorithm and it provides very similar results with significant gains regarding computation time when it is executed on graphical processors.

In addition, determining the texture of precipitations, in particular their continuous or intermittent nature, is important to properly characterize the sensible weather but it is not handled by the current algorithm. Preliminary experiments with a neural network trained on a very small set of manually labelled data provide encouraging results.

In the future neural networks could allow for the simultaneous detection of intensity and texture properties, and for a more detailed characterization of precipitation types including thunderstorms.

3

AROME-WMED reanalysis

Since 2010, HyMeX programme aims at improving the understanding and the modelling of the water cycle in the Mediterranean, with a special focus on the predictability and the evolution of the associated extreme events.

Many observation and numerical tools were deployed during the Special Observation Periods (SOPs). For the western Mediterranean, 2 SOPs took place during autumn 2012 and Winter 2013. A dedicated AROME version, named AROME-WMED that covers the entire western Mediterranean basin, was developed at CNRM to provide real time forecasts to the HyMeX operational centre and for the decision making for the observation deployment and instrument operation.

To take advantage of all research observations acquired during the campaign, a re-analysis using as many observations as possible was carried out. These data come from water vapour lidars (ground-based and airborne), boundary layer pressurised balloons, data from five Spanish radars and high resolution radiosoundings. Reprocessed data from ground GNSS stations and from wind profilers were also assimilated in the AROME-WMED model re-analysis. This re-analysis benefits from progress in the last model developments. 24% of additional observations were assimilated compared to the real-time version.

This re-analysis is closer to the observations than the previous versions. Comparisons of forecast with GNSS observations showed that the integrated water vapour content was improved up to the 42-h forecast range. In addition, atmospheric fields of the forecasts fit better with the radiosondes and precipitation below 10mm/24h are improved.

AROME-WMED meteorological fields are available in the HyMeX database for process studies.

4

Integrated flash-flood nowcasting

Flash floods regularly affect the Mediterranean regions. The speed of these phenomena is a major issue for warning people and planning emergency management in crisis time. Therefore, accurate flash-flood forecasts, especially in the short range (up to a 6 h range), are of great importance.

A hydro-meteorological integrated approach allows to forecast flash floods and runoff at these ranges driving dedicated hydrological models by rainfall nowcasts. Although extrapolation techniques based on radar data are skilful at 1-2 h lead time, numerical weather prediction is necessary beyond this forecast horizon. The nowcasting system AROME-NWC is a numerical model optimized for nowcasting purpose with rapid update cycle, based on the AROME model but with a reduced assimilation time window. It provides forecasts ranging from 30 minutes to 6 h, every hour. PIAF, the fusion product of radar extrapolation and AROME-NWC data, delivers precipitation forecasts up to 3 hours every 5 minutes and allows a continuous transition between these two sources of information. The benefit of rainfall nowcasting products for flash-flood forecasting is to be estimated with the study of the rainfall averaged over the watersheds and the simulated discharges at the outlets. For the rainfall averaged over the watersheds, a study conducted on seven study cases between 2015 and 2018 showed that AROME-NWC obtained better results than PIAF on forecast lead times ranging from 45 minutes to 3 h and worse results than AROME for lead times from 3 to 6 h. The use of time-lagged ensembles based on the AROME-NWC and PIAF nowcasts for driving hydrological models is currently being evaluated.

5

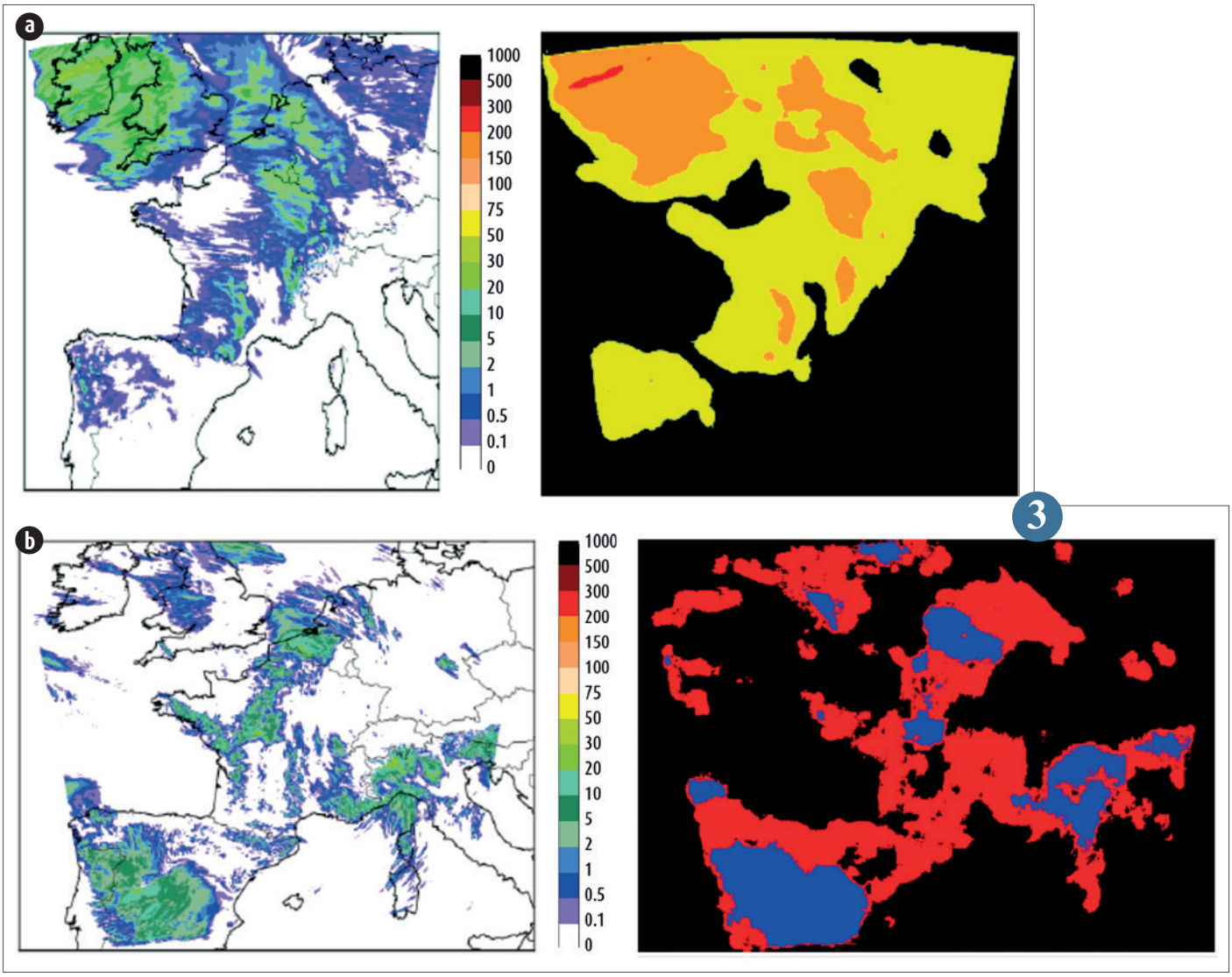

(a) 6 h-accumulated precipitation forecast from the AROME model (left) and objects corresponding to total (yellow), moderate (orange) and heavy (red) precipitation detected by the neural network (right).
(b) 6 h-accumulated precipitation forecast from the AROME model (left) and objects corresponding to continuous (blue) and intermittent (red) precipitation detected by the neural network (right).

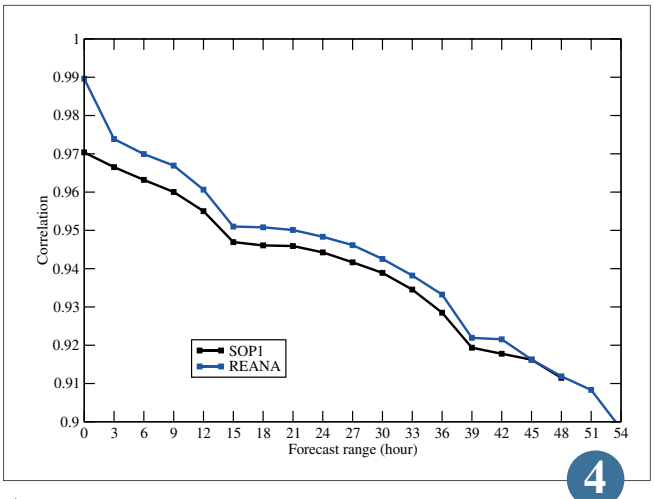

Correlation between integrated water vapour observation and forecast from the AROME-WMED reanalysis (in blue) and the real-time version (in black) as a function of the forecast-range

Scheme of the integrated flash-flood nowcasting system.

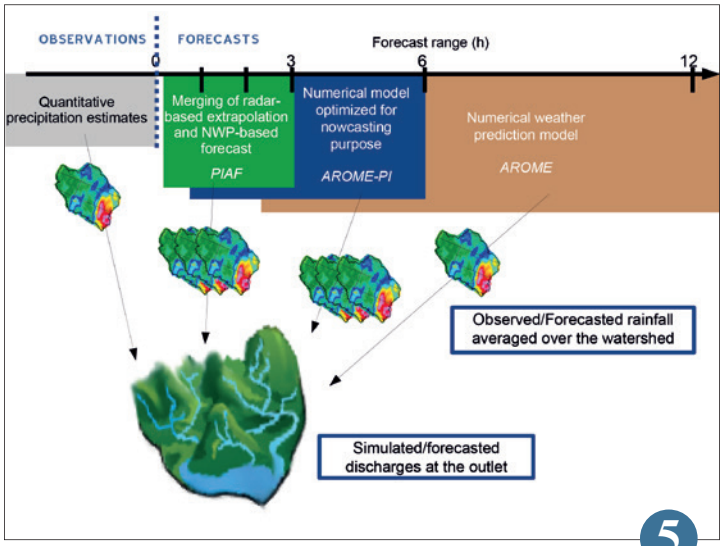

Probabilistic thunderstorm forecasts

Until now, thunderstorm forecasting has been mostly done manually. A new method to automate this task has been developed in the framework of the 3P/Alpha project. The idea is to merge most available numerical prediction data, on all needed ranges and locations, as heterogeneous ensemble forecasts (i.e. that combine several numerical models). Diagnostic algorithms extract the relevant physical information that is expressed differently by each model. Machine learning software is used to homogenise the data and to present it in a form that is simple to interpret, even for the layperson. The resulting forecasts are both accurate and consistent; the method is scalable to vast data volumes. Complementary information is combined from models that are as diverse as AROME, ARPEGE, ECMWF's IFS, or nowcasting tools. Objective and subjective evaluation has been performed using past cases, it shows that the forecasts are competitive with pre-existing products, and could be used for routine real time forecasting. It is recognized that for high impact events, human expertise remains essential for correcting the weaknesses of automated algorithms, and for efficiently expressing warning information to the public.
This approach will be applied to other parameters such as precipitation.

6

AROME Ensemble Forecast for Tropical Cyclones

A prototype for an Ensemble Prediction System (EPS) based on the oversea version of the limited-area model AROME has been developed at LACy in 2018. Several cases which affected La Réunion and the French Caribbean islands in 2017 and 2018 have been selected for a first validation of this system.
The AROME-oversea EPS is a direct adaptation of the AROME ensemble system which run operationally over France. But unlike its France counterpart, which is initialised and coupled at the lateral boundaries with the global model ARPEGE, the initial condition and the lateral boundaries of AROME-oversea comes from the ECMWF-IFS. Another specificity of the oversea system is that it is coupled with a prognostic parametrisation of the oceanic mixed layer (OML) which is initialised by MERCATOR analyses.
For this first prototype, 12 between the 50 members of the IFS-EPS are selected by a clustering method. The initial and lateral boundary conditions of the AROME-EPS coming from the 12 selected members contain the large scale perturbation which largely controls the spread of the AROME ensemble. The initial sea surface temperature and the initial vertical profile of the OML are also perturbed with a random large scale pattern and the Stochastically Perturbed Parametrization Tendency (SPPT) scheme is activated during the simulation.
The results for the tropical cyclone Fakir which impacted La Réunion at the end of April 2018 show several scenarios which could have alerted the forecasters of the fast propagation velocity and deepening of the cyclone which had been underestimated by the deterministic models and by the IFS-EPS (figure).
This new EPS prototype has also been adapted to the Caribbean domain of AROME-oversea. It is used for re-forecast of the 2017 hurricanes in the context of the TIREX project. It will also be used as a quasi-operational system during the field experiment campaign ReNovRisk between January and April 2019 in the SWIO.

7

High-resolution numerical simulation of eye-wall replacement cycle during Tropical cyclone Fantala (2016)

Tropical cyclone Fantala is one of the two most intense cyclones ever observed in the southwestern Indian Ocean basin. With a lifespan of nearly 3 weeks (4-27 Apr 2016) and wind gusts reaching nearly 360km/h, this exceptional cyclone completely ravaged the Farquhar archipelago (Seychelles), over which it passed 3 times in less than a week. In addition to these exceptional characteristics, Fantala also shows properties typical of extreme cyclones, such as the occurrence of several eye-wall replacement cycles (ERC). This phenomenon, generally visible in microwave satellite imagery, is one of the main intensification processes of tropical cyclone. It nevertheless remains poorly predictable using numerical weather prediction systems.
In order to better understand the mechanisms responsible for ERC triggering, high-resolution (500m) numerical simulations were performed with the Meso-NH/CROCO coupled system over a period of time encompassing one of the two ERCs experienced by Fantala. These simulations demonstrate the model's ability to realistically reproduce this phenomenon (spatial and temporal shift of about 50km/9 hours). The temporal evolution of the main meteorological parameters within the cyclone (temperature, humidity and wind speed in the vicinity of the two eye-walls) is thus very close to the climatological trends observed by airborne aircraft in the cyclones of the North Atlantic basin. Preliminary analysis of these simulations also shows that ocean-atmosphere interactions do not seem to play a major role in triggering Fantala's ERC. Indeed the ERC is present in both coupled and uncoupled simulations – although slightly shifted in time in coupled simulation- even if the temporal evolution of the intensity of the system is much more realistic when ocean coupling is activated (see figure).

8

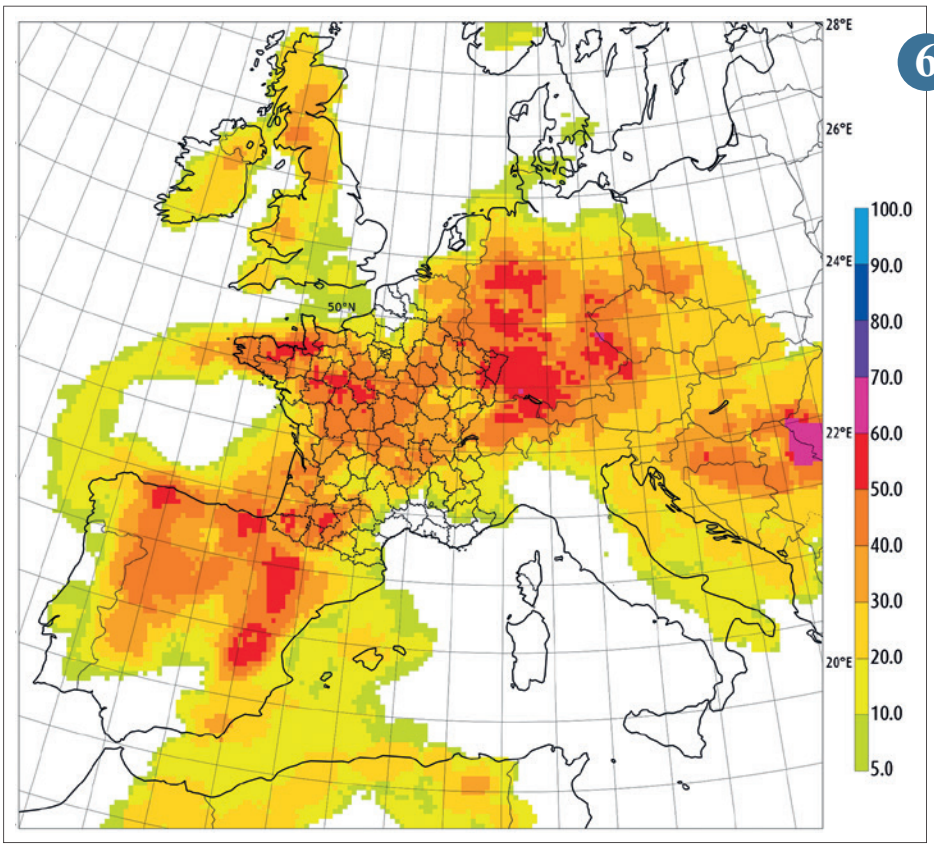

6

Example of thunderstorm probability forecast map that blends the AROME, ARPEGE and IFS ensembles, expressed as a risk index between 0 and 100%.

Plume charts for the probability of Pmin for the EPS (ECMWF) and for the PE-AROME-OI. Case of cyclone Fakir (S. Kébir)

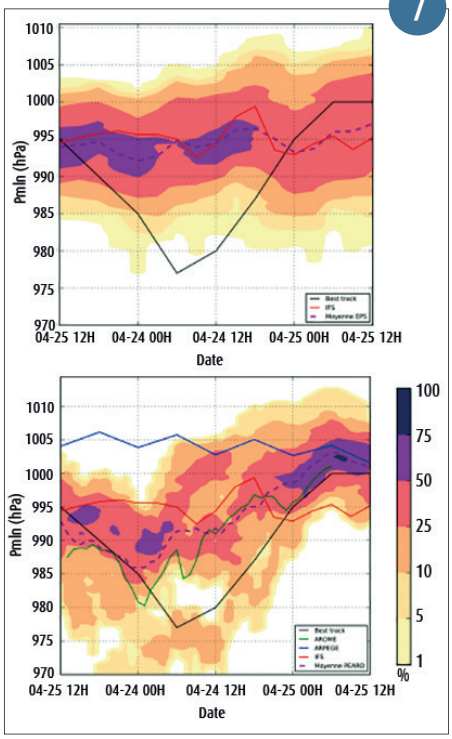

7

Horizontal cross-section of reflectivity in tropical cyclone Fantala as simulated by Meso-NH on 16 April 2016 without (left panel) and with (right panel) 3-D ocean coupling at 16 UTC and 18 UTC, respectively. The insert shows the temporal evolution of the system intensity in both configurations over the simulated 24-hour period (best-track in black).

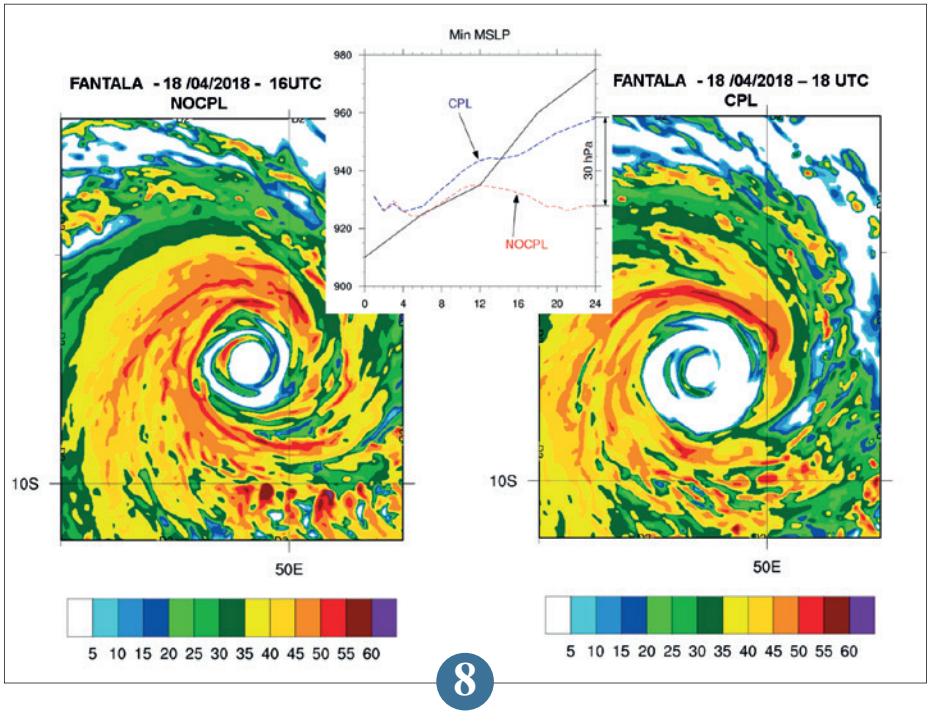

8

The 2017 hurricanes in the Antilles: hindcasts, uncertainties and impacts

The 2017 hurricane season in the Atlantic was exceptional for several reasons. It has witnessed the landings of two category-5 hurricanes over the Antilles, which is unprecedented since the beginning of meteorological records. The persistence of Irma's extreme sustained winds and Maria's rapid intensification have been particularly dramatic.

Météo-France's DIRAG seeks to study these exceptional phenomena and to characterize the related uncertainties in order to better understand their impacts. In the framework of the ERDF C3AF project, a review of Météo-France's productions provided a first assessment aiming at better anticipating the potential impacts of future cyclonic activity with more frequent major hurricanes. The ANR TIREX project builds on field surveys that were performed late 2017 in the Antilles by several members of the C3AF project (UMR GRED, LC2S, University of the French West Indies/LARGE). In this context, Météo-France's DIRAG, DIROI, LACy and CNRM collaborate to further reconstruct these tropical cyclones with AROME hindcasts at higher resolution.

On the other hand, the associated uncertainty will be assessed with Ensemble Forecasts and will provide the basis for a discussion of future improvement of hurricane warning.

9

New products to help weather forecasters

Fog snow, hail or freezing precipitation: all these weather events can be dangerous. They significantly impact the activities of our citizens by disrupting the train circulation, air and road traffic, or causing damage to crops for example. Different algorithms have been integrated into numerical weather forecast models (ARPEGE for the global forecast and AROME for the France or Overseas-centered forecast), in order to provide complementary and synthetic elements to weather forecasters.

Two expected visibilities are now produced by the models: the first one is a value due to haze or fog. The second one is due to rain, hail or snow. The algorithm is introduced into the physics of the models in order to better take into account the liquid water, cloud ice, but also rain and snow.

In a second step, a discrimination of the type of precipitation forecasted by the models has been implemented into their physics. This algorithm applies thresholds on the microphysics and thermodynamics parameters in order to determine the most frequent type of precipitation in the previous hour, but also the most dangerous one. Some of these thresholds are common to the HYDRE weather data fusion product so that forecasters can easily relate observations to forecasts. The figure shows the situation of February 28th, 2018, around Toulouse.

The next step will be to produce these new fields in ARPEGE and AROME ensemble forecasts and to develop a relevant synthesis of these parameters in a probabilistic form.

10

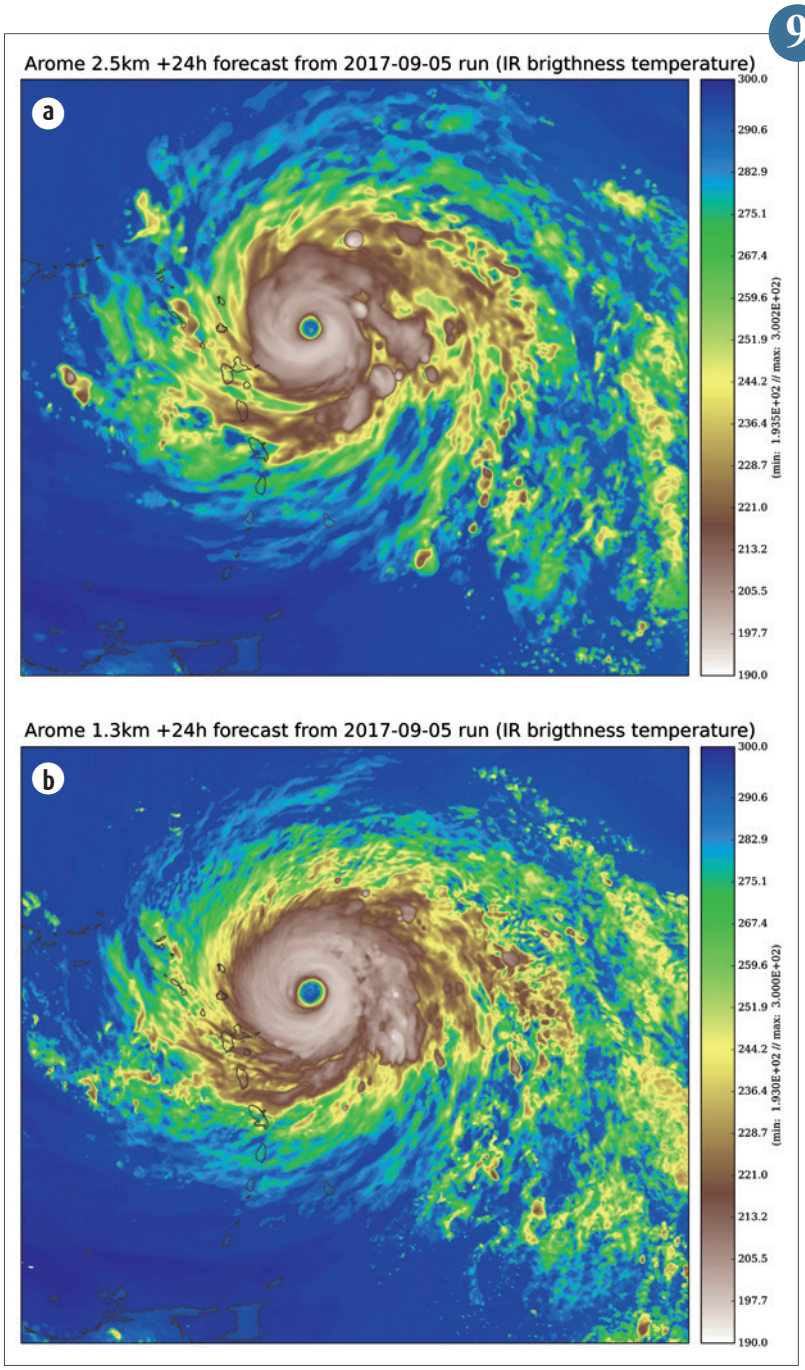

9

Infra-red brightness temperatures (K) simulated by 2 versions of AROME-Antilles: 2.5 km (a, operational version) and 1.3 km (b, research version).
+24h forecast of September 5 at 0 h UTC.

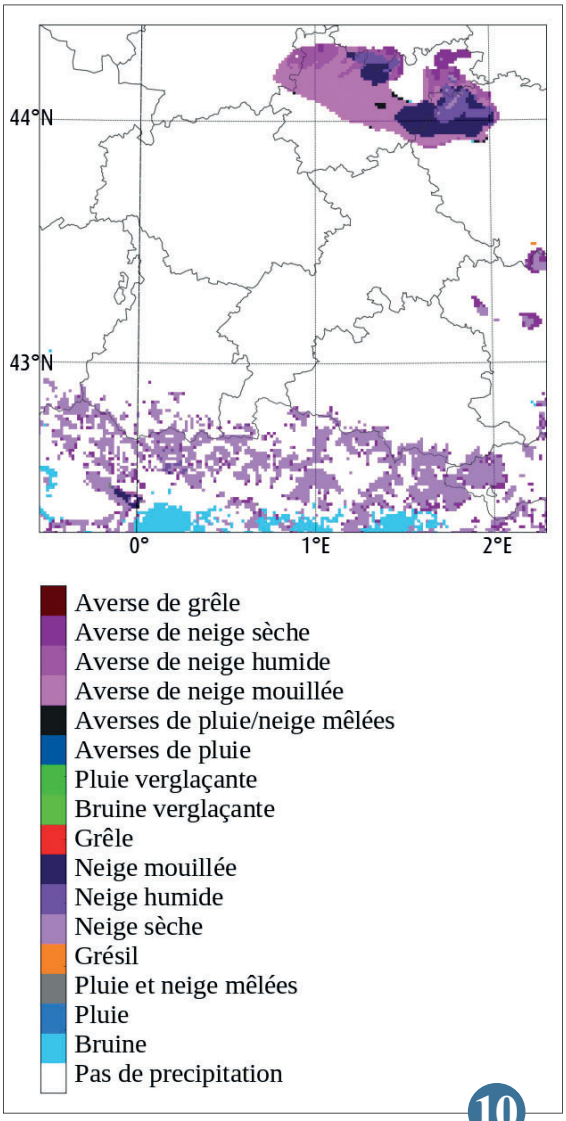

10

The most frequent precipitation type over the previous hour, February 28, 2018 at 12 UT around Toulouse

Process studies

The overarching goal of the process studies is to improve the representation of these processes in Météo-France's numerical weather and climate prediction models and in the design of relevant weather and climate services for the various weather-dependent economic sectors. The methodologies implemented to advance our understanding of processes are generally based on the combine use of observations from field campaigns and instrumented sites and numerical experiments.
The following examples illustrate, among other things, the use of observations from the international NAWDEX field campaign and Meso-NH model simulations to study diabatic processes involved in warm conveyor belts of Atlantic storms, as well as the use of observations from the Météopole Flux instrumented site in Toulouse to assess the biases of the surface water balance predicted by the ARPEGE and AROME numerical weather prediction systems. This year was also devoted to the preparation of the international SOGOG3D field campaign on fog, which will take place from autumn 2019 to the end of winter 2020 in southwestern France.
Detailed or idealized numerical simulation is also an essential instrument for process studies and assessment of their representation in models, as illustrated hereafter with the study on the effects of the numerical discretization of the ARPEGE model on tropical waves. The figure below is another example that illustrates an original approach using reference calculations of radiative transfer based on Monte Carlo methods applied to a simulated cloud field at very high resolution by the Meso-NH model to assess the three-dimensional effects of clouds and the importance to represent them in the radiation parameterizations of climate and weather prediction models.
Another series of articles below illustrates the progress made in modelling atmospheric processes and surface-atmosphere interactions, with outcomes expected on the capacities and performance of decision-making tools in the areas of urban adaptation to climate change, energy transition and agriculture.

1

Development of a photovoltaic power forecast tool

The continuously growing share of renewable energies on the electricity market has raised a need for improved production forecasts, to ensure grid stability and avoid financial penalties resulting from inaccurate forecasts. In this context we have developed a numerical model that converts atmospheric variables (direct and diffuse radiation, temperature and wind) into photovoltaic (PV) production. Radiative fluxes are routinely computed by the atmospheric models used at Météo-France, but PV production also depends on other parameters, among which panel technology and orientation. The model we developed accounts for all the physical processes through which solar radiation is converted into electric power. Contrary to existing models which rely on commonly distributed outputs of atmospheric models (generally broadband solar radiation with no distinction between the diffuse and direct contributions), our model takes advantage of internally computed variables which contain much more information. Indeed, at Météo-France solar radiation is computed in 14 spectral bands, the detail of which allows to finely represent the interaction with the solar panel, itself characterized by a strongly wavelength dependent efficiency (solar panels generally cannot convert radiation beyond approximately 1100 nm into electricity).

The model has been validated against observations from the *Site Instrumental de Recherche par Télédétection Atmosphérique,* and has further been coupled to AROME outputs to create atlases of PV production. The figure shows the simulated PV production for January and July 2017, a kind of information that can be very helpful in planning the development of new solar farms.

2

Synthesis image of a cloud field simulated by the Meso-NH model.
It has been produced by a radiative transfer simulation tool capable of processing the surface and volume complexities associated with clouds and terrain.

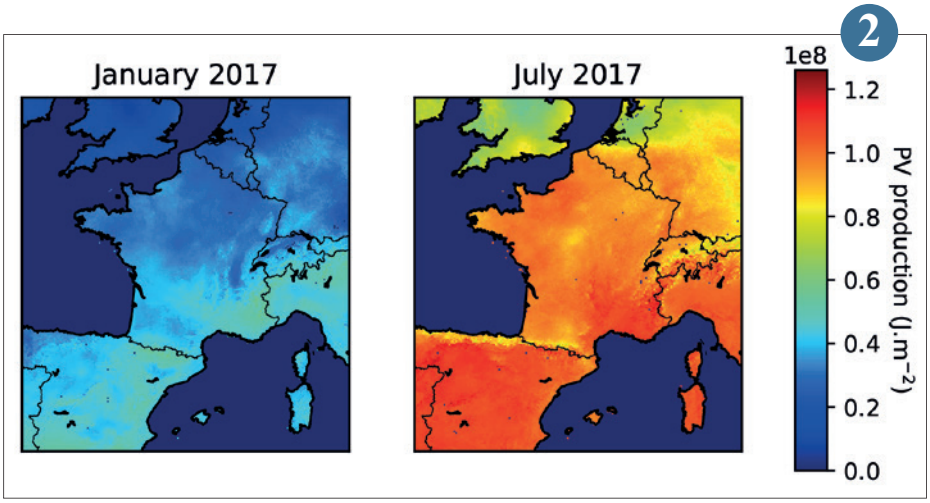

Photovoltaic production estimated from hourly AROME analysis for a monocrystalline solar panel facing South with an inclination of 37°, cumulated over January and July 2017.

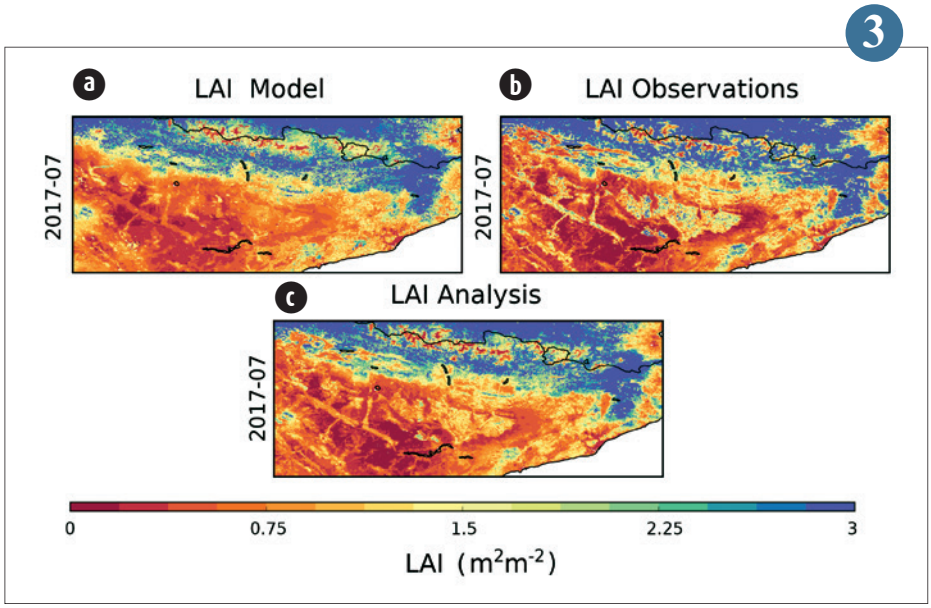

Impact of assimilating satellite-derived leaf area index (LAI) observations into the ISBA land surface model over north-eastern Spain (Ebro basin) The analysis represents the best compromise between the model and the observations.

Towards the assimilation of high resolution satellite data over land

Detecting and monitoring droughts involve numerous variables of the soil-plant system. For example, soil moisture and the vegetation leaf area index (LAI).
The ISBA land surface model developed by CNRM is able to simulate these variables and can be operated at various spatial scales, from the local scale to the global scale. One of the limitations to the use of the model at a high spatial resolution, for example using grid cells of 1km or 300m, is that analyzed atmospheric variables are not available at these scales. Such uncertainties can be reduced through dynamic integration of satellite-derived LAI observations in the ISBA model using data assimilation techniques. LAI observations are now regularly available in near real time at a global scale, at spatial resolutions of 1km and 300m.
The land data assimilation system implemented by CNRM (LDAS-Monde) is able to integrate satellite observations into the ISBA model. It can work at a global scale and at the regional scale at spatial resolutions of 0.25 degree and 1km, respectively. The enclosed Figure presents the impact of the assimilation of a LAI product over the Ebro basin in northeastern Spain, in July 2017. In the LAI observations, irrigated areas are clearly visible at the center of the domain. On the other hand, they are not visible in the simulated LAI map. The main reason for that is that irrigation is not represented in this version of the model.
The assimilation permits incorporating geographic information into the model, reducing the uncertainty "cascade" affecting the simulations, and compensating for missing processes.

Impact of stretching on tropical waves spreading on an aqua-planet

The resolution of global weather prediction models is too low to solve the dynamics of deep convection. It is therefore necessary to parametrized the effect of this unresolved phenomenon.
The aqua-planet configuration is an idealized framework that makes it possible to study the behaviour of parameterizations and their impacts on global circulation. In this configuration, the movement of tropical atmospheric waves which propagate freely in the absence of continents can be studied. In ARPEGE, the resolution varies according to the position on the globe. Therefore, the effect of the change of resolution along the tropical band on the displacement of these tropical waves can be studied. To measure this impact, we consider two aqua-planet simulations, on the one hand the model ARPEGE without stretching (figure a), on the other hand the model ARPEGE stretched (figure b) for which the variation of resolution along the equatorial band is maximum. In order to study the movement of tropical waves, we focus on the intensity of precipitation along the tropical band and more particularly in their spectral characteristics (wave number and pulsation). In figures c and d the wave energy as a function of the wave number and the pulsation is drawn in colour for both configurations. Solutions of the linearized shallow water model are added in black lines.
It is shown by the results that for both configurations the Kelvin waves are very present. A little signal of gravity waves and equatorial Rossby waves is also shown. The similarities between the graphs allow us to conclude that the resolution variation along the equatorial band does not affect the propagation of tropical waves.

4

Ice injected into the tropical tropopause by deep convection

Stratospheric water vapour has a strong impact on climate and stratospheric ozone. Quantifying the quantities of total water (water vapour and ice) injected by deep convection from the upper troposphere to the lower tropical stratosphere (~12-20 km altitude) is important for estimating the impact of convection on the entry of water vapour into the stratosphere.
The study uses ice and precipitation measurements from 2004 to 2017 from various satellite instruments (limb space-borne MLS and SMILES and, nadir space-borne, TRMM) to quantify the average ice concentrations injected into the upper troposphere and tropical tropopause. Thus, it is shown that ice concentrations in these layers increase proportionally with precipitation during the convective growing phase (figure).
The results provide information on the diurnal cycle of ice in these atmospheric layers according to different regions: Pacific Ocean, South America, South Africa, Indian Ocean, Maritime Continent (islands and seas in north of Australia). The results will help to better understand the processes impacting the entry of water vapour into the tropical stratosphere on these convective regions.

5

Warm Conveyor Belts in the NAWDEX campaign

Warm Conveyor Belts (WCBs) are dynamically important airstreams in mid-latitude cyclones. They correspond to the ascent of warm and humid air masses from the lower atmospheric layers to the high troposphere. WCBs represent the cloudy part of the depression. Heat release associated with the formation of cloud species could have a strong impact on the dynamics of these depressions. Representation of these badly known processes could constitute an important source of uncertainty for the prediction of these depressions.
The NAWDEX measurement campaign was aimed at improving knowledge about them. It occurred from 19 September 2016 to 16 October 2016 off the Iceland coast. Embedded instrumentation on Falcon et Gulfstream V planes (LIDAR, RADAR, drop-sonde) allowed the reconstitution of wind and reflectivity profiles of cloudy species in WCBs. These observations are compared to simulation results obtained with the model Méso-NH. Different parametrizations for the representation of cloud species are evaluated and confronted to measure made by the RASTA airborne radar (see figure). This cloud system is overall well simulated by the two models used. However, a systematic study of the different processes, and of their representation, associated with heat release during the given WCB case should allow the clarification of uncertainty sources and ways of improving the parametrizations to be opened.

6

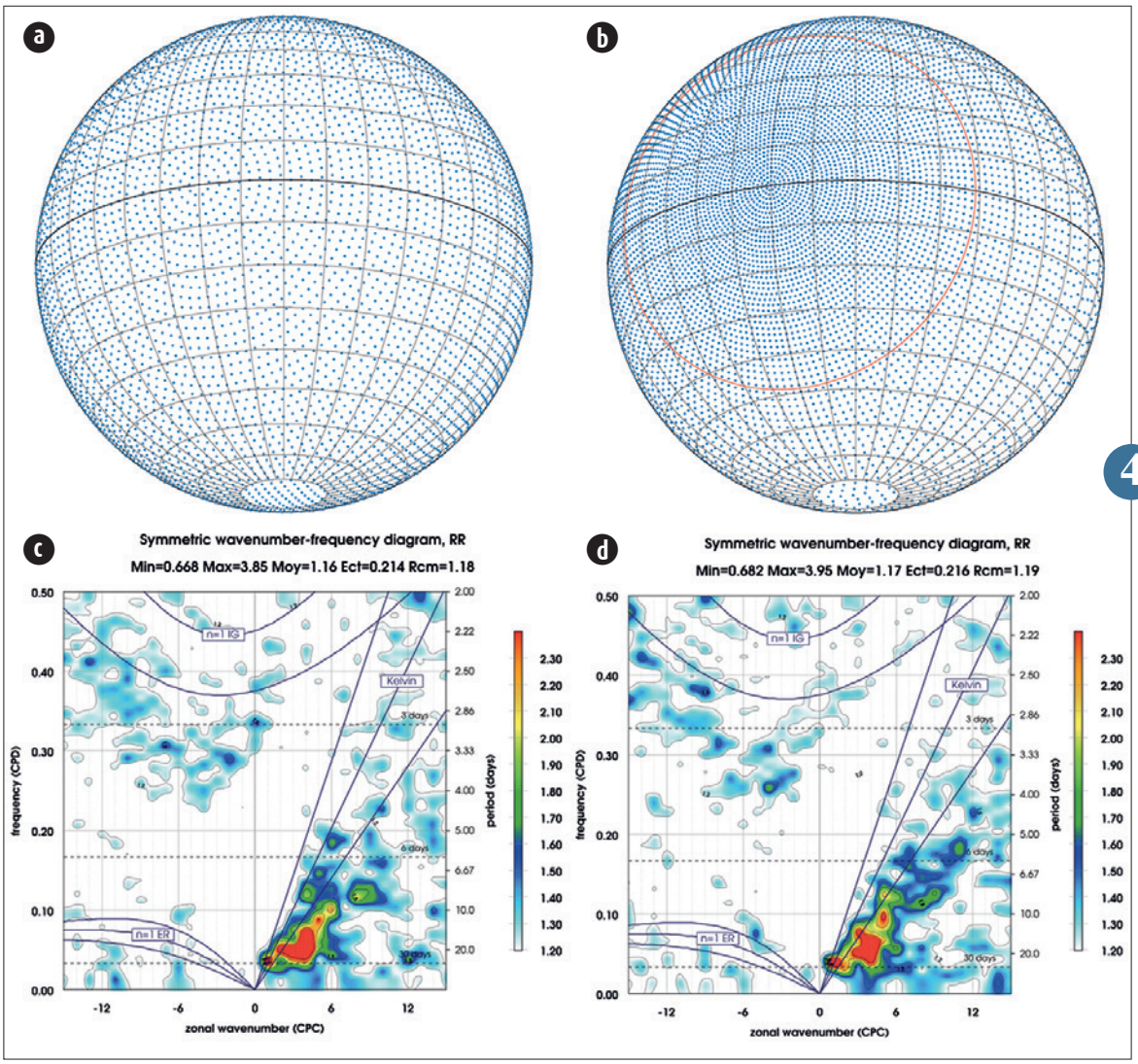

4

Grid points for the non-stretched configuration (figure a) and the stretched configuration (figure b). Four periods means of 120 days of total precipitation spectral transform for the non-stretched configuration (figure c) and the stretched configuration (figure d)

Diurnal cycles (South Africa, South America and the Maritime Continent) of ice measured by SMILES in the troposphere (blue) and tropical tropopause (red) and precipitation measured by TRMM (black) in December-February 2009-2010 (*Dion et al.,* 2018).

5

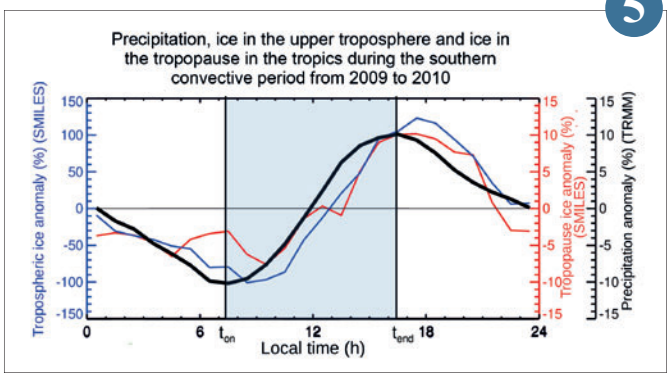

6

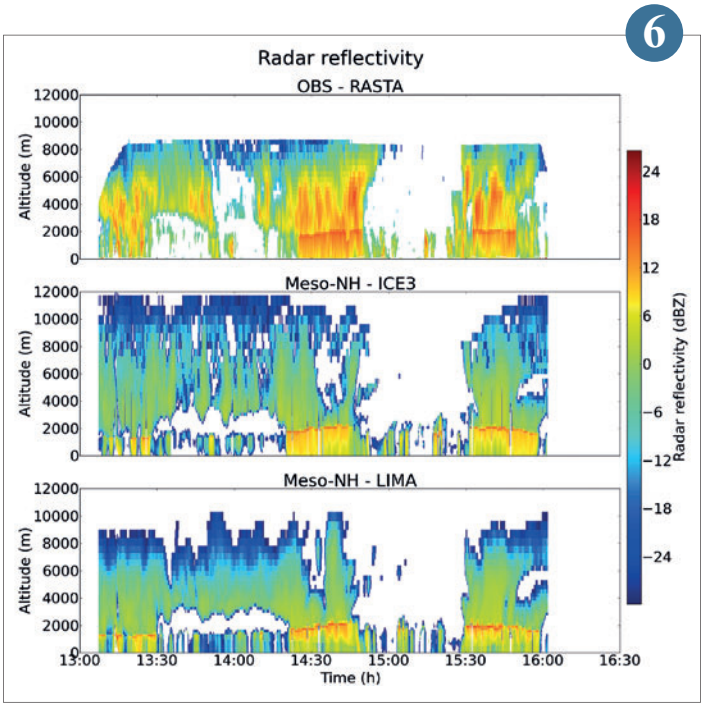

A comparison of RADAR reflectivities as measured (top) in the case of a warm conveyor belt on 1 October 2016 and simulated by Méso-NH using either ICE3 (middle) for the cloud representation or LIMA (bottom).

Performance evaluation of the MESCAN precipitation reanalysis system in mountainous areas at kilometre scale

The spatialization of surface precipitation data over complex terrain is crucial for hydrology, avalanche hazard warning and water resources management. This precipitation field is currently provide by the SAFRAN operational surface analysis system which will be replaced by the MESCAN system which still in development. The new one merges a 2D precipitation field from the operational numerical prediction weather AROME model at 1.3-km grid spacing with 24h accumulated rain gauge data. During snowy event, the precipitation gauges can collect less than 50% of the actual amount of solid precipitation when wind speeds exceed 8m/s. A correction method of wind-induced precipitation measurement errors has been developed in order to remove the negative bias in the rain gauges precipitation data. This method is based on the estimation of snow water equivalent of the daily snow fresh measurement at the weather stations.
The bias correction method was evaluated with off-line simulations, made by the French land surface model SURFEX over mountainous areas during the winter 2015/2016. The model was driven by meteorological forcing from the SAFRAN analysis system combined to the MESCAN precipitation reanalysis data. The comparison of the simulated snow depth with in situ observations shows that the bias correction method improve the performance of the MESCAN surface analysis precipitation system. This work will be used in a near future in the production of a high resolution and long-term reanalysis data set over France.

7

Validation of the surface water balance in the operational weather forecast models with measurements of Météopole-Flux instrumented site

Since 2012, the Météopole-Flux experimental system located at Toulouse, has continuously measured the surface flux of water vapour, rainfall, and soil water content up to 2.20m. These long-term measurements of surface processes allow us to make systematic comparisons with the AROME and ARPEGE operational weather forecast models.
A study of the surface water balance from the observations allowed us to analyse for the first time the behaviour of the different terms of the water budget in the model. The figure illustrates this comparison over two periods of the year (spring and summer). A significant overestimation of the evapotranspiration flow is highlighted in the model, while rainfall and water balance in the soil are more similar. Thus, the balance of these terms thus produces a significant residual in the model which will have to be studied more thoroughly with the help of the observations. This work opens new perspectives for the improvement of the representation of exchanges with the surface in AROME and ARPEGE.

8

Improved simulation of thermal comfort by taking into account urban vegetation strata

Improving the description of vegetation in urban canopy models is essential for a better simulation of urban climate.
For this purpose, the urban canopy model TEB, which simulates the interactions between cities and the atmosphere, has a new parameterization that makes it possible to distinguish tree layers from the natural surfaces on the ground. It takes into account the radiative, energetic, and aeraulic effects of trees, interacting with the buildings, the ground and the air in the street. Since the level of sophistication of this parameterization requires the knowledge of the distribution of vegetation strata within cities, a methodology, as generic as possible, has been established to build a detailed database, by combining the BD-TOPO of the IGN and Pleiades satellite images.
These developments were applied and evaluated for a neighbourhood of Toulouse where measures were collected. Thanks to the new parameterization, but also to the more realistic database (figure a), the micro-climatic variables are better simulated. But tree canopy modelling also improves the simulation of thermal comfort in the city, which depends on different environmental variables (figure b). During the day, the improvement comes mainly from taking into account the slowing down of the air flow by trees. At night, taking into account the infrared radiation emitted by the trees in the model limits the reduction of the thermal comfort index, in accordance with observations.
These new developments will allow for a more realistic evaluation of the performance of greening scenarios to adapt cities to climate change.

9

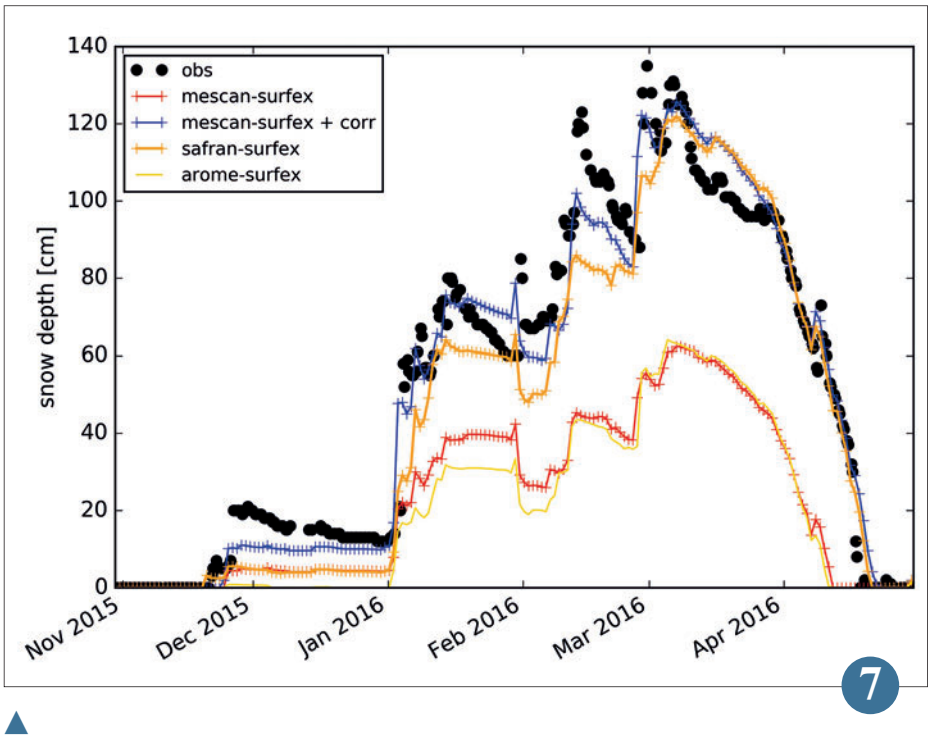

7

Simulated snow depth at Bessans located in the Haute Maurienne Valley at 1710m altitude (France) for different precipitations data set.
- SAFRAN reanalysis (orange)
- MESCAN reanalysis without the bias correction method (red)
- MESCAN reanalysis with the bias correction method (blue)
- MESCAN precipitation background from AROME model (yellow)

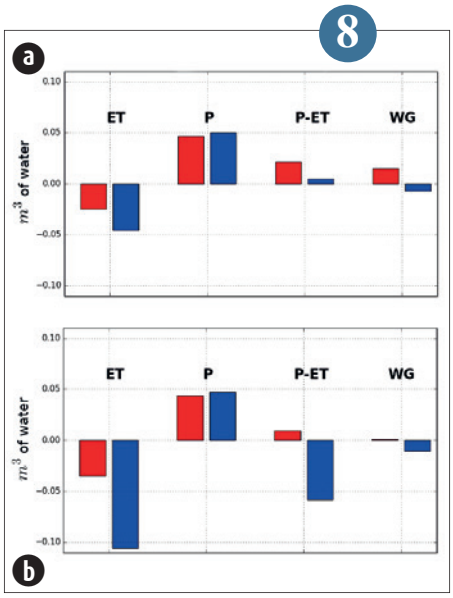

8

Comparison of different terms of surface water budget : evapotranspiration (ET), rainfall, (P), and variation of soil water content (WG) for periods from March 22nd to April 4th of 2017 (a), and July 17th to August 9th of 2017 (b). Observed values in red and simulated values by AROME in blue colour.

a) Ortho-photography of part of the residential neighbourhood simulated (left) and detailed urban land use established from the BD-TOPO of the IGN and Pleiades satellite images (right).
b) Evolution of the level of thermal comfort (UTCI, Universal Thermal Comfort Index), measured and simulated for a residential neighbourhood in Toulouse (Papus), with and without the new tree canopy parameterization. Observations come from the EUREQUA campaign, spring 2014.

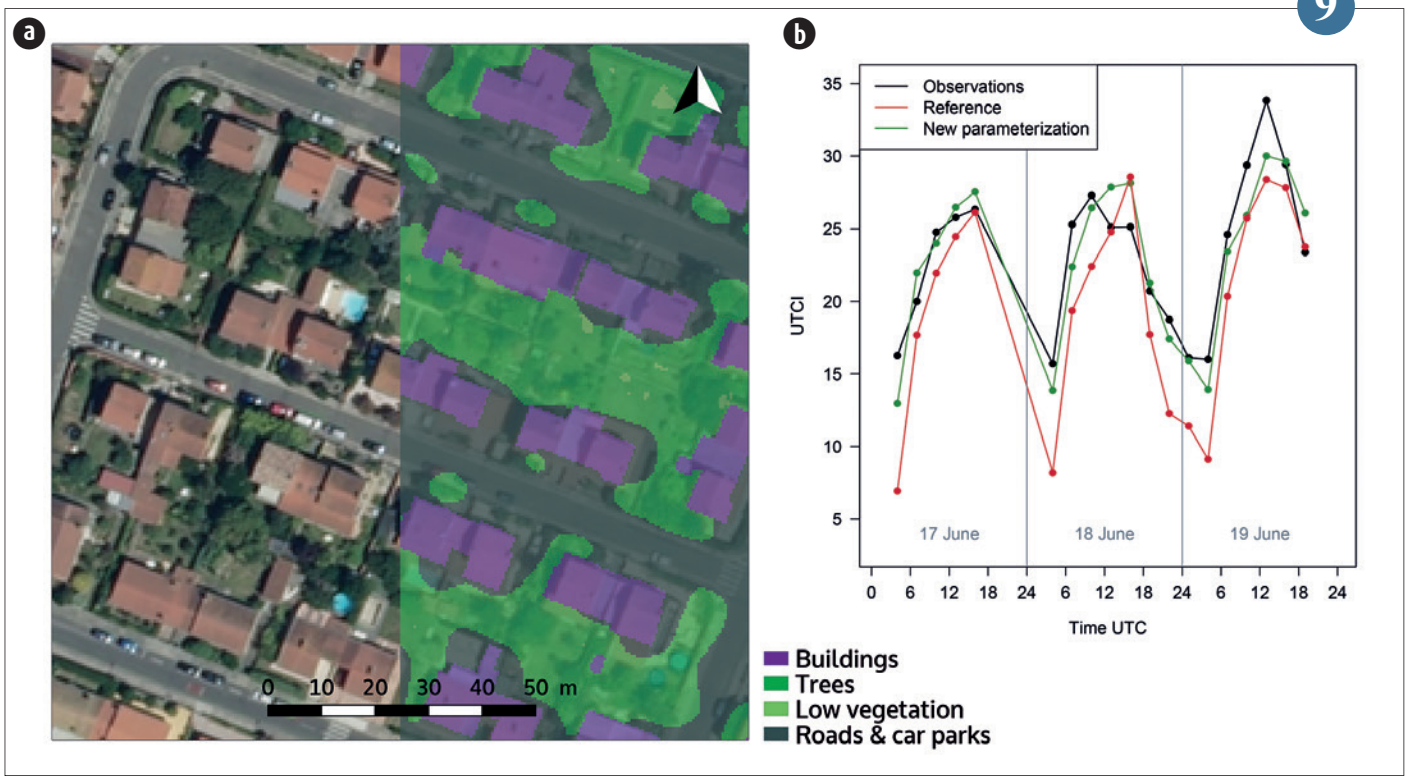

9

Influence of urban morphology and regional climate on the urban heat island intensity of French cities during the summer season

The urban heat island is defined as the temperature difference between a city and the adjacent rural areas. It can reach an intensity of 5 to 10 K, especially during the night and degrade human thermal comfort and health. The Urban Heat Island Intensity (UHII) is usually higher for larger urban agglomerations, in densely built-up areas, and for meteorological situations with clear sky and low wind speed. The UHII also depends on geographical factors like the distance to the coast and the presence of orography.

The goal of this study is to investigate the influence of urban morphology and regional climate on the nocturnal UHII of an ensemble of French cities. Urban morphology is characterised via the Local Climate Zones (LCZ) defined by Stewart and Oke (2012), regional climate via the French regional climate classification of Joly et al. (2010). The urban heat island of 42 French urban agglomerations is simulated with the urban climate model TEB coupled to the mesoscale atmospheric model Méso-NH for a meteorological situation during the summer season favourable to the development of a strong urban heat island. The simulated UHII (Figure 1) varies between 7 K in the centre of Paris and about 2 K in the centre of medium-sized cities close to the Atlantic and Mediterranean coast. The LCZ explain about 40% of the UHII variation. Mainly due to sea and mountain breezes, the UHII is on average lower in the Mediterranean, Atlantic and mountain climate than in the semi-continental climate.

In the follow-up, a similar analysis will be conducted for other meteorological situations and the interaction between the urban heat island and building energy consumption will be quantified.

10

Sub-seasonal forecast over West Africa as part of the CREWS-Burkina project

The CREWS program was launched at the COP21 with the objective of strengthening the information and early warning systems in the most vulnerable countries. CREWS-Burkina Faso is a pilot project covering the climatic zone of the Sahel, funded by the World Bank and coordinated by the World Meteorology Organization for a 3-year period (2018 to 2020). Météo-France is in charge of the development of the seasonal to sub-seasonal forecast component of the project. Concerning the sub-seasonal scales, Météo-France is currently exploiting the ECMWF 45-day ensemble forecast with a focus on rainfall, despite the low forecast scores for this variable. Taking advantage of results from previous projects over West Africa – AMMA and MISVA – this project seeks to improve the forecast of rainfall at the sub-seasonal scale by relying on variables, such as "precipitable" water and the mid-tropospheric wind, that drive the occurrence of precipitation and which have a better predictability. This also entails strengthening of the observational ground network over this region where few observational data are available to evaluate weather forecast systems.

During this first year of the project, a workshop between ANAM and Météo-France took place, resulting in the setting up of weekly briefings during the 2018 rainy season. This allowed an initial evaluation of existing forecast products and of observational datasets. In particular, a network of 150 automatic stations in Burkina Faso has been installed by ANAM. The ground rainfall estimate often confirms the large-scale structures detected by satellites, such as the measurements over the two dry regions in the south-west and north-east of Burkina Faso (see figure). This step of validation of the rainfall data is essential since it will serve as a basis for the evaluation of the forecast products developed within the project. New diagnostics are currently being developed with the objective of making them available on a dedicated website for the 2019 season.

12

Fog formation by stratus lowering

Fog strongly perturbs aviation, marine and land transportation and accurate forecasts are thus required to reduce its impact on human activities. Although relatively frequent, fogs formed by stratus lowering are the most difficult to predict, and the least explored so far. To improve their forecast, it is essential to improve our understanding of the keys processes driving such cloud life cycle.

Several stratus lowering events occurred during the field experiments conducted during the 2015 and 2016 autumns at the atmospheric station of the ANDRA (Agence Nationale pour la gestion des Déchets Radioactifs) in Houdelaincourt (Meuse). Of the 20 events recorded from October to December 2016, 10 led to fog occurrence at ground.

The case study of the night from 01 to 02/12/2016 was sampled with the CNRM's tethered balloon (see figure a) equipped with the specially adapted version of a CDP (Cloud Droplet Probe) microphysical probe which allows measurement of the size distribution of water droplet between 2 and 50µm in diameter. Figure b shows the evolution of the stratus cloud base height measured by a ceilometer, and the values of the liquid water content derived from the CDP data along the flight track of the balloon. It appears that the stratus, located at about 300m above ground level at 18h UTC, lowers during the night in several steps before the fog formation at ground from 6h to 10h with a thickness of up to 250m. During this process, measurements reveal an extremely complex evolution of the vertical structure of the atmospheric boundary layer: several cloud layers at different altitudes interspersed with clear air have thus succeeded the relatively thick stratus.

A high-resolution numerical simulation performed with the Meso-NH model is being analysed to investigate the various processes involved. The preliminary budget analysis shows that the advection processes seem crucial to feed the stratus and to favour the ascent of the cloud top and the lowering of its base.

11

10

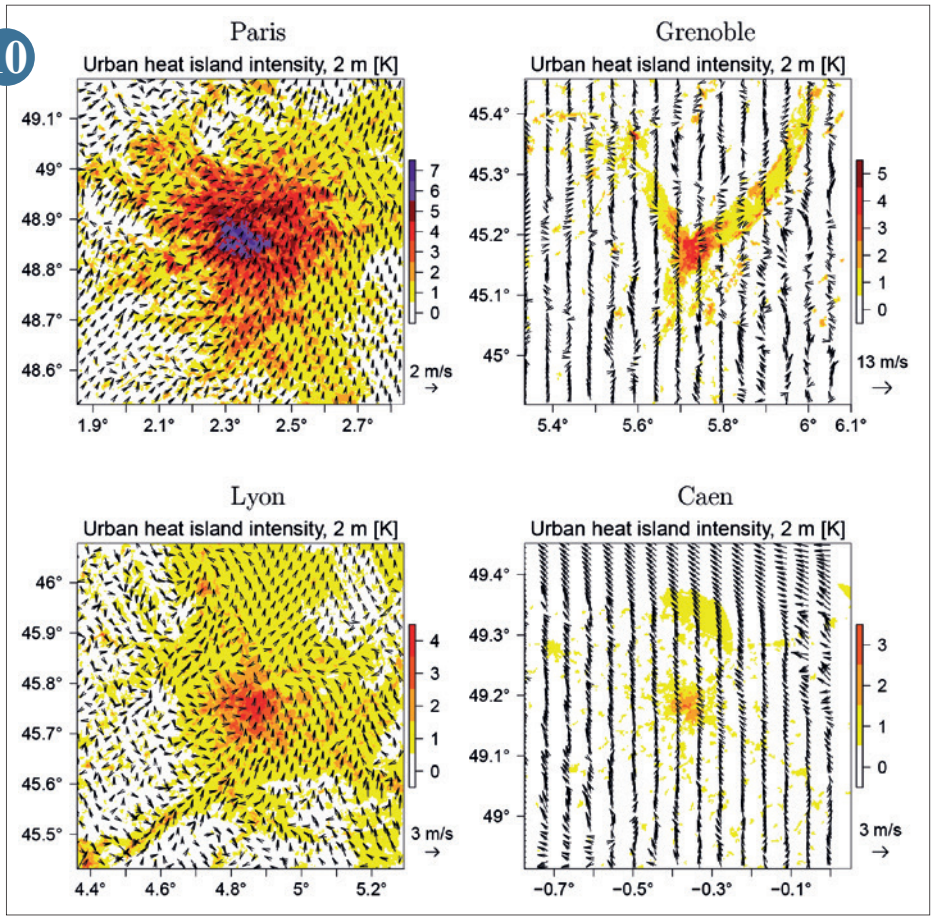

Nocturnal urban heat island intensity for a meteorological situation during the summer season favourable to the development of a strong urban heat island for a selection of French cities

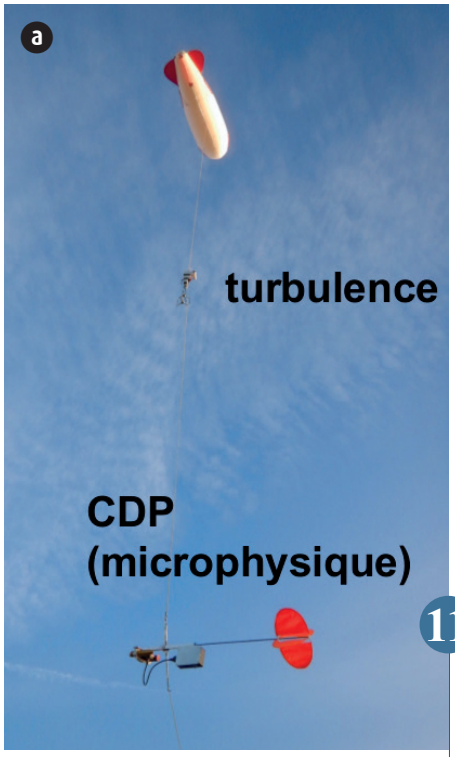

11

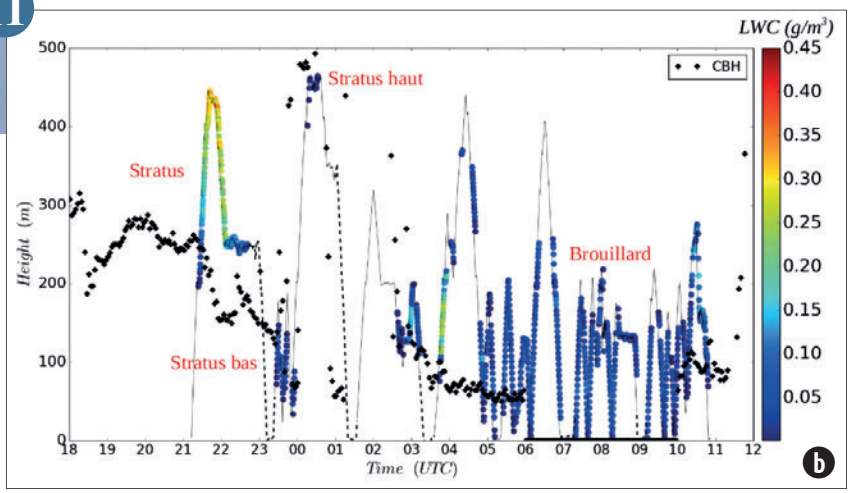

a) The payload below the tethered balloon: the turbulence probe (above) and the adapted CDP for cloud microphysics (below).
b) Temporal evolution of the height of the cloud base measured by a rangefinder (black diamonds) during the night of 01 to 02 December 2016 The values averaged over one minute of liquid water content obtained by the CDP (coloured dots) are superimposed on the trajectory of the balloon (grey or dashed line when the battery of the CDP is empty).

12

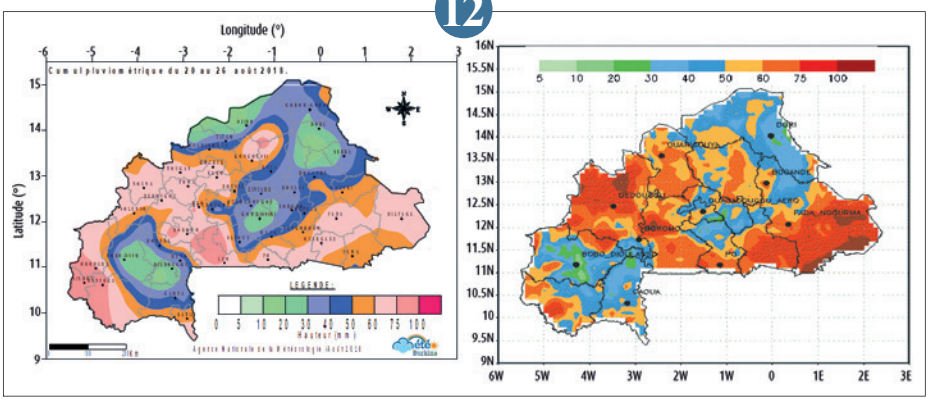

Precipitation observed by the ground network of automatic stations from ANAM (left) compared to ARC2 satellite estimation (right), during the 20-26 August 2018 week.

Climate

The international inter-comparison project CMIP6 aims to study model biases, climate response to forcings, variability, predictability and climate change. On an unprecedented scale, it will feed numerous scientific studies and the IPCC 6th Assessment Report (scheduled for 2021). The CNRM is involved in 17 of the 21 CMIP6 sub-projects.
In association with CERFACS, CNRM is contributing to the project with 3 different models of different resolution and complexity. These different coupled models result from the coupling of the ARPEGE-Climat V6 (atmosphere), Surfex V8 (continental surfaces), CTRIP (rivers), Nemo 3.6 (ocean) and Gelato 6 (sea ice) models by the Oasis3-MCT coupler. CNRM-CM6-1 and CNRM-CM6-1-HR have a resolution of approximately 100 and 50 km respectively. The CNRM-ESM2-1 Earth System Model also includes all the Earth System components used at CNRM, including the global carbon cycle, interactive tropospheric aerosols and stratospheric chemistry (figure 1). The set of simulations carried out with these 3 models will allow a better understanding of the role of resolution or complexity in the uncertainties of future climate projections.
Among the first results that emerge, that CNRM-CM6-1 simulates the observed climate and global warming over the recent period in an even more realistic way than its predecessor used for CMIP5. The equilibrium sensitivity of the new model to an increase in atmospheric CO_2 is significantly higher, resulting in an increase in global warming of about 1°C for the RCP8.5 scenario compared to the previous version. Several other international models have similar behaviour, which remains to be understood. In addition, the CNRM-ESM2-1 Earth system simulates a slightly lower warming than CNRM-CM6-1 (Fig. 2), partly due to differences in the representation of vegetation.
Beyond that, the massive production of data for CMIP6 will make it possible to feed new regionalization studies on the metropolis and overseas territories. It should also be noted that the modelling effort for CMIP6 also serves seasonal forecasting and associated services, as the new system 7, which will be operational at the end of 2019, will be based on the high resolution version of CNRM-CM6-1.

1

Diagnostic, study and climate modelling, from season to century

Interactions climate / biomass fires in the South-East Atlantic

The representation of aerosol-cloud-radiation interactions remains one of the major uncertainties for regional and global climate studies. In the South-East Atlantic, during the period from May to October, intense biomass fires located in Central Africa generate high concentrations of atmospheric particles. These plumes are then transported to the Southeast Atlantic region characterized by the presence of low stratiform clouds. Located above these clouds, these aerosols can cause a positive radiative forcing at the top of the atmosphere (warming), a sign contrary to that generally exerted by aerosols (cooling), and which remains very difficult to represent in climate models.

This scientific question was addressed using the ALADIN-Climat model, taking into account the optical properties of biomass burning particles. Simulations were conducted for the summers of 2016 and 2017, which corresponded to the AEROCLO-sA (FR), ORACLES (US) and CLARIFY (UK) measurement campaigns for which research aircraft were deployed.
The simulations indicated an aerosol transport mainly between 2 and 4km above the Atlantic, in agreement with the airborne observations. Although the ALADIN-Climat model underestimates the frequency of stratocumulus in this region, it allows to simulate a positive radiative forcing at the top of the atmosphere, of about ~+20 and +40Wm^{-2} at the regional scale with strong contrasts between the continent and the oceanic region (figure). The next step in this work will be to address the impact of aerosols on the properties (water content and albedo) of low clouds.

2

1

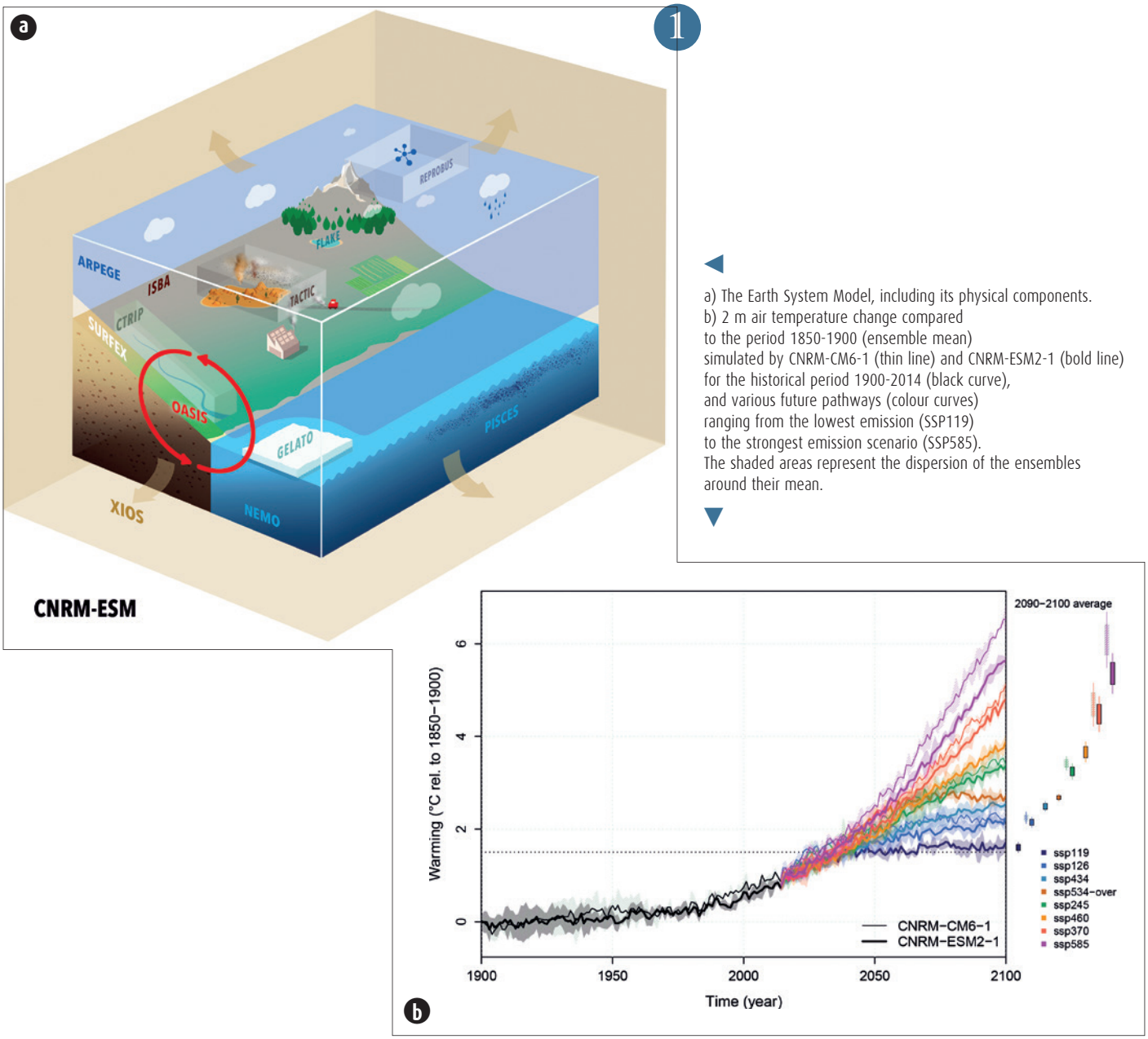

a) The Earth System Model, including its physical components.
b) 2 m air temperature change compared to the period 1850-1900 (ensemble mean) simulated by CNRM-CM6-1 (thin line) and CNRM-ESM2-1 (bold line) for the historical period 1900-2014 (black curve), and various future pathways (colour curves) ranging from the lowest emission (SSP119) to the strongest emission scenario (SSP585). The shaded areas represent the dispersion of the ensembles around their mean.

2

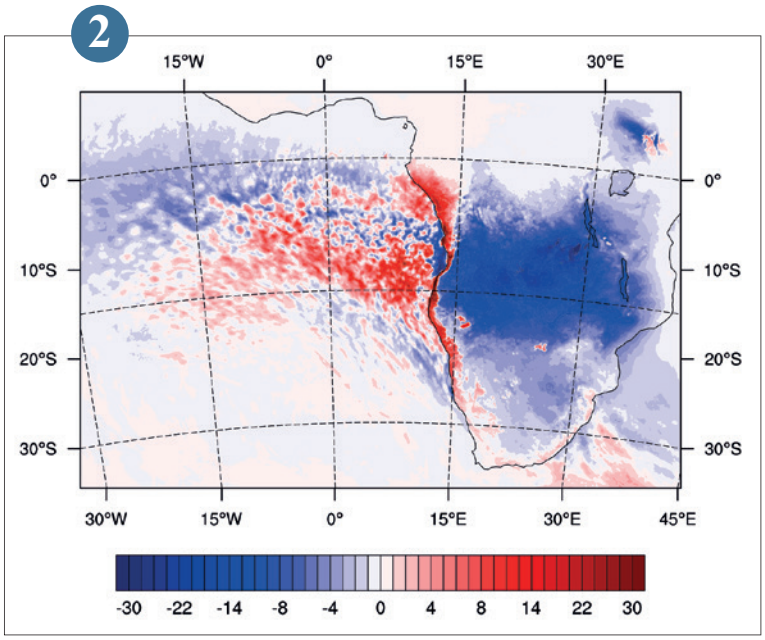

Direct (visible) radiative forcing due to biomass burning aerosols at the top of the atmosphere (in cloudy skies conditions) for the period of September 2016.

Method of downscaling ADAMONT adapted to France

The use of climate projections to drive different impact models dealing with water resources, biology or energy for example requires regionalized climate projections with high space and time resolution. The need is also to specify diagnostics on several sectors and territories.
The ADAMONT procedure, developed by Météo-France, is a method of downscaling and bias adjustment of regional climate scenarios based on a quantile-quantile correction against a set of observations or re-analyses and that takes weather regimes into account. It allows to obtain continuous de-biased scenarios at 1h-time step for surface variables such as 2m-temperature, 2m-humidity, 10m-wind speed, solar radiation (direct and diffuse) and infrared, rain and snow.
This chain, which has been primarily developed by the CNRM for the alpine and Pyrenean areas, has been adapted to the whole French country using SAFRAN-France reanalysis as a reference. ADAMONT has been applied to some regional climate scenarios of the EUROCORDEX project (see http://euro-cordex.net/). It has produced datasets covering the entire 21st century for the RCP4.5 and RCP8.5 scenarios.
These downscaled data were used to drive some hydrological models, including SURFEX-ISBA-MODCOU for impact studies for the Meuse River discharge in the frame of the CHIMERE21 project.
The ADAMONT results are now being evaluated. Once evaluated, the produced data will make available to the scientific community on the DRIAS website.

3

New hydrological simulations on the north-eastern France as part of the CHIMERE21 project

CHIMERE21 is a project funded by the Rhine-Meuse Water Agency and associates Irstea, EDF, the University of Lorraine and Météo-France. It aims to quantify the impact of climate change on the low water levels of the Meuse river basin. Particular attention is paid to the quantification of uncertainties from different sources (climate scenarios, climate models, downscaling, hydrological modeling).
The numerical tools for this work are fed by the results of the EUROCORDEX database models, in which projections from 5 global and regional model associations were selected. These data were used to perform a downscaling to generate the meteorological parameters used by the hydrological models. Two downscaling have been implemented, including one by Météo-France (ADAMONT method, see previous article). They will make it possible to carry out hydrological simulations with 3 hydrological models, including the SIM2 model of Météo-France.
To ensure the quality of the results, hydrological simulations of the historical period (1950-2005 or 1970-2005) were carried out and compared to the analyzed discharges. The first simulations of Meuse river discharge in future climate were conducted with SIM2 (see figure) and will be completed in the coming months.
The project partners will soon have a set of data and tools to simulate the flows of the Meuse until the end of the century. By combining these results and approaches, they will be able to qualify the uncertainties and thus better help managers in their decision-making process in the face of climate issues.

4

Sensitivity of the methods of spatial analysis for climatological normals to the density of the observation network

The network of rain gauges of Météo-France is today facing major changes. The manual stations forming the Réseau Climatologique d'État, managed by volunteers, consisting in around 2300 stations will disappear in the next years. Around 700 of them will be replaced by automatic stations. The spatial density of daily data of rain gauges will therefore decrease drastically. An analysis of the consequences of such a change for the climatological productions was necessary.
The production of the next climatological normals, for the period 1991-2020, will be launched in 2021. The standard spatial analysis of climate normals of Météo-France, on a one kilometre grid resolution, is today produced with the method Aurelhy, using the longest and most comprehensive possible time series available. The number of such long time series, without gaps, will decrease strongly. A new daily spatial analysis, also on a one kilometre grid, over a time series of 60 years, was implemented recently at the Direction de la Climatologie et des Services Climatiques (project Prescilia : PRÉcipitations Spatialisées Contraintes par une InitiaLisatIon Aurelhy). This daily spatial analysis can be used for the production of rainfall accumulation over all the time steps interesting the climatology (monthly, yearly, decadal, 30 years).
This product Prescilia will benefit of all the daily observations available over the period 1991-2020, finally allowing to produce climatological normals with a better density of observations than that would have been possible with Aurelhy.
A study of the sensitivity of Prescilia and Aurelhy to the density of the network of observations is presented here. This study is based on a virtual exercise of reduction of the network, progressively, from a random selection, covering the years 2004 to 2007. The climatological performances of Prescilia and Aurelhy are then estimated over the period 2001-2010 against a reference sample of 1400 stations in a k-fold cross-validation exercise. The performances are evaluated in three different situations: (i) the full network with the density existing today, (ii) the network with a progressively reducing density, (iii) the network with the future final density (all the manual stations closed). The study showed that Prescilia is performing better than Aurelhy with the future low density network.

5

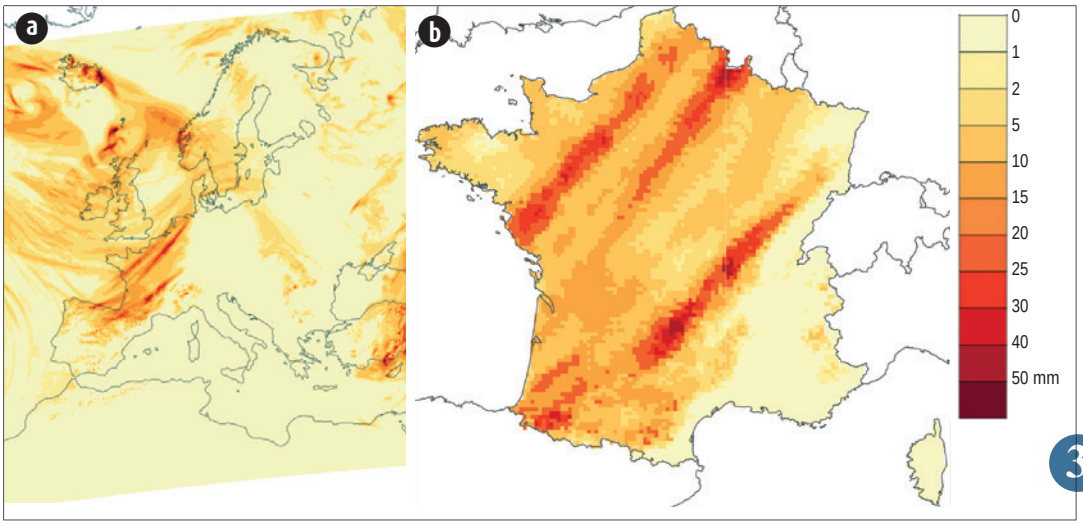

a) The daily total precipitation range in mm from the model CNRM-ALADIN5.3 driven by CNRM-CERFACS-CNRM-CM5 for March 30, 2092, scenario RCP8.5.
b) Same total precipitation field in mm, de-biaised and at a 8 km x 8 km resolution after application of the ADAMONT method on the day of March 30, 2092.
Same colour scale for both fields.

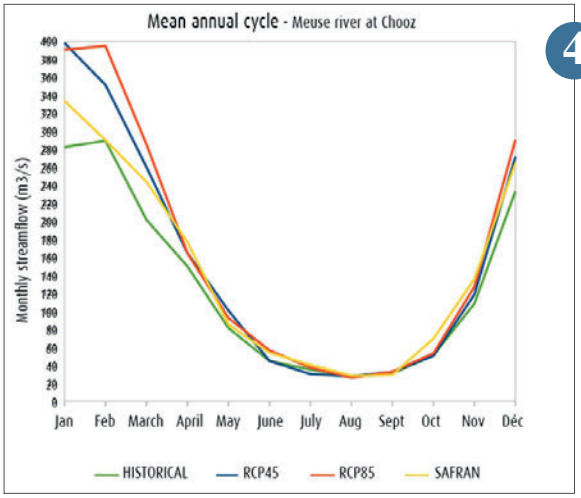

Average annual cycle of monthly streamflows of the Meuse at Chooz simulated with the SAFRAN reanalysis (period 1979-2008, in blue) and the scenarios produced with the CNRM-ALADIN53 / CNRM-CERFACS-CNRM-CM5 pair for the historical period (1950-2004, in green) and the future period (2005-2100) under RCP4.5 (in red) and RCP 8.5 (in yellow) assumptions.

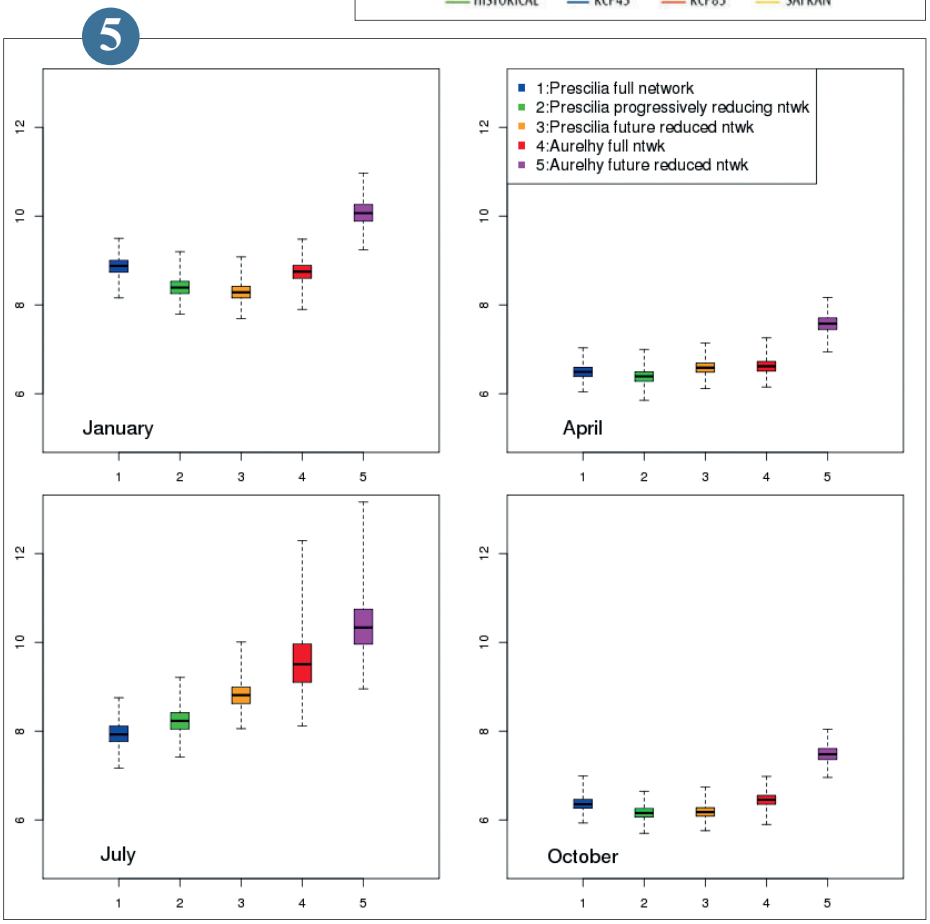

Mean relative absolute error (%) for 1400 reference stations after a k-fold cross validation for 5 experiments over the period 2001-2010
(1: Prescilia full network;
2: Prescilia network progressively reducing;
3: Prescilia future reduced network;
4: Aurelhy full network;
5: Aurelhy future reduced network).
Aurelhy future reduced network shows always the worst results.

Re-building of long snow height series in the Pyrenees for climate change analysis

The Clim'Py project contributes to the development of the Pyrenean Observatory of Climate Change and its geoportal (https://www.opcc-ctp.org/fr/geoportal), by documenting the past and future climate in the Pyrenees, especially for the snow trends. Several approaches have been implemented and combined to describe the snowpack evolutions: in situ observations, physical modelling and remote sensing (MODIS and SENTINEL2 data).

Météo-France is involved in this project through the complementary skills of the CNRM-CEN team for snowpack modelling, of the DCSC and the DIRSO departments for climate change analysis.

An inventory of the snow height series available on the whole massif has been achieved and around 60 series (more than 10 years old whom 20 series with more than 30 years old) have been identified on the French and Spanish versant.

Its series, coming from the nivo-meteorological network, cover the period from December to April with data availability according to the ski-resort opening. To optimize the use of its data for climate change analysis, a specific action of data control and re-building has been designed from a version of the snowpack model CROCUS including an assimilation code of the snow height observations.

A selection of long series over the Pyrenees has been used to assess the method and evaluate uncertainties. A new climatology of the snow has been achieved and several indicators have been calculated to highlight variability and climate change: seasonal and monthly mean value, number of days upper than several thresholds.

With a strong inter-annual variability, the snow trends prove to be very sensitive to the date start or end of the series (see Figure). The most robust result concerns the diminution of the snow conditions at the spring (April) while the temporal deepness of the series (35 years old maximum) remains too short to really detect the climate change effects on the snow variable.

6

Contribution to Climate Data Rescue in the frame of Copernicus C3S

The Copernicus Climate Change Service (C3S) supports coordination and harmonization of in situ data rescue activities around the world. In the frame of the Copernicus C3S/311a, 14 partners, including Météo-France, have been involved in development of a Service to facilitate climate data rescue: the C3S Data Rescue Service (C3S DRS).

The C3S data rescue portal will provide data rescue activity information, a registry service for metadata related to rescued data, data rescue tools, guidelines for best practices for climate data rescue to facilitate all steps of the data rescue procedure.

Météo-France is contributing to the Metadata registry, is taking part in writing guidelines for best practice for climate data rescue and is respondent to the activity annual survey.

Since this year, it is possible to get information about the key valorisation initiatives of the climate archives of Météo-France and the National Archives (Semaphores and lighthouses in mainland France 1879-1930, French Polynesia 1935-1980 et West Indian Ocean) on the International I-DARE Portal. Each initiative is geo-located and the progress is regularly updated.

For details on C3S Data Rescue Service:
https://insitu.copernicus.eu/news/the-c3s-data-rescue-service
and https://rmets.onlinelibrary.wiley.com/doi/full/10.1002/gdj3.56

8

Impact of groundwater on climate sensitivity in CNRM-CM6

Groundwater amounts for about 30% of the total freshwater resources. It can also affect the atmosphere through exchanges of water with the uppermost soil layers. For these reasons, CNRM-CM6, the Météo-France climate model, recently implemented an aquifer scheme, thus becoming the first global climate model to include a 3D representation of groundwater.

The addition of aquifers in CNRM-CM6 did not have a significant impact on present-day climate, but things can be different in a warmer climate, such as projected for the end on the 21st century. We investigated the influence of aquifers on "climate sensitivity", that is to say on the model's response to an abrupt quadrupling of the atmospheric CO^2 concentration ($4xCO^2$), compared to pre-industrial levels. We showed that locally (in Ukraine and eastern Europe), aquifers could reduce by 1° to 2° the increase of daily maximum temperature, which corresponds to 20% of the simulated warming. This finding can be explained by an increased recharge of aquifers in winter due to larger rainfall rates in the $4xCO^2$ climate. In summer, the water table depth remains high enough for the aquifer to actually cool down the low levels of the atmosphere through the evapotranspiration fluxes, whereas without aquifers, all the excess of soil moisture has evaporated by the time spring comes.

The existence of such feedbacks underlines the necessity to represent groundwater in global climate models. In return, it will allow us to understand better the evolutions of groundwater resources and water table depth in future climates.

7

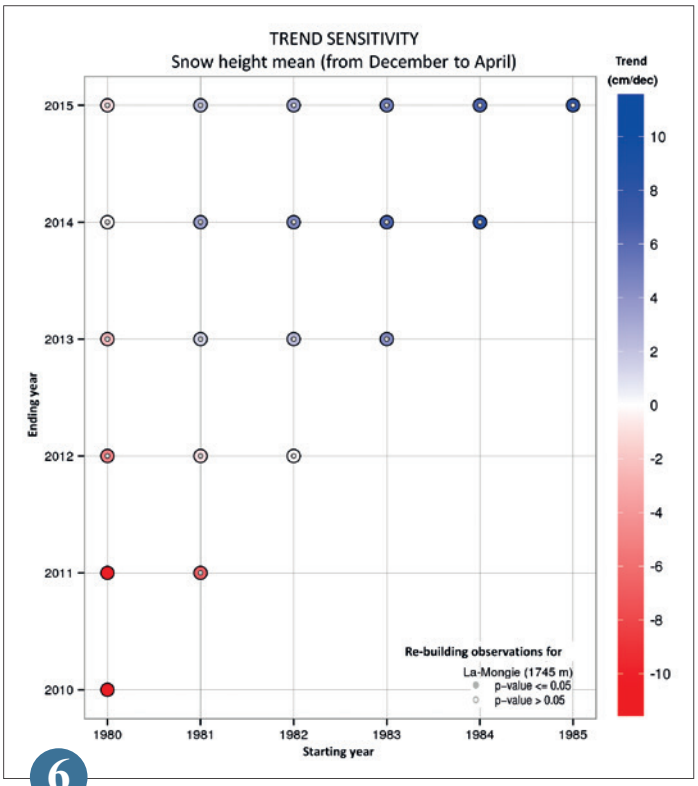

6

Sensitivity of the snow height mean trends (December to April) according to the starting/ending year taken into account for the serie of "La Mongie" (1745mslp) in the Pyrenees. The positive trends are in blue colour and the negative ones in red. Full circles represent the significant trends with the Mann Kendall test (p value lower than 0.05).

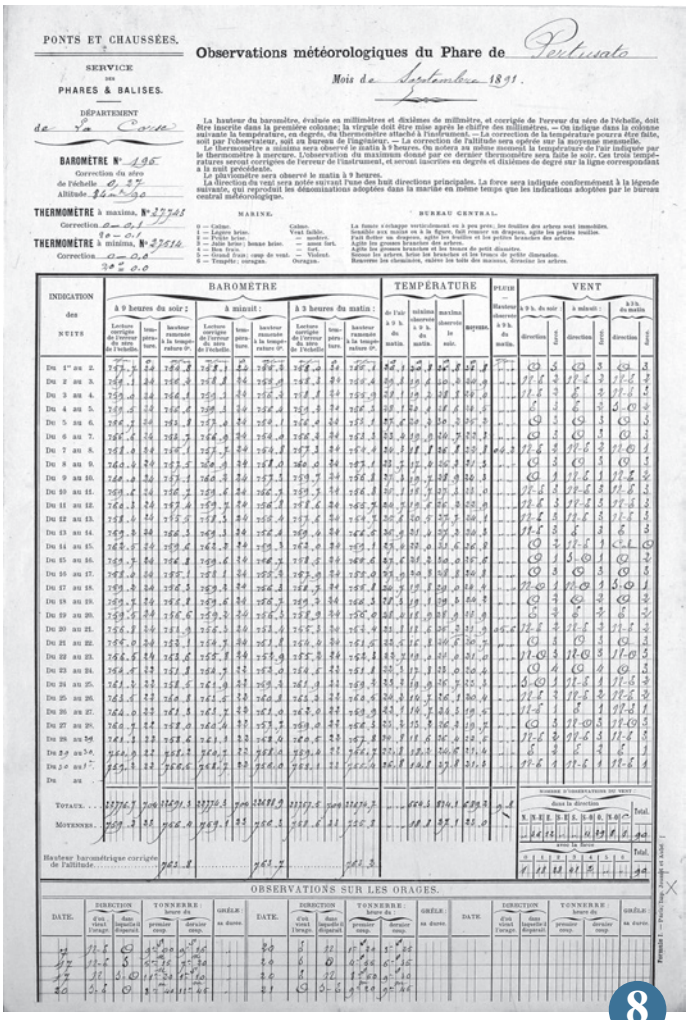

8

Meteorological observation sheet of the Pertusato lighthouse (Corsica), September 1891.

Impact of groundwater on daily maximum temperatures (K) in CNRM-CM6
a): differences in pre-industrial climate between the experiments with aquifers (Aqui) and without (Ref);
b): differences in 4xCO2 climate between the experiments with aquifers (Aqui) and without (Ref);
c): impact on climate sensitivity (b - a).

7

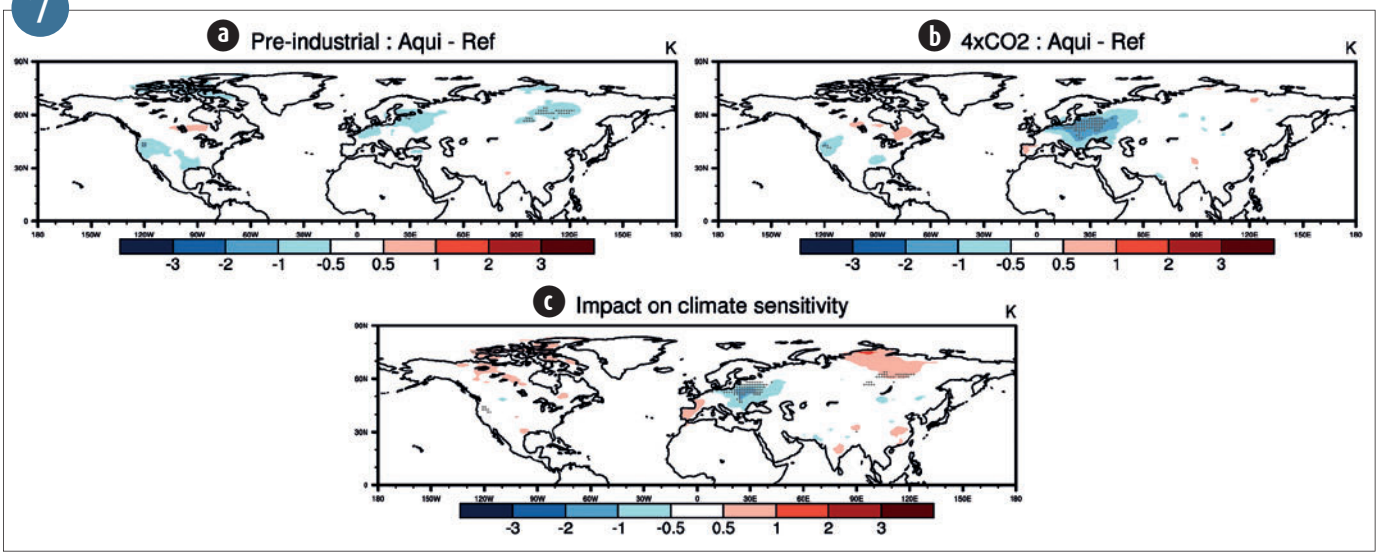

Role of soil moisture in a summer seasonal forecast

The summer climate variability of several mid-latitude regions is partly linked to the superficial soil water content. Over these regions, including Southern Europe, soil moisture anomalies strongly impact energy and water exchanges between the land surface and the overlying atmosphere, and thus temperature and precipitation. However, taking into account these soil moisture anomalies when initializing seasonal predictions, translates into a moderate and localized forecast improvement, for the summer season.

To better estimate the potential role of soil moisture in terms of seasonal predictability, idealized experiments have been carried out with two regional climate models, ALADIN and RACMO, over the Euro-CORDEX domain at a 0.22° horizontal resolution. For each of these models, they consist of ensemble initialized simulations of the 1993-2012 summer seasons, for which soil water content is daily constrained to pseudo-observations. These experiments ('SOIL') are compared with control simulations (' CTRL '), in which soil moisture evolves freely. The figure highlights the significant increase of the correlation between observed and simulated summer precipitation when soil moisture is prescribed.

This improvement, also noticeable for temperatures and downward surface solar radiation, concerns most of the domain, including very northern regions of Europe. Results are consistent between the two models, and suggest that soil moisture could contribute to improve summer forecasts in regions located further North than those previously identified.

9

Seamless production and publication of CMIP6 climate projections

CNRM contribution to the sixth CMIP program is essential, both with respect to its institutional duty in climate study and for its international recognition. Practically, it has an unprecedented size and complexity: running more than 200 climate simulations which were specified by 17 distinct sub-programmes and which represents more than 24.000 years of simulated climate; this is achieved using three main configurations of CNRM's climate models: two in ocean-atmosphere coupled mode (one at high resolution: 50km for the atmosphere), and a third one in "earth system" mode (which also includes a representation of the carbon cycle, atmospheric chemicals and aerosols); other configurations are also used: "no-ocean", 'ocean-only' and "land-only".

The complexity occurs in three domains:

- in the detailed specification of those variables which have to be simulated, which varies for each simulated year, and which is handled in a complex database, the CMIP6 "Data Request";
- in the number, variety and details of the metadata which the CMIP programme requests to associate to the data;
- in the specifics of the data delivery system which is prescribed by CMIP6 (an ESGF "node").

CNRM addressed these challenges very early by:

- investing in a 2 petabytes ESGF node, and in the necessary expertise for running it;
- developing a workflow based on three major components: the ECLIS framework for running the simulations, the Xios library (by IPSL), and a module, "dr2xml", which translates the "Data request" in Xios configuration data. This workflow allows for a seamless production of results which comply to the CMIP6 norm.

This allowed CNRM to be among the very first climate research centres to massively deliver its results, in due time for the next IPCC assessment report, and so to improve its international recognition in climate simulation.

10

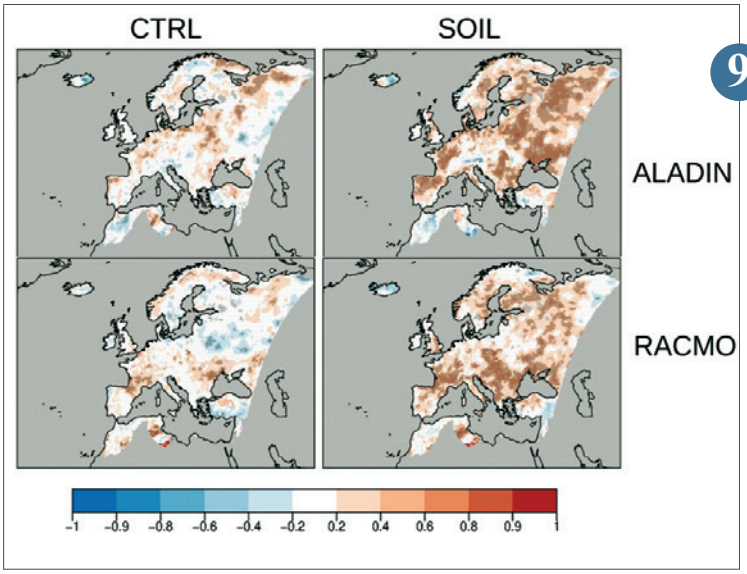

9

Correlation of simulated summer precipitation (June-July-August) with corresponding EOBS observations, over the 1993-2012 period

10

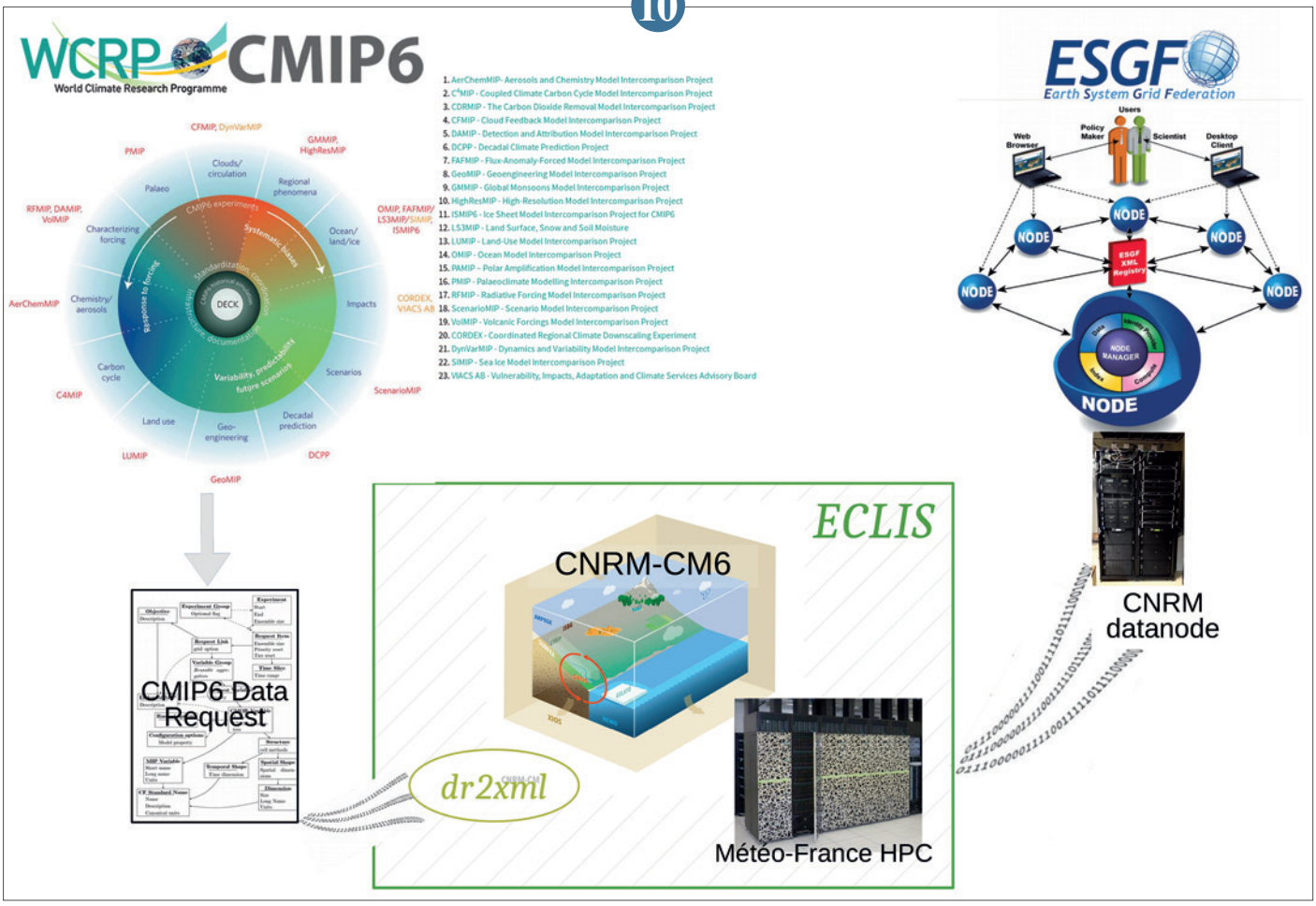

The 23 CMIP6 sub-programs (acronyms in red, names in green) fed a complex database ("Data Request") which specifies the results to produce.
The ECLIS framework drives both its translation by "dr2xml" in directives for the model component Xios, and the running of simulations on Météo-France's High Performance Computing centre. This feeds directly (without any further processing) a CNRM owned data node of the worldwide ESGF climate data dissemination system, with more than 200 simulations and 24 000 years of simulated climate.

Impacts and adaptation

Defining single extreme weather events in a climate perspective

Retrospective analyses of extreme events are common in order to provide a fine picture of a given weather event, in particular through the description of its characteristics (e.g. typical scale: length, extent) and rarity (e.g. via an evaluation of the occurrence probability of that event). In a climate change context, such retrospective analyses can also be extended to attribution diagnoses, in order to assess any potential human contribution to that event.

The definition of the event itself is critical in such analyses. For instance, the European Heatwave of 2003 has been sometimes described in the literature as a ~10-day long event in early August, over a particular city or region of interest, and sometimes as a summer-long event (June-July-August), covering Europe as a whole.

In order to define a singular extreme event objectively, we propose to systematically investigate what was the most extreme in that event. For this purpose, we assess the occurrence probability of the event (accounting for climate change as much as possible) for a vast collection of temporal and spatial windows (figure). The smallest probability indicates the period of time and the spatial domain over which this event was the most extreme. Applied to the European Heatwave of 2003, this method selects a 8-day time window in early August, and a relatively small spatial domain (~500km) in the vicinity of Paris. Results also suggest that this method do not bias attribution results, which use to be highly sensitive to the spatio-temporal scale.

The advantage of the proposed approach is that it can be used for any meteorological variable or type of event, including precipitation, wind, etc. Therefore this method presents a clear interest for climate monitoring.

11

SIOD direct and indirect impact on tropical cyclone activity over the south west Indian Ocean basin

Thanks to satellite imagery, tropical lows can be thoroughly studied since 1998 over the south west Indian Ocean basin (30E-90E, 0S-40S). It becomes then possible to establish links between inter annual variability of cyclone activity and large scale climatic disturbances such as ENSO, IOD, SIOD. As a reminder, SIOD stands for subtropical Indian Ocean dipole. A positive (resp. negative) SIOD event is associated with above (resp. below) average sea surface temperature south east of Madagascar and below (resp. above) average sea surface temperature west of Australia.

From recent work achieved by computing ACE (accumulated cyclone energy) from CMRS-cyclone de La Réunion reanalysis, we can state that strong positive SIOD events (1998/1999, 2008/2006, 2010/2011 and 2016/2017) are associated with very low cyclone activity from November to the end of February (see figure).

GNSS derived integrated water vapour (IWV) time series and ERA interim reanalysis shows that the area between 50 and 80E and 5-20 S are drier than they usually are from October to February during strong SIOD positive events. This dry anomaly is associated with subsidence anomaly over the western Indian Ocean which tends to dry the mid troposphere but also generates an anomalous east-west pressure gradient, reinforcing the trade winds in the tropics and advecting dry air from the south. Dry air and lower than normal low level convergence seems to bring an explanation to the weak cyclone activity during the 4 strong SIOD positive events.

Attention can be brought on higher than average cyclone activity over the central south Pacific basin 1 year prior to strong SIOD positive events. Studying cyclone activity within other southern hemisphere basin could improve seasonal forecast in our own in the matter of strong SIOD positive events.

13

Mediterranean Sea Marine Heatwave on the Rise

Episodes of anomalous ocean warming have been observed in recent decades, with widespread ecological impacts and important socio-economic implications. Superimposed on the underlying warming trend of the ocean, these events referred to as Marine Heatwaves (MHWs), occur regionally from coastal to open ocean and may force changes in marine ecosystems and fisheries in a matter of weeks or months. They can be persistent in time and extended in space.

A general increase in their occurrence throughout the global ocean surface was indicated over the last century, while regional and global-scale projections suggest more intense and longer-lasting events in the 21st century with higher global warming rates.

In the case of the Mediterranean Sea -a well-known "Hot Spot" region for climate change-, little is known about past or future MHW trends. A significant annual mean SST rise (+1.5°C to +3°C, depending on GHG emission scenario) projected for the basin by the end of the 21st century, is expected to accelerate future MHW occurrence. To assess for the first time this evolution, we used satellite-derived sea surface temperature observations as well as the fully-coupled, high-resolution Med-CORDEX model ensemble (www.medcordex.eu) in a multi-scenario approach.

In response to increasing GHG forcing, events seem to become stronger and more intense under RCP8.5 than RCP2.6. Particularly for RCP8.5 2071-2100, simulations project at least one MHW every year, up to 4 months longer and about 4 times more intense than present-day events (HIST) (figure). Meanwhile, their surface coverage at peak increases from an average of 40 % (HIST) to almost 100 % and events like the observed MHW 2003 become the new normal. While RCP8.5 is the business-as-usual scenario RCP2.6 is the closest to Paris agreement limits, which could restrain future MHW mean intensity and duration.

12

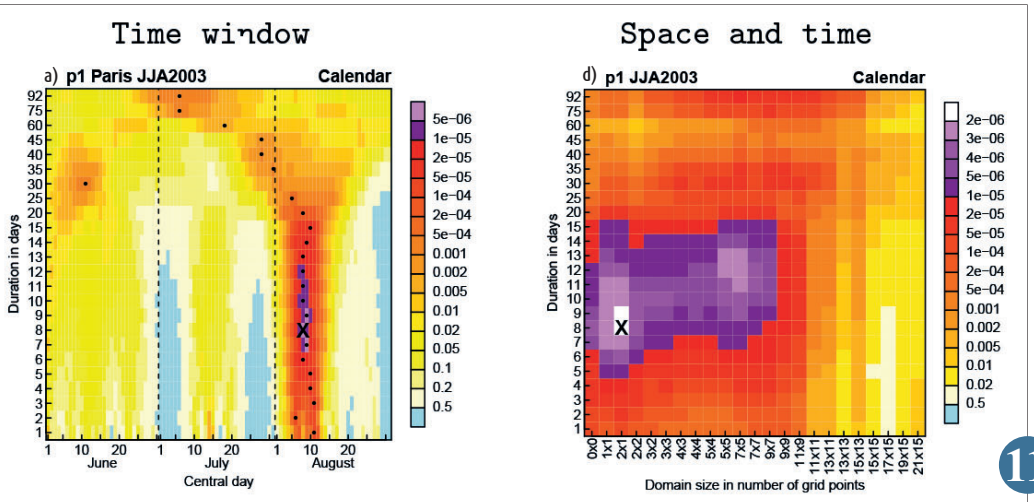

11

Occurrence probability of the 2003 European Heatwave in Paris, as estimated for a collection of time windows and spatial domains. Values correspond to the probability (estimated from the historical record) to observe a temperature lower than that observed in 2003. Maximizing these values allows us to highlight the spatio-temporal scale characterizing the event.
Left panel: time period is investigated first, through selecting the date (center of the time window, from 1st of June to 31st of August, x-axis) and duration (y-axis, in days), in Paris. The highest value is found for an 8-day event occurring in early August.
Right panel: spatio-temporal domains are investigated through the size of the spatial domain (x-axis, one unit corresponds to a 2.5°x2.5° square, all domains include Paris), and the duration (y-axis, in days).

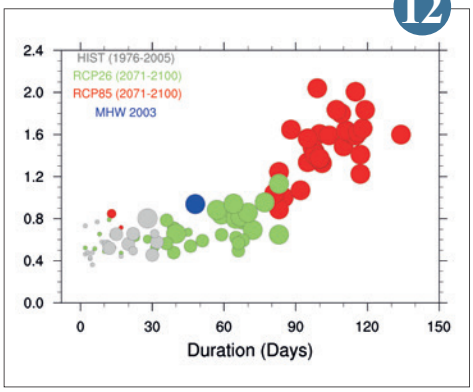

12

MHW evolution in the Mediterranean Sea at present-day and at the end of the 21st century using the CNRM model of the Med-CORDEX ensemble
Historical run (HIST) is indicated in grey, high-emission scenario RCP85 in red and low-emission scenario RCP26 in green.
Observed MHW of 2003 is also shown in blue.
Size of the bubble refers to the maximum surface coverage (%) of each event.

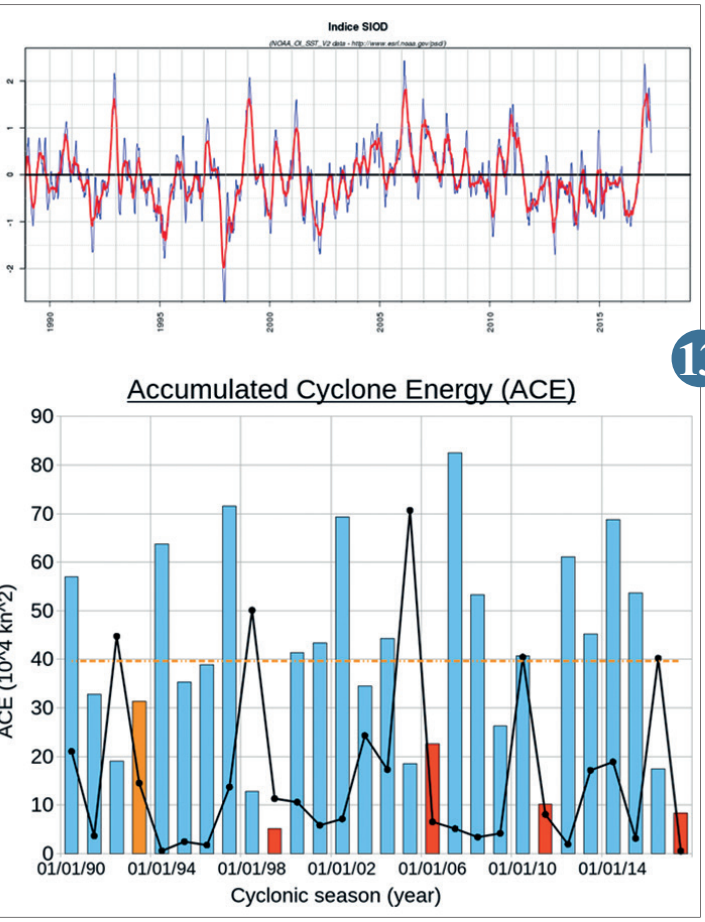

13

Top panel represents 1990 to 2017 SIOD index in °C.
Bar plot in the bottom panel is ACE for South West Indian Ocean basin between November 15th of year n-1 and February 28th of year n.
Year with strong positive SIOD are in red. Orange dashed line stands for mean ACE in south west Indian Ocean basin between November 15th of year n-1 and February 28th of year n. Black curve represents ACE for the South Pacific basin east of the date line between November 1st of year n-1 and May 1st of year n.

Agriculture: using cover crops to mitigate the effects of climate change

In Europe around 20% of land surface area is covered by agricultural fields. During fallow periods, soils often remain bare. In a special issue of *Environmental Research Letters* dedicated to climate change, *Carrer et al.* (2018) quantify how cover crops could be used during fallow periods to mitigate the effects of climate change. Using satellite data from all over Europe, they modelled the effects of changes in albedo – the fraction of energy reflected by the land surface – resulting from the introduction of cover crops in agricultural fields (figure a).
The results of the study suggested that the introduction of cover crops could mitigate approximately 7 % of the annual greenhouse gas emissions from Europe's agricultural and forestry sector (using 2011 emissions as a reference) by simultaneously increasing albedo, reducing the need for fertiliser, and increasing carbon sequestration. The albedo effect accounts for 10 to 13 % of this total effect. The European countries for whom this technique holds the most promise are France, Bulgaria, Romania, and Germany in order of relevance (figure b).
It remains to be determined how viable this approach is compared to other climate engineering techniques, given possible climatic and ecological feedbacks, economic constraints, and ethical concerns. A significant advantage of this method is that it can be put into place progressively and reversed at any moment.

14

Seasonal hydrological forecasts in France using the new Météo-France System 6 model

Since spring 2018, the Météo-France's operational seasonal forecast model (Météo-France system 6) has been used by DCSC (Directorate of Climatology and Climate Services) to produce hydrological seasonal forecasts over France.
The forecasting chain comes from research works (in particular Stéphanie Singla PhD in 2012). Additional work, in the framework of the EUPORIAS project, has been completed in conception and assessment of decision making products. In partnership with EPTB Seine-Grands Lacs (manager of dams in the upstream part of the Seine basin), this co-design has led to the implementation of a regular production of hydrological indices, henceforth updated each month.
Initial states (in particular snow pack, underground water levels, soil wetness, river flows) are provided by the operational analysis chain SAFRAN-SURFEX-MODCOU, for a long time used for water resource monitoring in France. The hydrological predictability comes partly from these initial conditions, knowing that their influence could extend to weeks up to months.
Among available output variables, one can firstly mention river flow. Forecast scores show for some basins, during favourable spells (for instance snow melting times for mountainous basins), good predictability up to several months ahead. Such forecasts could be precious tools for water resource management, for example dam release planning during low flow season. Soil wetness and snow pack forecasts offer opportunities that still need to be exploited. From this « real time » chain, several technical improvements are planned, like introducing medium range or monthly forecasts at the beginning of simulation, using a finer downscaling method on meteorological forcing or using other seasonal forecast models. In parallel, in the MEDSCOPE project, we are testing a similar chain on several European regions. And last, there is still a major effort to be make in pedagogy and support to users: this is fundamental for these products to become pillars of a true climate service.

16

Groundwater resource seasonal forecasts in France

The Aqui-FR project aims at producing and forecasting groundwater resources over France. This initiative gathers regional hydrogeological applications that simulate daily groundwater levels by using surface runoff and drainage from the SURFEX surface model platform.
The predictability in hydrology has been proven for river flows, which was improved by taking into account the aquifers (especially regarding the low flow sustainability). Using the atmospheric forecasts from the ARPEGE System 6 climate model, it is possible to forecast groundwater levels for the next six months. An initialization in spring or at the beginning of winter allows us to anticipate potential risks of drought or flooding by a rising water table. These forecasts consist in multiple scenarios (or members) giving as many output scenarios. Based on this range of possibilities and on an historical simulation (or reanalysis, REA) over a hindcast period (1993-2016), groundwater levels are converted into standardized piezometric level indexes (SPLI, figure a) which define an hydrogeological status rather wet or dry up to 6 months in advance. A comparison with ground measurements (OBS) shows a good performance of the seasonal forecasts (PSE) starting in May during the low flow season (figure b).
These forecasts are under evaluation and the Aqui-FR platform is in constant evolution with the addition of new regional hydrogeological models.

15

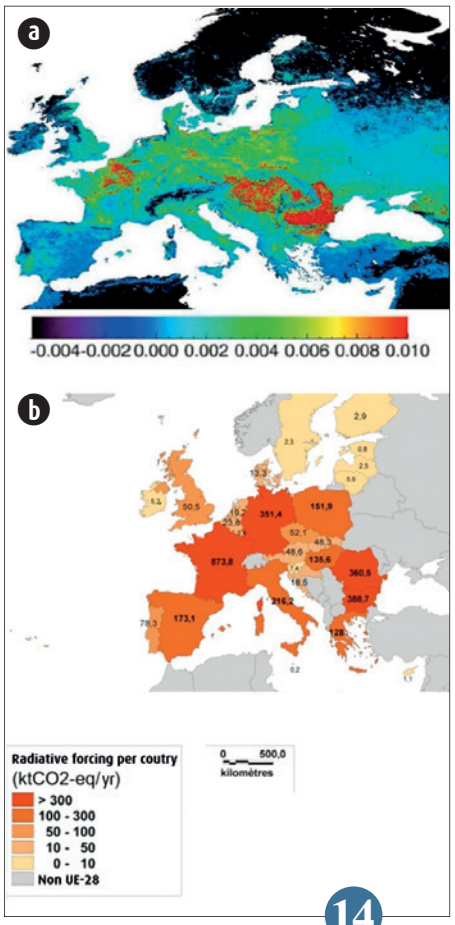

Maps showing (a) the annual increase of surface albedo resulting from the introduction of cover crops and (b) the climate mitigation potential related to the increase of albedo over croplands due to the introduction of cover crops (in thousands of tonnes of equivalent CO_2 per year for each country of the UE-28).

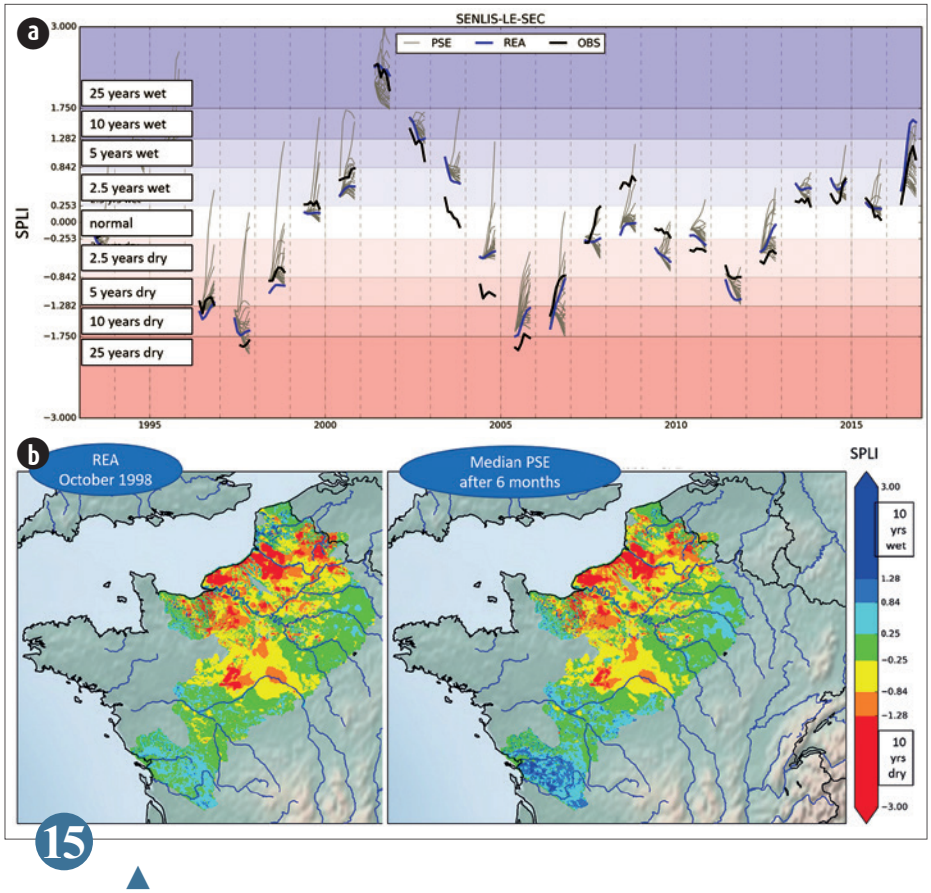

a) Time series of the standardized groundwater level index (SPLI) of the piezometric in situ station near Senlis-le-Sec (Somme region) between May and October from 1993 to 2016 using the observations (OBS), the historical simulation (REA), and the seasonal forecasts after 6 months (PSE). b) SPLI map of October 1998 over France using the historical simulations (REA, left panel) and the median of the seasonal forecasts after 6 months with an initialization in May (right panel).

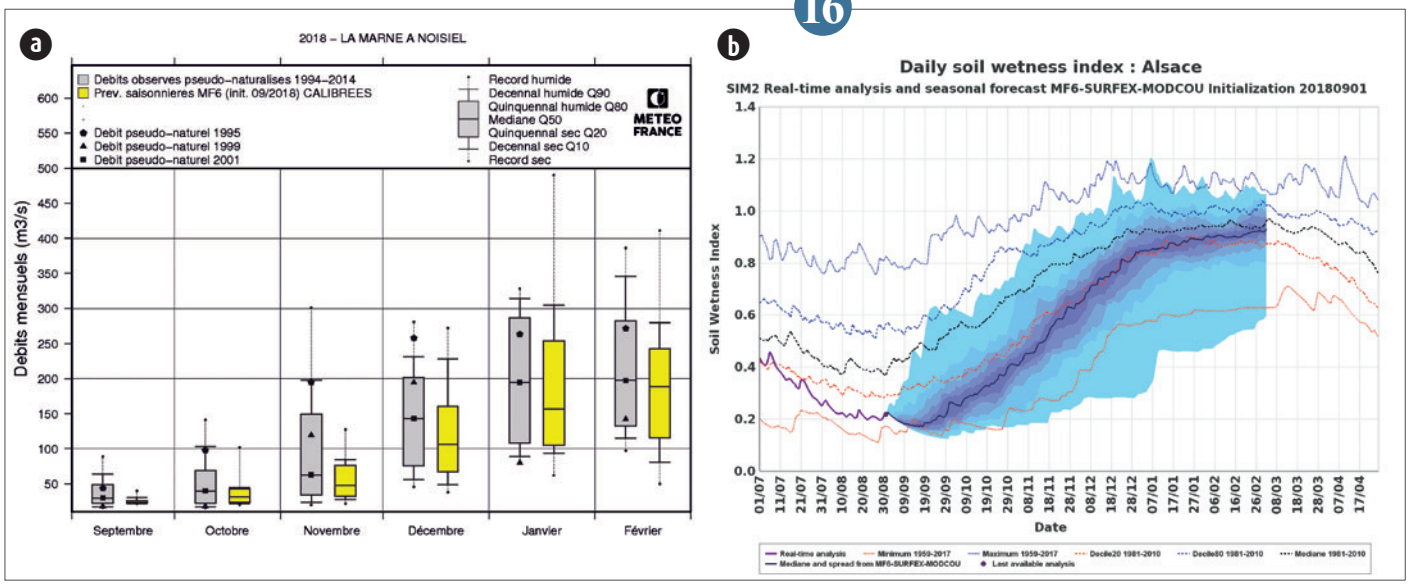

a) Seasonal forecast of monthly mean river flows at Noisiel (Marne river), initialised September 1st 2018, for the period from September to February. For each forecasting month, historical monthly means are drawn in grey (1991-2014), seasonal forecast from Météo-France System 6 in yellow. b) Seasonal forecast of soil wetness for the Alsace region, initialised September 1st 2018, for the period from September to February, from Météo-France System 6 ensemble forecast.

Chemistry, aerosols and air quality

The Copernicus Atmosphere Service (CAMS) became operational in 2015 and provides users with open and free data on the composition of the atmosphere (aerosols, reactive gases and greenhouse gases) worldwide at a resolution of 50km and on Europe at 10km. Météo-France coordinates the «Regional» operational production of CAMS (over Europe), and develops the related services based on research activities in atmospheric chemistry modelling and linked surface processes. Two MOCAGE operational chains cover Europe, one of them with assimilation, and a third one feeds the national Prév'Air platform for air quality forecasts in France together with INERIS. Météo-France is also in charge of forecasting the dispersion of dangerous and polluting species in the atmosphere over France («MOCAGE-accident» chain) but also on the Europe-Africa domain as a Regional Specialized Meteorological Centre of the World Meteorological Organisation. Another version of MOCAGE can be activated to provide information on backward plumes related to possible nuclear tests. As a Volcanic Ash Advisory Centre, Météo-France is also in charge of monitoring volcanic plumes over a large area covering continental Europe, Africa, the Middle East and West Asia as far as India.
The Institution will continue to improve its services based on advances in atmospheric composition research and models. This requires, in particular, to better understand the physico-chemical processes involved, as was the case this year, for example, on the basis of analyses of observations from the Passy-2015 campaign. Concerning online modelling, activities focused in particular on taking into account the dry deposition of gases in C-IFS-MOCAGE. Concerning assimilation, promising work shows the added-value of the Météo-France lidar network for the prediction of volcanic ashes and air quality through a quasi-operational chain running at CNRM. Finally, work completed this year has demonstrated the benefits of the new FCI imager embarked on the future MeteoSat 3rd generation satellite for the prediction of a particulate matter pollution episode.

1

Dry deposition of gases in C-IFS: towards an integrated approach

In the frame of the European program Copernicus Atmosphere Monitoring Service, CNRM contributes to the development of C-IFS model. C-IFS is the version of the operational weather forecast model IFS of ECMWF in which the chemical composition is included.
Near the surface, one of the main processes determining the concentrations of gases in the atmosphere, including pollutants with health impacts, is the so-called "dry deposition". This process corresponds to the absorption of the chemical compounds by soil, vegetation, buildings, sea water, ... It depends of the surface characteristics, the chemical compounds and the meteorological conditions. To represent this process in C-IFS, climatologies corresponding to averaged deposition were used until now. They were calculated by CNRM through the use of an independent model. Recent work done by CNRM and ECMWF has led to the implementation within C-IFS of the calculation of instantaneous dry deposition. It was tested with two chemistry schemes, C-IFS operational one and MOCAGE from CNRM. The results were evaluated over one year by comparing with measurements of dry deposition and pollutant concentrations close to the surface. The impact of the changes is positive on the dry deposition, in particular giving a better representation of the day-night variations as shown in the figure. It is of lesser importance on the concentrations since other processes act at the same time on the amount of pollutants.
This work has shown the utility to represent the instantaneous variations of dry deposition of atmospheric gases in C-IFS and also provided uncertainties associated to the dry deposition model used. This analysis will serve for future improvements.

2

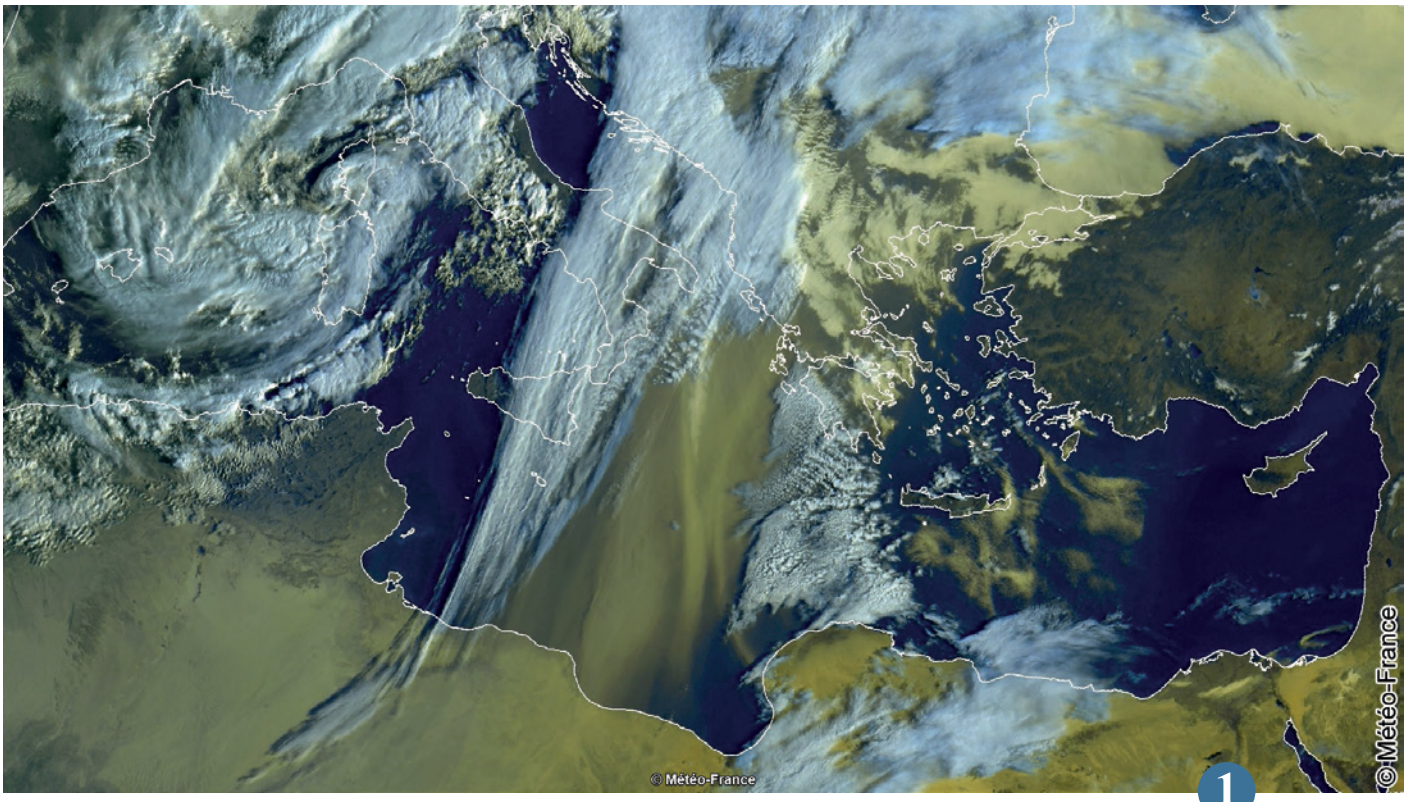

Satellite image from METEOSAT10, on 29/02/2016 at 07:00 UTC
On the eastern flank of a marked low-pressure system on Corsica, sand dust from the Sahara desert is transported to the Greek coast by strong southerly winds over hundreds of kilometres.

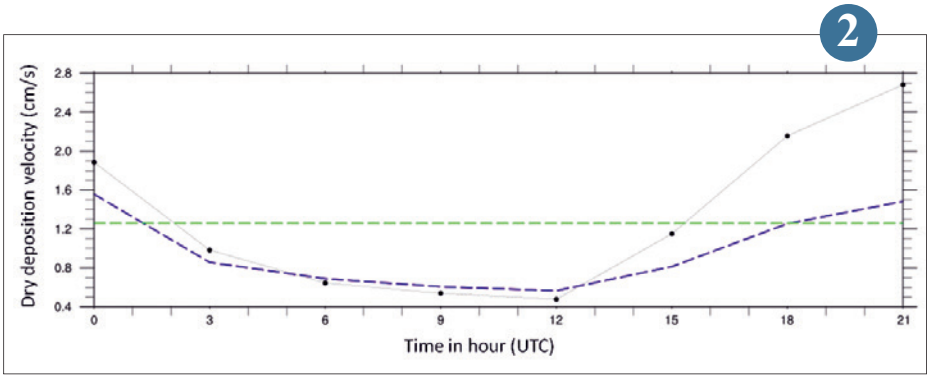

Dry deposition velocity as a function of the time of the day
Comparison between the observations at a measurement station located in USA (black dots) and C-IFS results using the dry deposition climatology (green) and those using the integrated calculation (blue).

Fine scale circulations in the Arve valley and impacts on winter air quality

Air quality issues are frequent in urbanized alpine valleys, particularly under wintertime anticyclonic conditions. Pollution episodes develop due to the combination of increased emissions and atmospheric stratification that inhibits vertical mixing and isolates the valley atmosphere from large-scale dynamics. The transport and dispersion of pollutants then become mainly driven by local thermally driven flows, which are only partially represented by NWP models.
The deployment of a scanning Doppler lidar during the Passy-2015 field experiment allowed the 3D tracking of these flows in the Passy basin (Haute-Savoie) which currently represents one of the hot spots for wintertime pollution in France. The combination of observations and high resolution numerical simulations highlighted the role of local circulation on disparities in pollutant spatial distribution. During the day, mass exchanges preferentially occur between the sunniest valley sections, leaving the shaded areas poorly ventilated. At night, the convergence of flows from tributary valleys along with local orography induces a strong sheared flow structure. All these characteristics tend to limit ventilation in the most polluted areas of the basin. In addition, snow cover plays an important role in the dispersion of pollutants by supporting the development of secondary circulation cells.
Fine scale characteristics of topography and surface conditions therefore appear to be key parameters for forecasting the dispersion of pollutants in mountainous areas.

3

Role of the Météo-France aerosol lidar network in improving volcanic ash and air quality forecasts

The assimilation of aerosol products is an important topic for Météo-France with multiple applications ranging from air quality to volcanic ash forecasting as part of the responsibilities of Météo-France as a Volcanic Ash Advisory Centre (VAAC).
Due to the eruption of the Icelandic volcano in 2010, which caused major air traffic disruptions in Europe, Météo-France decided to install a network of MPL lidars on the French territory in order to detect and quantify the transport of volcanic aerosol during a major eruption event. The CNRM has also developed a pre-operational assimilation chain capable of assimilating observations from this network in order to improve the representation of the three-dimensional distribution of different aerosol types, including volcanic ashes. Ultimately, this assimilation chain must become operational and will be used to feed the MOCAGE-Accident model during volcanic eruption events.
In order to illustrate the ability of different datasets assimilation to improve the representation of volcanic aerosol in the MOCAGE model, a simulation of a volcanic eruption on the Terceira Island (Azores) was performed. The beginning of the eruption was simulated on 28/06/2018 at 09h30. figure (a) shows the volcanic aerosol optical depth from the MOCAGE model and that from the combined assimilation of the MODIS imager with the MPL network measurements. The difference between the modelled and assimilated fields highlights the capability of the assimilation to improve the dispersion of the volcanic plume.
Another case study (realistic) related to the air quality forecasting is presented in figure (b). It shows the time series of surface concentrations of particulate matter (PM10 and PM2.5 in µg/m3) over the Guipry station (FR19008) from different products during the first 15 days of June 2018. This figure highlights the improvement in air quality forecasting in terms of PMs using the simultaneous assimilation of MODIS and the lidar MPL network.

4

What is the potential benefit of assimilating data from the future FCI imager on-board MeteoSat 3rd Generation for predicting air pollution in Europe?

The 3rd generation of MeteoSat satellites, scheduled to be launched from 2021, will provide the meteorological community with an unprecedented wealth of data. The FCI (Flexible Combined Imager) imager, aboard MeteoSat 3rd Generation, has been designed specifically for aerosol detection. As part of a thesis co-funded by Thalès Alenia Space and Météo-France, we have quantified the potential contribution of FCI to the monitoring of particulate pollution in Europe. The study focused mainly on the VIS04 channel, whose central wavelength (444nm) is the shortest of all the channels and whose fine particle detection potential is a priori the strongest.
The study consisted in developing and implementing observation system simulation experiments using the MOCAGE chemistry-transport model. From a MOCAGE reference configuration, synthetic observations representative of the FCI VIS04 channel were generated. These synthetic observations are then assimilated in another MOCAGE configuration: the differences between a simulation without assimilation and a simulation with assimilation enable to quantify the contribution of the assimilation of FCI/VIS04 data.
Figure NN thus shows the contribution of assimilation during a spring particulate pollution episode that covered Western Europe. Thanks to the assimilation of VIS04 channel data, surface particle concentrations are significantly increased and are closer to the reference. The assimilation of FCI/VIS04 improves the representation of the intensity and spatial extent of the pollution episode.
This work allowed to identify the potential of the future FCI imager and thus to prepare us to assimilate this future data into Météo-France models as soon as they arrive.

5

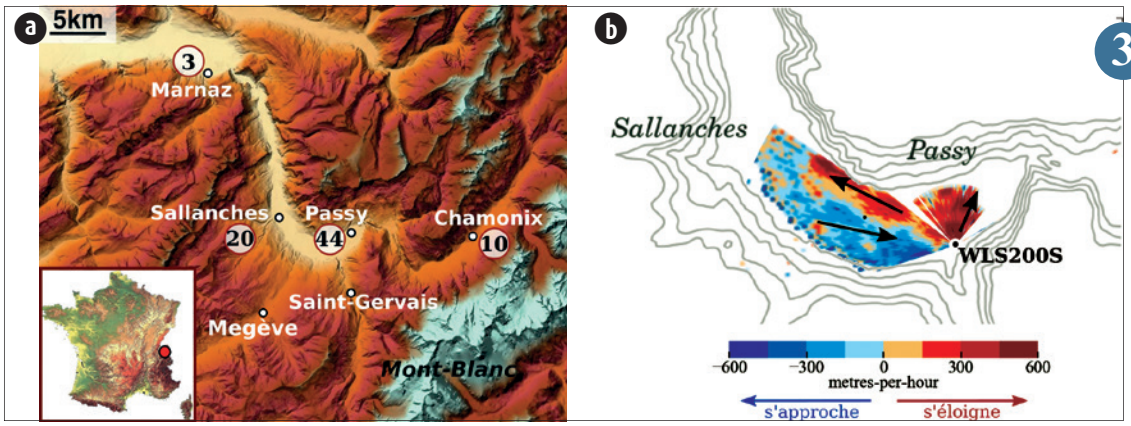

a) Location of the main towns in the Arve valley with the billhook like shape Passy basin in the centre of the figure. The annual numbers of days exceeding the regulatory daily PM10 concentration threshold are indicated in the circles, the critical value not to be exceeded being 35 days/year (data provided by Atmo Auvergne Rhône-Alpes).
b) Daily averaged radial velocity field determined from the scanning Doppler lidar (WLS200S) during anticyclonic conditions typical of wintertime particulate pollution episodes.

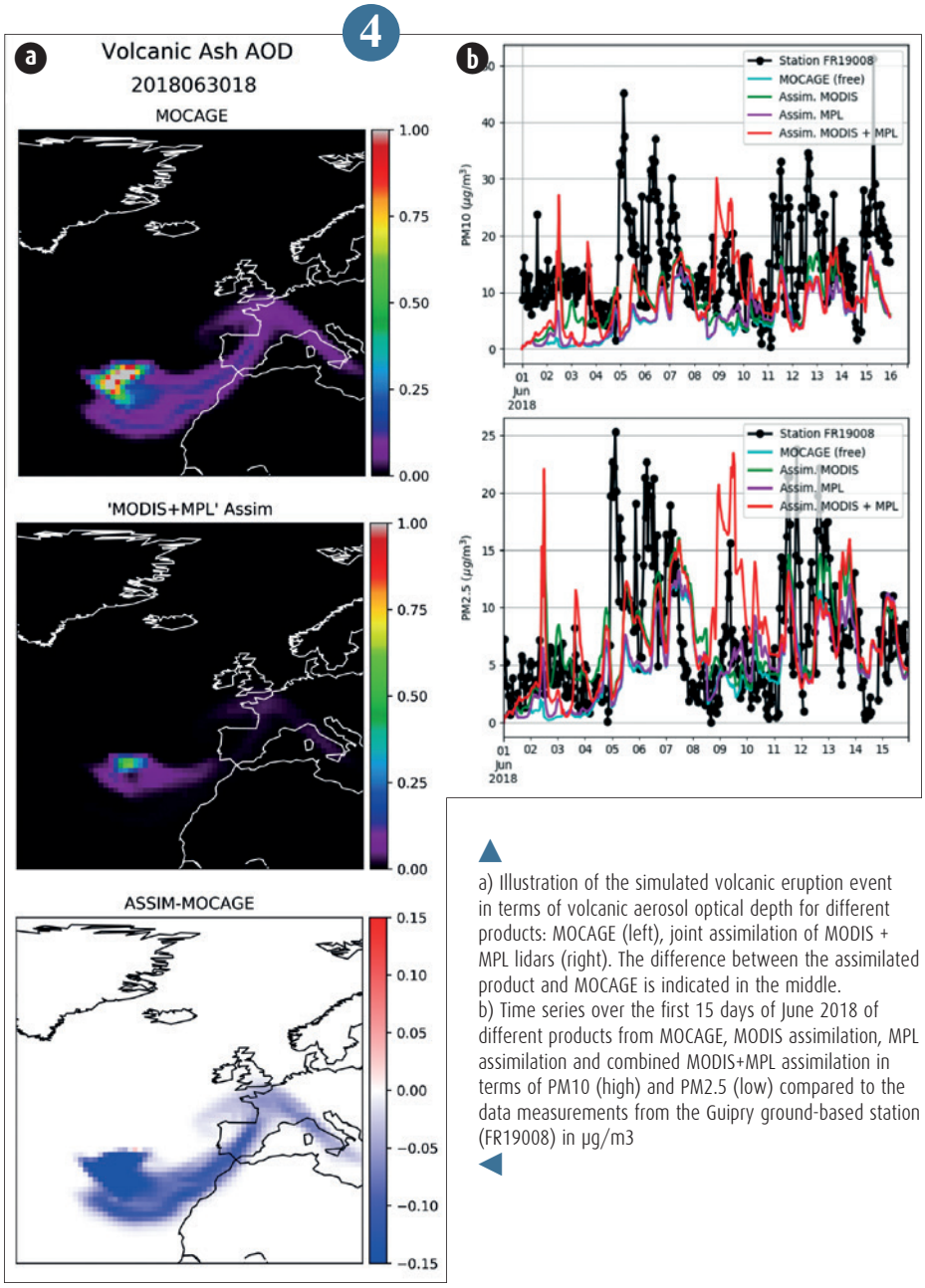

a) Illustration of the simulated volcanic eruption event in terms of volcanic aerosol optical depth for different products: MOCAGE (left), joint assimilation of MODIS + MPL lidars (right). The difference between the assimilated product and MOCAGE is indicated in the middle.
b) Time series over the first 15 days of June 2018 of different products from MOCAGE, MODIS assimilation, MPL assimilation and combined MODIS+MPL assimilation in terms of PM10 (high) and PM2.5 (low) compared to the data measurements from the Guipry ground-based station (FR19008) in µg/m3

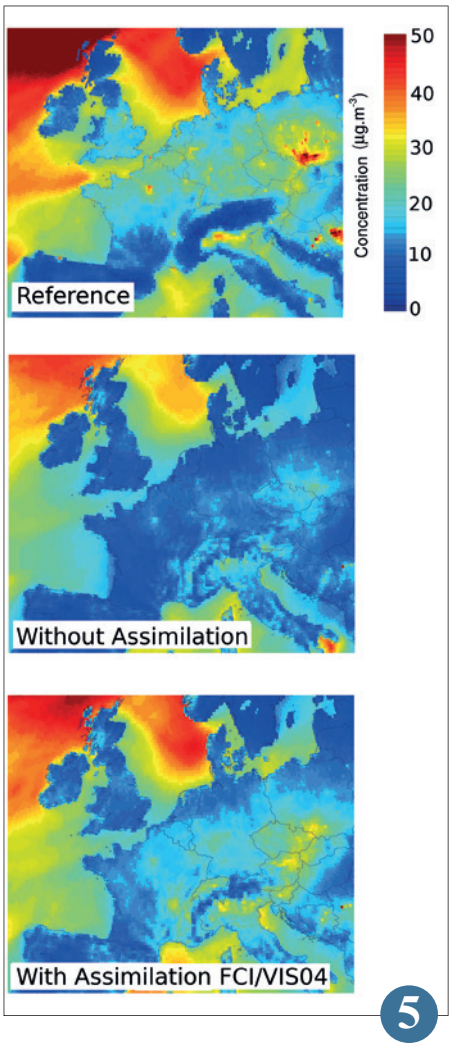

Average concentration (in µg.m^{-3}) of fine particles (less than 10 microns in diameter, PM10) during the pollution episode from 6 to 15 March 2014 Top: Reference MOCAGE simulation, from which the synthetic FCI/VIS04 satellite observations are derived for assimilation. Bottom: MOCAGE simulation without (left) and with (right) assimilation of FCI/VIS04 observations. The assimilation gets closer to the reference and thus significantly improves PM10 concentrations.

Snow

Snow on the ground is one of the most fascinating materials on Earth. It plays a key role in the functioning of the climate system, with a pivotal role for the regulation of water availability at the regional scale. In mountain regions, snow governs ecosystems functioning and has wide ranging implications for socio-economic systems in the energy (hydropower), agriculture and tourism sectors. Natural hazards, such as avalanches or floods, directly or indirectly stem for the state of snow on the ground.
Météo-France, in particular the Snow Research Center (CEN, Météo-France – CNRS, CNRM), carries out research activities to better understand and predict the evolution of snow at various time and space scales, especially in mountains. In 2018, several major advancements were achieved, disseminated and transferred into operational services. The model SYTRON, built on top of the operational mountain snow prediction system, explicitly accounts for blowing snow impacts in the mountains. It was thoroughly described and evaluated in a scientific publication, and model results are now provided in real time to operational divisions. Data assimilation plays a growing role on snowpack modeling, where it helps to reduce the effects of prediction errors, either due to errors in the estimation meteorological conditions or snowpack modeling errors. A new milestone was achieved in 2018, with the development of a system for data assimilation of optical satellite data in the Crocus snowpack model, thereby confirming the potential of this approach, as long as complex terrain effects are duly accounted for. CEN has coordinated an international study to evaluate various tools using cone penetration tests to characterize snow physical properties. This work was complemented with a detailed study on the microscopic and macroscopic behavior of snow, combining material physics, signal-processing and in-situ and laboratory experimental work.

1

Analysis of snow profiles measured by digital penetrometers

The cone penetration test consists in measuring the force required to vertically drive a rod with a conic tip into the studied material. It is commonly used to characterize snow vertical heterogeneity, for instance by the observers reporting snow conditions to the avalanche forecasters of Météo-France.
Nowadays, digital penetrometers such as the SnowMicroPenetrometer can measure snow penetration strength at a very high vertical resolution. The measured strength fluctuations contain a valuable information about snow microstructure. Recovering this information requires an inversion model and knowledge about the involved mechanisms. A common assumption is to consider that macroscopic strength results from the brittle failure of bonds between snow grains. Based on this assumption, we proposed a new inversion model which considers the penetration profile as a non-homogeneous Poisson process and which is able to account for the transient penetration regime (Fig. a). To evaluate the main model assumptions, we conducted experiments that consisted in imaging the 3D structure of snow samples by X-ray tomography before and after a penetration test (figure b). We were able to relate the grain contact density measured by tomography to the one derived from the resistance signal. In addition, using grain tracking and image correlation methods, we reconstructed the deformation field induced by the presence of the cone (figure b) and thus determined how the extension of the plastic zone depends on the snow type.
In the future, these studies should make it possible to derive, in an objective way, the stratigraphy of the snowpack from a simple and fast field measurement.

2

Assimilation of visible satellite images (MODIS) for ensemble numerical simulation of the snowpack

Météo-France is operating a snowpack modelling system in support to avalanche hazard forecasting at the scale of the French mountain ranges. However, these simulations suffer from numerous errors and uncertainties which limit their use by the forecasters. In order to mitigate these errors, a twofold approach is being developed: use of ensemble modelling, to account for those errors, and satellite data assimilation to reduce them. To that end, the use of MODIS images (visible/near infrared) is under investigation.
Indeed, these data allow to monitor every day (for cloud free conditions) the snowpack surface properties at high resolution (250m) suitable for mountainous areas, and thus to better constrain model state variables of the snowpack model Crocus, such as light absorbing particles content and specific surface area, which is related to the surface snow type. In order to evaluate the potential impact of assimilating such data, a comparison of time series from the ensemble simulation and MODIS observations was carried out for winter 2016-2017 in the Grandes-Rousses massif (Central French Alps) (figure 1). High correlations (0.7-0.9) are noted between these time series, which are strongly influenced by the snowfall chronology. However, a strong negative bias for MODIS data (identified by a comparison with Sentinel 2 data), prevents from directly assimilating them. Computing ratios of reflectance in several MODIS bands can be used to circumvent this bias. This could allow to take advantage of the wealth of information content in the observations while coping with the raw data bias. For that reason, we are confident that MODIS data assimilation in Crocus model will become possible and efficient in a near future.

3

1

Observation site of “Col de Porte”.

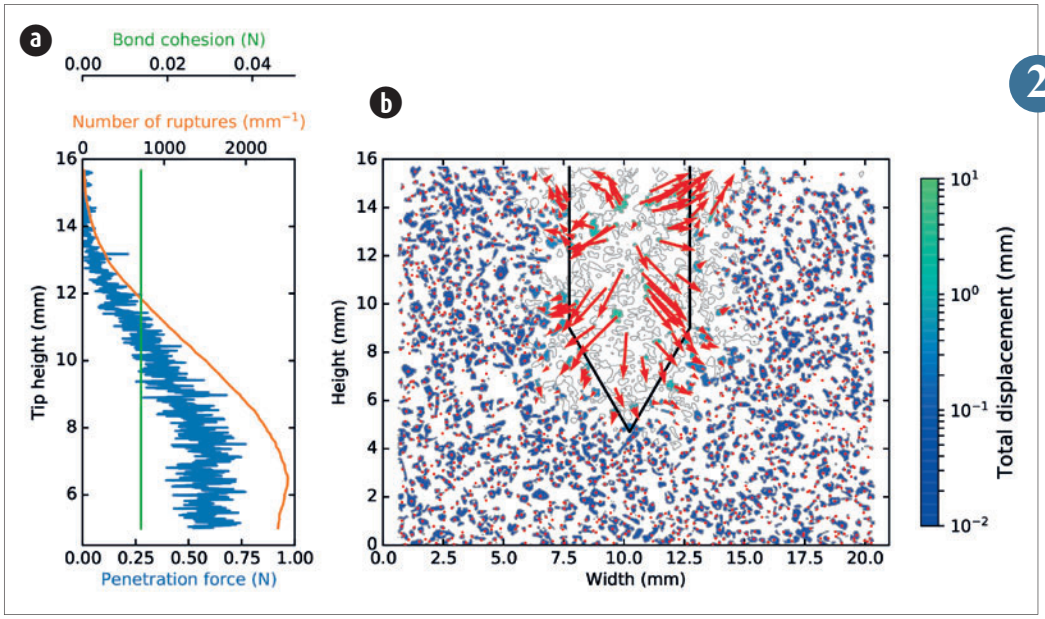

2

A cone penetration test in a snow sample composed of rounded grains:
(a) penetration strength profile and, as obtained by our model, its inversion in terms of microstructural bond strength and number of ruptures per millimeter;
(b) sample microstructure measured before the cone test (black contour) and the displacement field (color and arrows) induced by the cone, measured by X-ray tomography. For some grains (colored in white), the displacement was not measurable.

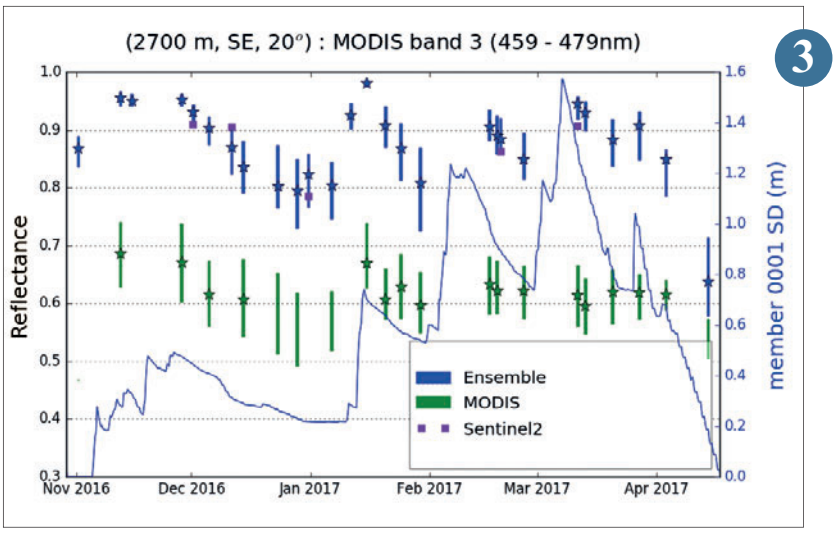

3

Time-series of snowpack reflectance (460nm) simulated by the ensemble (quartiles in blue, stars for medians) and observed by MODIS (same, in green) and Sentinel2 (medians in purple), together with the Snow Depth (SD) simulated by the first member of the ensemble (blue curve) in Grandes-Rousses mountain range, at 2700m, South- East aspect and 20 degrees slope, during 2016-2017 winter..

Development of an operational system for blowing snow forecasting in mountainous terrain (SYTRON)

Blowing snow transport strongly influences the evolution of avalanche hazard and must be taken into account by avalanche hazard forecasters when preparing their daily bulletin. To improve blowing snow forecasting, an operational system, named SYTRON, that explicitly simulates blowing snow in mountainous terrain, has been deployed at the beginning of winter 2016/2017. It provides the forecasters with complementary information to the existing operational system for avalanche hazard forecasting SAFRAN-SURFEX/ISBA-Crocus-MEPRA.

SYTRON simulates the evolution of the snowpack over the different French mountain ranges. It combines information on wind intensity and direction with simulated physical properties of surface snow, to determine the occurrence of blowing snow and the amount of snow redistributed by the wind between different slopes. SYTRON provides forecasts for the next 48 hours for each mountain range of the French Alps, Pyrenees and Corsica. These forecasts are available in 300-m elevation steps for a variety of aspects. Daily-updated synthesis graphics for each mountain range are provided to the forecasters (see figure.).

Performances of SYTRON were evaluated for winter 2015/2016 using 11 stations measuring blowing snow fluxes in the French Alps. SYTRON provides a satisfying estimation of blowing snow occurrence at the regional scale with a low rate of false alarms. The increase in resolution of the future system for snow and avalanche hazard forecasting will allow a more accurate representation of the strong spatial and temporal variability of wind-induced snow transport in the French mountains.

4

Example of visualization of data from the modelling system SYTRON provided to the avalanche forecasters for the Vanoise massif (French Alps) on February 9 2016. This figure represents, for the four main aspects (North, East, South and West), the evolution of wind for each 300-m elevation step over a 72-hour period: 24 hours of analysis before February 9 06 UTC, and 48 hours of forecasting after this date. Blowing snow intensity is represented by a colour code on a four-level scale (erosion: red, accumulation: blue).

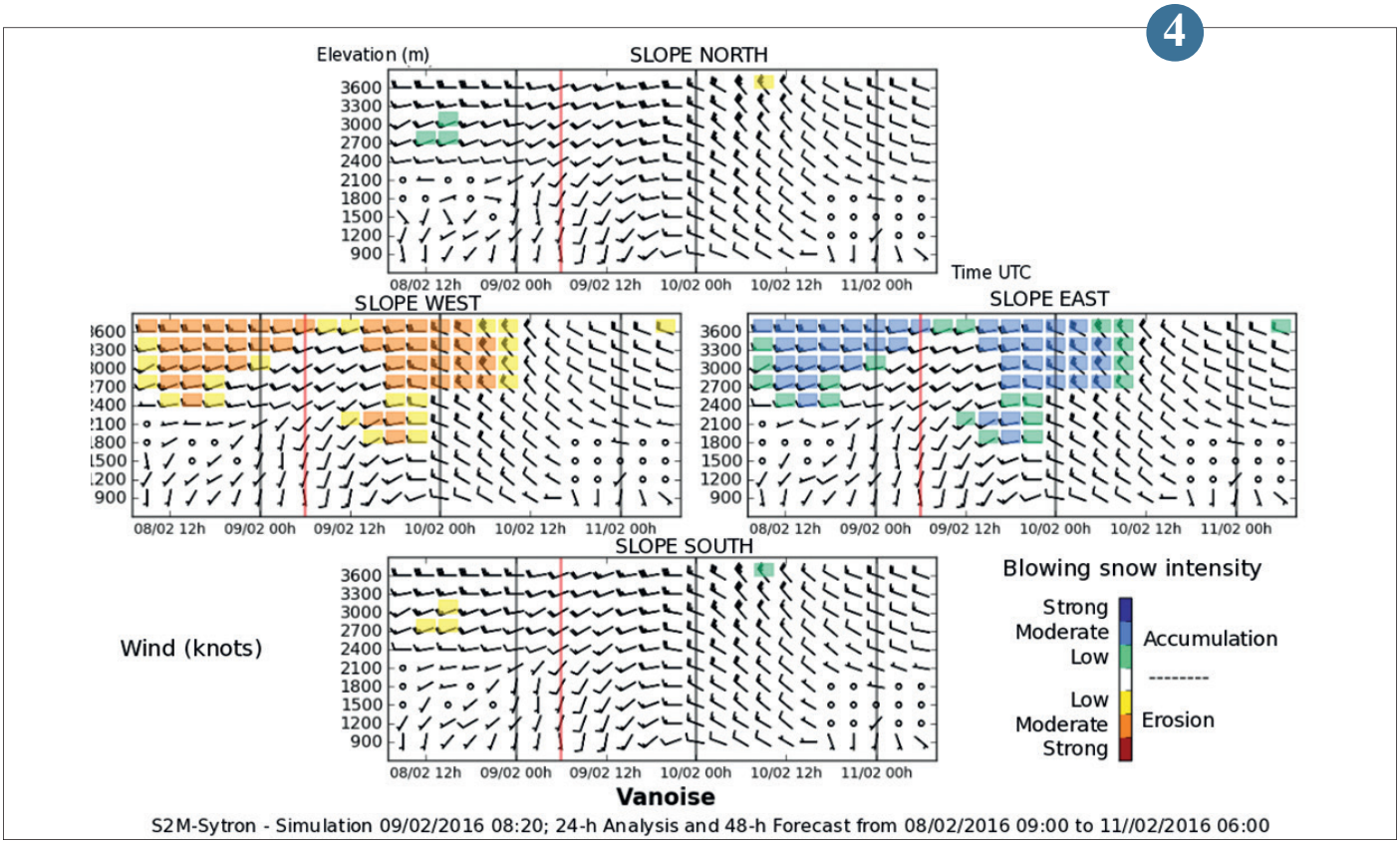

Oceanography

Ocean and atmosphere interact at all time and space scales. Extreme events with strong impact on human activities occur at the interface, where air and water concur to create storms or cyclones. Their coupling is also at stake to impose slow variations of the Earth climate, for which ocean is the slowly varying component.
In order to predict such events, detect trends, analyse their governing processes, considering the surface is not enough. One must have the head in the sky and the feet deep inside the oceans!
This is the reason why Météo-France works hand-in-hand with its partners in order to improve our understanding and the knowledge of the marine environment, the air-sea and ocean-land interfaces. In geosciences, observation and numerical modelling are the key approaches to get a deep insight into the system.
Surges, hurricanes, extreme sea states, storms are words with a meaning not only for mariners and sea operators, but nowadays with a meaning to every citizen. Each new meteorological event raises questions regarding the climate drift. Thermohaline circulation, water warming, reference measurements are other words that appear in the hereinafter papers: They show that the meteorologists do consider the planet with its complexity, just like the "Earth system".

1

1

▲
Waves and strong sea: West coast near the tip of Castagna, south of the Gulf of Ajaccio.
© Lapujade Alain - Météo-France

Storm surge forecast for the Lesser Antilles and Guyana

As part of the HOMONIM project, managed by Météo-France and SHOM, with the support of DGPR and DGSCGC, the hydrodynamic surge prediction model that turns on an area including the Lesser Antilles and Guyana has been improved during 2018. The new version of this model incorporates a more powerful barotropic solver and a new bathymetry with 500 meters resolution specially developed by the SHOM. It also includes a new computation of wind stress, now based on a parameterization of Pond and Pickard, more adapted to the extreme wind conditions existing in hurricanes.
The recordings of the two tide gauges of Marigot/Saint-Martin and Barbuda during the hurricane were used, as well as the wind and pressure forcing data of the AROME "Tropics" atmospheric model of the 5th September 2017 at 18 hours, to optimize the calculation of the source term due to wind in such cyclonic conditions. The figure shows the significant improvement in the calculation of the surge at Marigot by the new version of the model. This improvement in calibration of the model was made possible by the existence of exploitable measurements and also by a very faithful atmospheric model replay obtained with "AROME tropics", even if the maximum wind remains underestimated and the pressure in the center of the cyclone a little overestimated.

2

Using a model climatology for extreme waves diagnostics

We study the sensitivity of the forecast of strong waves affecting the Atlantic coast of Western Europe, sometimes leading to very significant retreats of the coastline.
When a wave model predicts an event of such intensity, the associated uncertainty must be documented. In this study, we study the behaviour of the MFWAM wave model, forced by the 35-member global atmospheric ensemble model PEARP. A hindcast database of MFWAM forced by PEARP is available over a 10-year period. Thanks to this reference also called climatology of the model, it is possible to compare the distribution of the values of the different members of a wave set forecast with the distribution of the values of the climatology to measure the unusual character of this forecast.
This calculation of the so-called Extreme Forecast Index (EFI) is particularly sensitive to the sampling of the climatology set up. In the case of the Eleanor storm of January 2, 2018, we show the impact on EFI of two model climatology set up, with two hindcast frequencies, 1 and 4 days, and the addition or not of a record winter 2013-2014.
On the figure, we can see very high values of EFI calculated for a frequency of 4 days and without the record winter. When the frequency of climatology is increased to 1 day and once winter 2013-2014 is added to the climatology, EFI values are significantly reduced to a ratio of 10%. Highest EFI values are more localized and more relevant in terms of expected impact.
In the case of extreme events, the use of a climatology of a probabilistic model improves the information produced by the forecast, all the more so if we maximize the representativity of this climatology.

3

Assimilation of new satellite data in wave models

To ensure continuously improvement of the operational sea state forecast of Météo-France, the assimilation of wave data in the model MFWAM is updated regularly with the arrival of new wave observations. The use of these satellite wave data contributes significantly to correct misfit induced by wind forcing from the atmospheric system.
Since May 2018 the altimetry mission Sentinel-3A (S3A) of the Copernicus Space Program has been implemented operationally in the assimilation system. This induces better global data coverage over the ocean basins. The model MFWAM assimilates significant wave heights from the altimeter S3A for global and regional configurations dedicated to overseas and Europe. In 2019, Sentinel-3B will join the altimetry constellation and thus enhance the improvement of wave products provided to the Copernicus Marine Service (CMEMS).
Since the launch of the France-China satellite mission CFOSAT on 29th October 2018, the assimilation of new wave data from the instrument SWIM has been implemented in the frame of the Calibration/Validation phase. The SWIM instrument provides both the significant wave height from nadir and the directional wave spectra from several incidence angles on the ocean surface. Such directional wave observation is highly requested in order to improve the swell directional properties.
The first results of the assimilation are very promising and show a significant impact on the integrated wave parameters describing the sea state in the periods of analysis and forecast, as illustrated in figure. During the verification phase of CFOSAT mission, the SWIM instrument will be calibrated and the level 2 data processing will be upgraded to retrieve a better quality of the observed wave spectra. This will reduce the rejection of wave spectra in the assimilation process and therefore improve the impact of the model analysis.

4

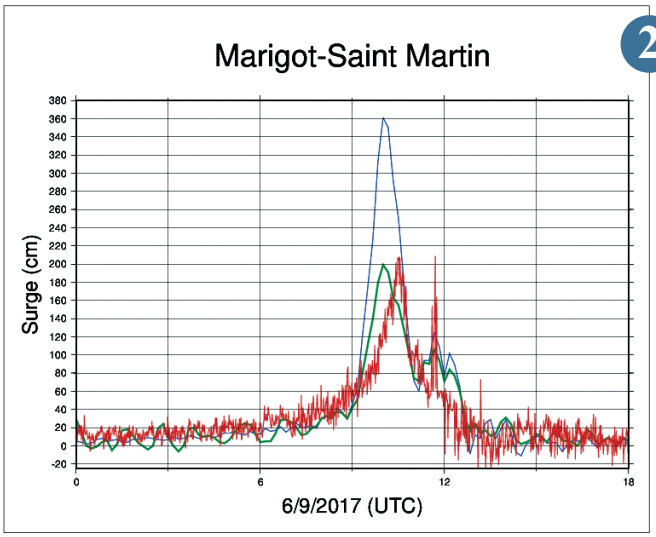

2

Comparaison entre la surcote mesurée (trait rouge)
et la surcote modélisée (trait bleu pour l'ancienne version, trait vert pour la nouvelle version)
à Marigot (nord de Saint Martin dans les Petites Antilles)
pour le 6 septembre 2017, jour du passage d'Irma.
Les deux versions du modèle sont ici forcées par le vent et la pression atmosphérique
de surface au pas de temps horaire du modèle AROME Tropiques de Météo-France
du réseau de production du 5 septembre 2017 à 18 h UTC.

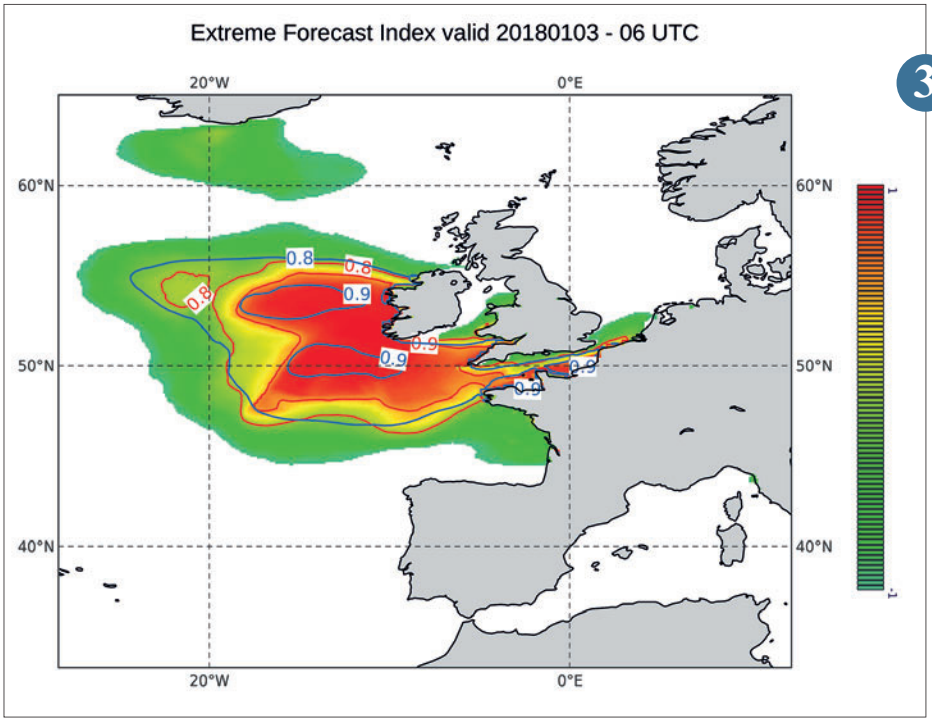

3

Color shadings show Extreme Forecast Index values
(between -1 and 1). Red contours correspond
to 0.8 et 0.9 EFI values with a climatology
with hindcast every 4 days
and without winter 2013-2014.
Blue contours show the same EFI values
but with a 1day-climatology and with winter 2013-2014.

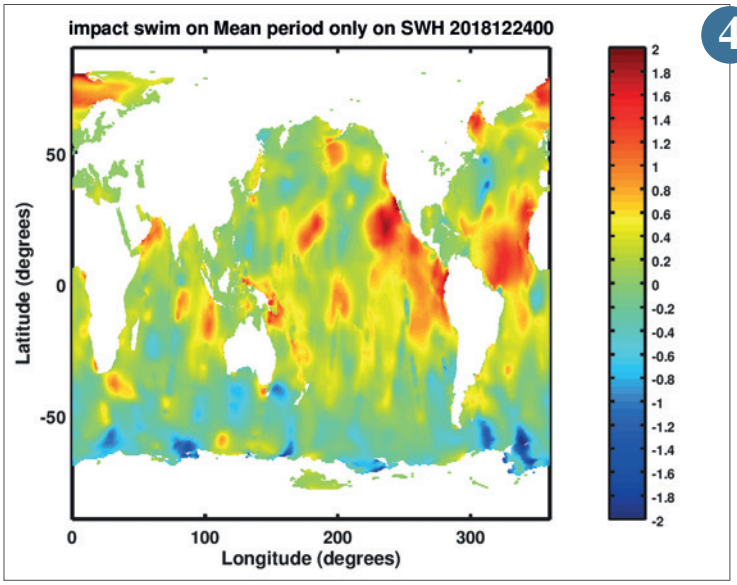

4

Difference of mean wave period (in seconds) from runs of the model MFWAM
with and without assimilation of CFOSAT wave data
on 24 December 2018 at 0:00 UTC.
Negative and positive analysis increment values
indicate an overestimation and underestimation
of mean period, respectively.

Where does the sinking of the Mediterranean Thermohaline Circulation take place?

For more than half a century, scientists have shown the presence of a so-called thermohaline circulation in the Mediterranean Sea, similarly to the global ocean. This circulation, referred to as the "oceanic conveyor belt", is activated by density gradients of seawater, which is of temperature ("thermo") and salinity ("haline". At the global scale, it plays a major climatic role by transporting heat poleward. If its magnitude were to decrease, its role of climate buffer would also be reduced.

The Mediterranean Sea warming, observed since the 1950's, has recently accelerated in higher proportions than the global ocean and has been accompanied of a salinization of its deep waters. It is therefore crucial to analyse its sensitivity to global warming and to understand its circulation, and in particular the location of the scarce convection areas, that is the sinking areas according to the historical vision.

Our team combined outputs from a Mediterranean Sea model and observation off the French coast to determine where and how this sinking occurs. The sinking was found to occur near the coast, away from convection areas which are predominantly offshore. We identified new key areas of sinking off the French, Libyan, Egyptian coasts and in the Aegean Sea, some of which are very distant from convection areas. The physical analysis shows the key role played by the Earth's rotation, which prevents any sinking from occurring away from the coast. This constraint, as old as our

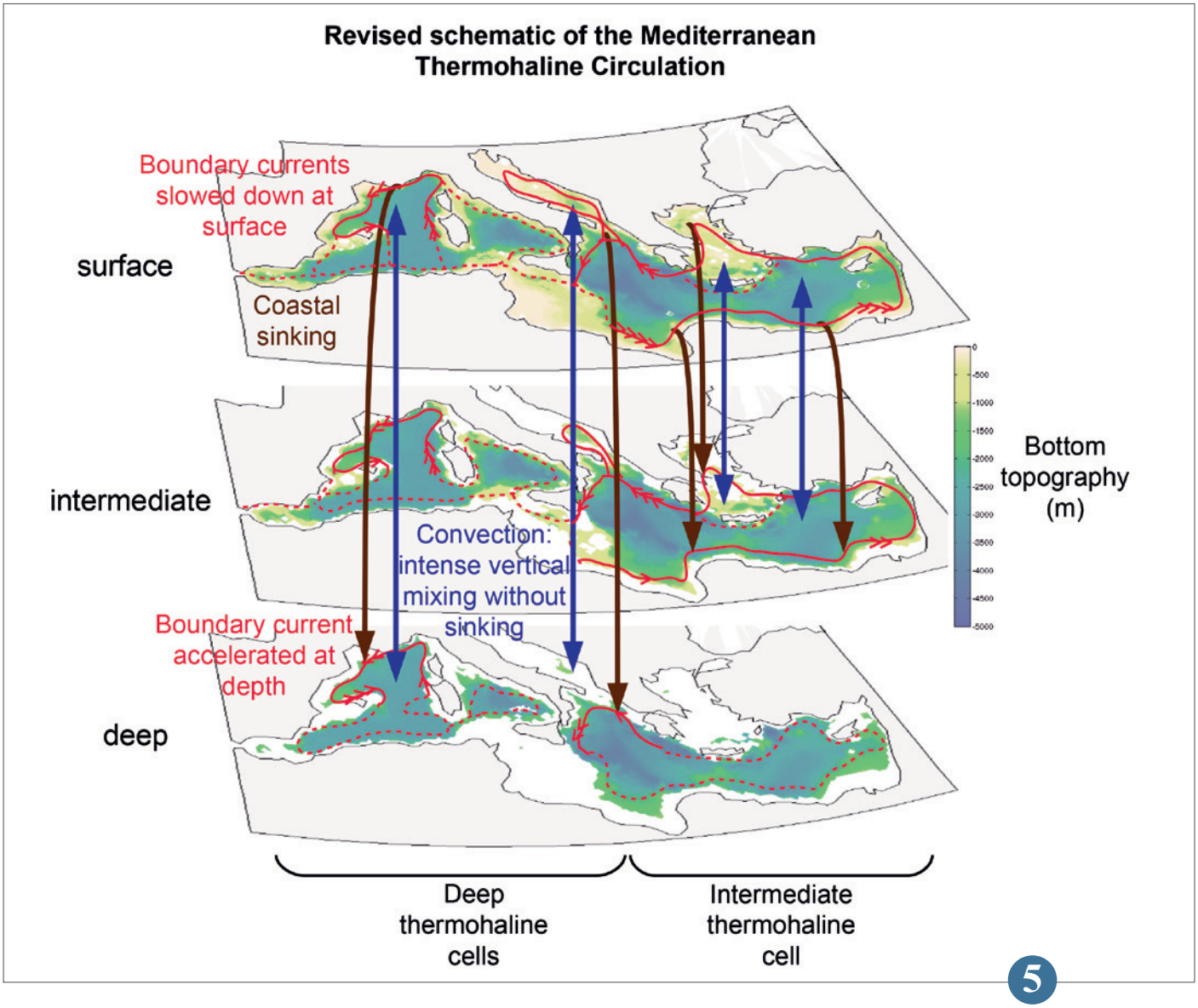

5

Revised schematic of the Mediterranean thermohaline circulation
Due to surface water and heat exchanges, the Mediterranean Thermohaline Circulation is characterized with a surface incoming and an outgoing at depth of its only open straits with the global ocean: Gibraltar Straits. Convection areas, historically seen as the sinking regions of this circulation, are actually only a location of intense vertical mixing between surface and deep water masses. Reversely, boundary currents are present almost throughout the basin and interact with the boundary and are the main sinking area. Thus, while boundary currents deepen, they weaken at surface and intensify at depth. We only present here the three main thermohaline circulations, two deep and one intermediate, the remaining circulation (dashed) is not detailed.

planet, implies that convection areas will never experience sinking, contrary to the former prevailing vision. Thus, our results replace the traditional vision of a “conveyor belt” sinking at convection areas by that of a “coastal sinking ring”.

5

Next-generation drifting buoy for Fiducial Reference Measurements of Sea-Surface Temperature

The 2016 launch of the first Copernicus satellite in the Sentinel-3 series inaugurated a new era: the monitoring of sea-surface temperature with unprecedented accuracy and resolution. The on-board radiometer was built under stringent specifications, exceeding previous attempts. Reaching the expectations for the retrievals from the radiometer measurements requires, in turn, advancing the in situ observing systems that are used in the process of calibration and validation.

A next-generation drifting buoy has been developed within the framework of a Copernicus project initiated by EUMETSAT. The buoy relies on the international standard for Lagrangian drifter with barometer. In addition, it carries a sea-surface temperature reference sensor that also measures the sensor immersion pressure. Hourly data, collected within minutes via the Iridium constellation, also contain information about the sea-surface variability.

The major innovation is to establish links to the calibration chain, at four steps during the buoy life-cycle. The sensor is calibrated in a metrology laboratory. After sensor integration in the buoy, the buoy is verified by the same laboratory. When the buoy is deployed at sea, a measurement is made by another precision instrument, which is regularly calibrated in laboratory. Finally, when the buoy is recovered at end-of-life, the sensor is verified again in laboratory to estimate any potential drift.

Even if not all buoys will undergo all these steps (only the first one is mandatory), this protocol will allow one to establish whether or not these buoys can be qualified to deliver Fiducial Reference Measurements. Two prototypes have been deployed so far, and a further 100 units will be deployed by 2021.

6

6

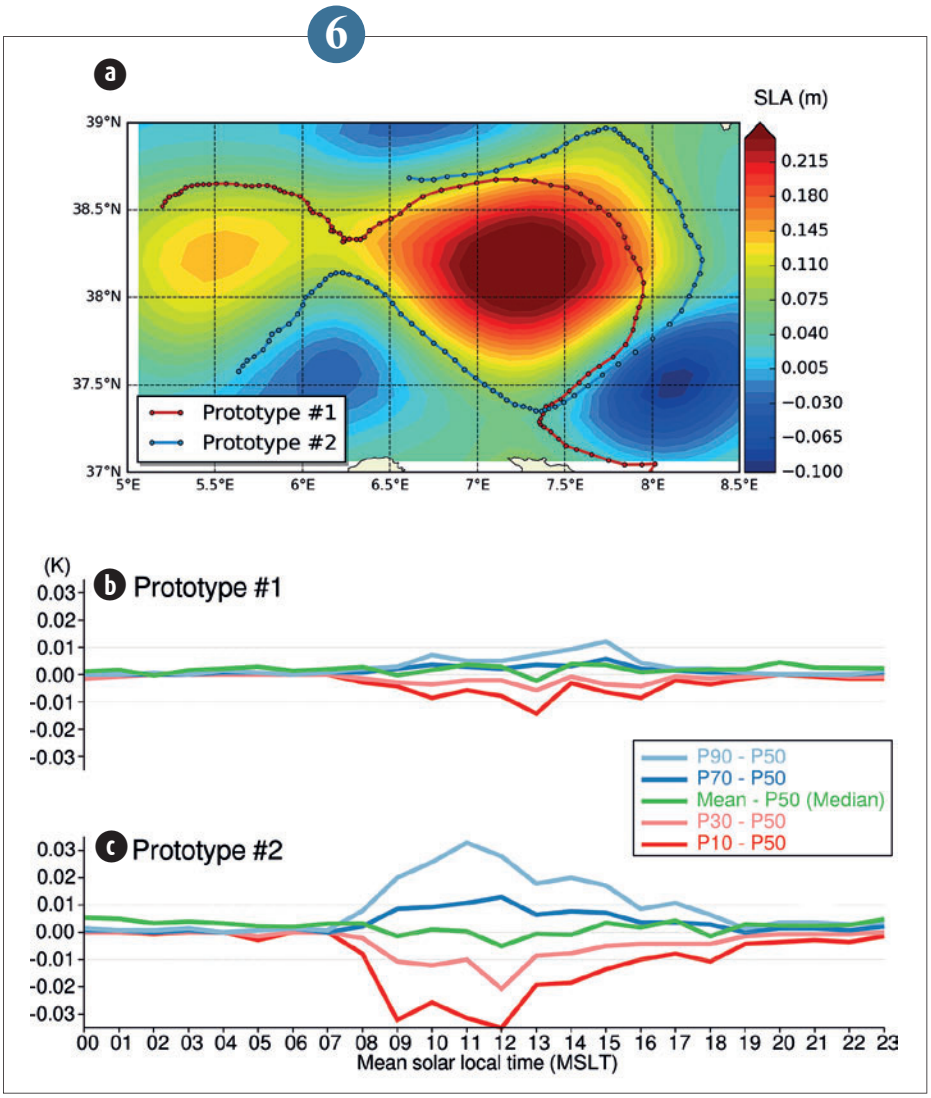

a) Tracks of the two prototype drifting buoys between 29 May 2018 and 13 June 2018 in the Mediterranean Sea overlaid on a mean sea-level anomaly map over the same time period.
b) Over the same time period, mean departures between percentiles from the distribution of 5-minute measurements sampled at 1 Hz and the median of the distribution, as a function of mean solar local time, for the first buoy.
c) Same but for the second buoy. The first buoy drifts in the vicinity of vortices, where the surface waters are well-mixed, whereas the second buoy travels farther away from vortices ; the distributions of sea-surface temperatures that are then observed indicate a more vertically stratified surface (given that the buoys oscillate, so the temperature sensors sample various levels underneath the surface). These differences matter when using the drifter data for cal/val of the satellite radiometer retrievals.

Engineering, campaigns and observation products

The prediction of clouds and precipitation is a challenge for weather services. With a size smaller than the resolution of models, clouds implement highly non-linear processes. Predicting the physical characteristics of clouds, their effect on the solar radiation, where, when and how much they produce rain or hail, is very difficult. This can be yet a crucial matter as the flush floods in the Aude region in October 2018 dramatically remind us. This is why research studies are conducted. They improve our ability to characterize clouds at global scale from space, or provide detailed measurements inside a cloud with Unattended Aerial Vehicles that follow it while it is moving, or give information on their electrical activity that can now be observed operationally and can be assimilated. The amount of precipitation can be monitored in real time with an increasing accuracy from real time observations of operational radars.
In 2018, Europe launched successfully the first satellite able to measure wind profiles all over the world, from the surface to the stratosphere. Called AEOLUS, the satellite should improve weather forecasts, in particular in the Tropics. Several satellites (MERLIN, MicroCarb, IASI-NG) will be launched by France and Europe in the coming years that can measure the concentration of greenhouse gases. Field campaigns are carried out in order to prepare these missions. They also provide useful information for the evaluation of air quality models.
More and more opportunity data are acquired by connected sensors. A new, original example is given with environmental sensors mounted on turtles by a marine biology center of La Réunion Island in the Indian Ocean. They should provide low-cost, useful observations at the interface between the ocean and the atmosphere in a region where cyclones are developing.
The acquisition of measurements by radiosondes, while the falling, has been practiced for a long time by researches. It is now becoming a reality in operational observation networks. This will improve the benefit of radiosondes to weather forecasts at a negligible cost.

1

Observation engineering and products

Improving observed radar accumulations by using simulated vertical profile of reflectivity from the AROME model

Estimating rain rate at the ground level from the reflectivity measured aloft by radars remains a serious challenge.
Today, to produce the operational radar accumulation Panthere, this evaluation is made through a simplified vertical profile of reflectivity determined from the radar volume scan and used indifferently over the entire radar domain. This technique shows its limits especially when the vertical structure of precipitation is very variable in the area (ex: upstream or downstream of a front).
The method proposed takes advantage of the fields produced by the nowcasting numerical weather prediction model AROME-NWC and in particular its ability to simulate more realistic precipitation profiles. The method allows in particular to consider different precipitation profiles at each point of the radar domain. In the vicinity of each radar pixel, the observed reflectivity data are compared to a set of simulated profiles (from +3h lead time). The precipitation rate associated with the simulated profile most in agreement with the observations is selected and used in the calculation of the accumulation.
First results obtained on March 3, 2017 rainfall episode are very promising (cf. figure). The 6-hourly accumulation estimates obtained with the new method are in much better agreement with the rain gauges than the current product. The use of AROME-NWC model profiles makes possible to better represent the evaporation of precipitation (virgas) under the radar beam at the East of the domain as well as the higher accumulations observed near the Pyrenees.
The next step will be to adapt the method to mountainous areas where the masks are more important and the variability of precipitation profiles is even greater than in the plains.

2

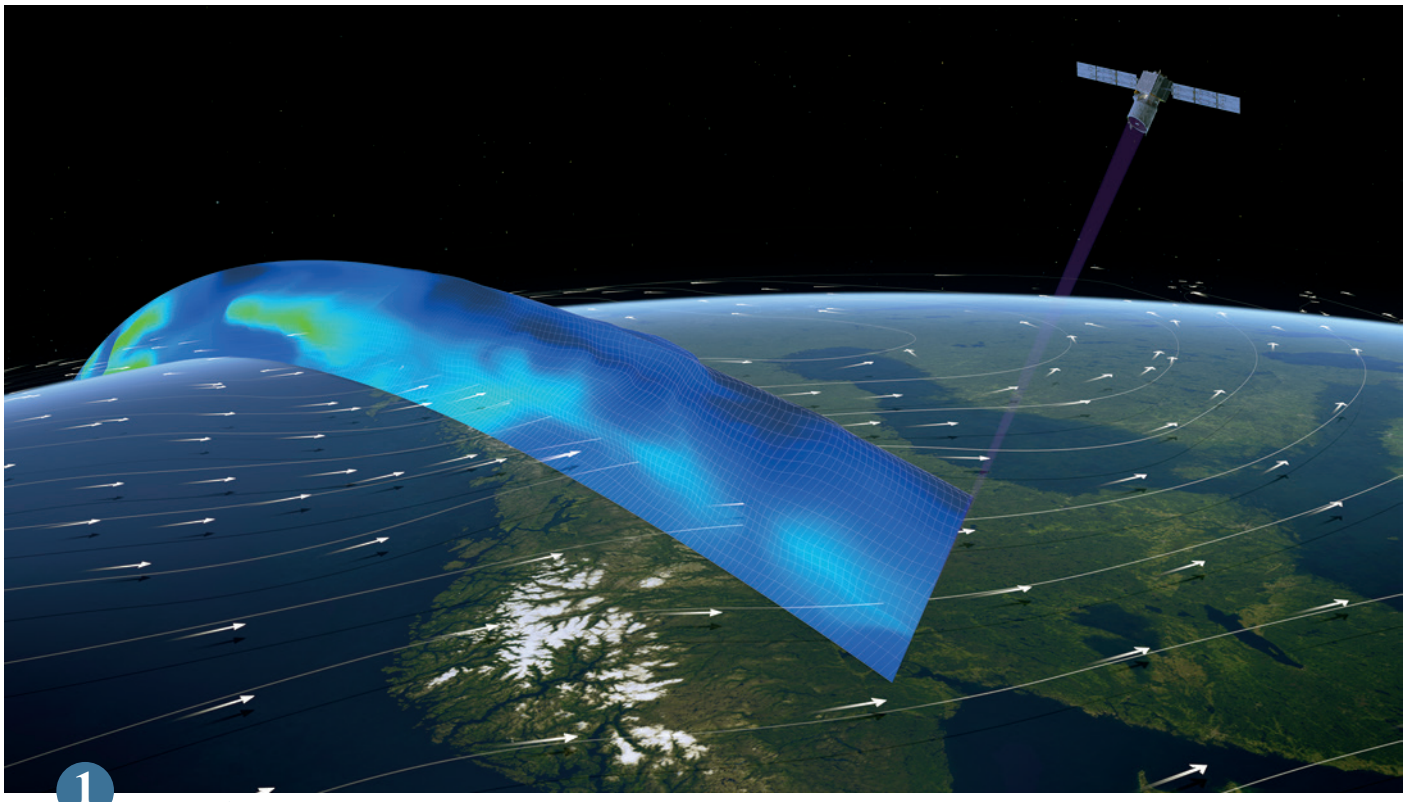

1

Artist view of the space borne wind lidar AEOLUS (launched on the 23rd of August, 2018) probing the atmosphere. © ESA

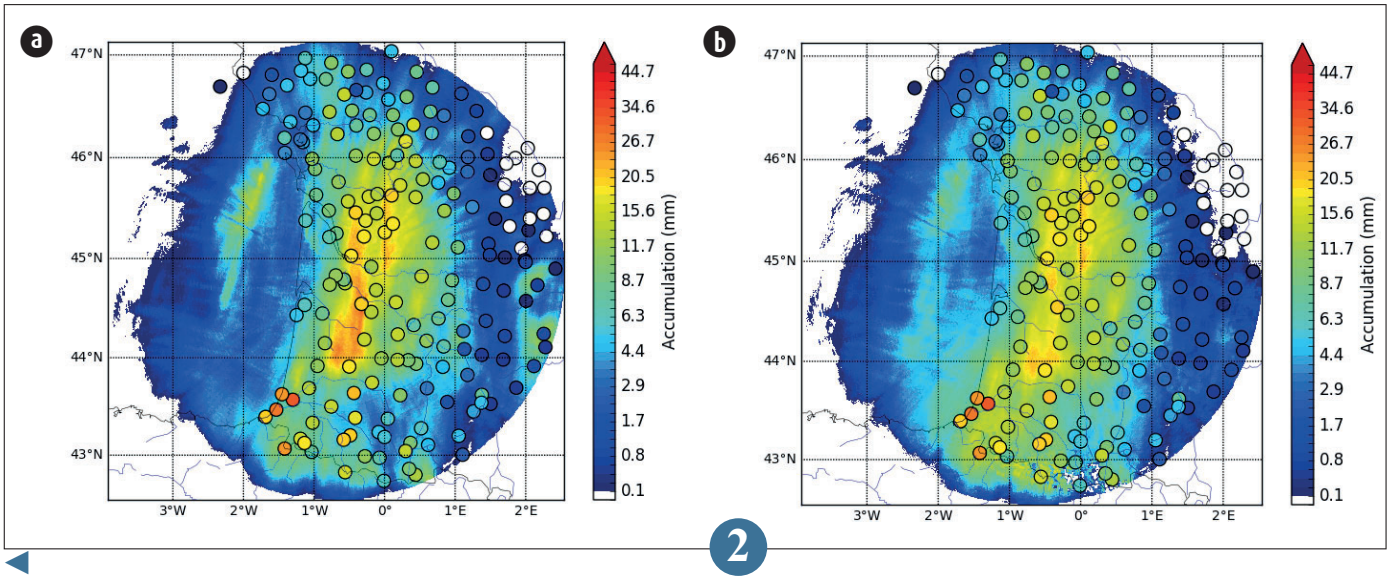

2

6 hours accumulations from the 03/03/2017 at 18 h UTC to the 04/03/2017 at 00 h UTC for the radar of Bordeaux (range of 255 km). a) Panthere;
b) with the new method by using AROME-NWC forecast. Circles indicate rain gauge accumulations.

Cloud microphysics retrieval at global scale from meteorological geostationary satellites

The imagers on board the second generation of meteorological geostationary satellites (MSG, Himawari8, GOES16/17) have channels in the visible, near infrared and infrared spectrum allowing the cloud microphysics retrieval. The mapping at a global scale of cloud top phase, particle size, ice and liquid water content is therefore now possible at high temporal frequency.

The Centre de Météorologie Spatiale is involved in the SAF-NWC project funded by EUMETSAT to prepare software modules to identify clouds and retrieve their height and microphysical properties from a set of meteorological geostationary satellites. The method used for microphysics is based on thresholding technics (for cloud phase) and comparison of measurements to simulations (obtained using DISORT) especially of near-infrared bands showing sensitivity to cloud phase and particle size. The validation is performed using measurements of A-train active space borne instruments (radar CPR on CloudSat and Lidar CALIOP on CALIPSO).

The software developed within the SAF-NWC is used by the Centre de Météorologie Spatiale to map cloud macro and micro-properties at a global scale. The figure illustrates the cloud ice water content retrieval while the Atsani typhoon was close to the Japanese coasts on 23rd August 2018. These cloud products, widely used by Météo-France, are also made available to the French research community.

3

Doubling the radiosounding network at lower cost with descent data collection

Despite progress in satellite observation, the global radiosonde network retains the privileged status of “backbone” of the atmospheric observation system. However budget cuts manage in triggering reductions of this network since this mode of observation remains expensive (between 100 and 300€ per ascent). In this context, the collection of observations at the descent of the sondes makes it possible to significantly increase the number of data, with almost no additional cost, in case of flat terrain. Germany and Finland have been producing such messages for over a year with Vaisala hardware. The four-dimensional data assimilation of radiosoundings accounting for the actual slopes of the ascending profiles would really benefit from this new descending data, provided that their quality is verified. Knowing that hardware and software are optimized for measurement on the climb, the same quality is not guaranteed at the descent. CNRM/GMAP monitored the data available over several weeks in the spring of 2018. Ascent data are used as a reference. The comparison with the ARPÈGE model shows an equivalent quality in the troposphere, especially if the fall speed is reduced thanks to a parachute. In the stratosphere, if descending temperature data are not so good, the wind data seem surprisingly better than for the ascent. This idea stems from an excessive reliance on the model. It is known from experience that model winds are of modest quality in the stratosphere. The high fall speed and the smoothing algorithms produce wind measurements that are quite uniform on the vertical. If the radiosonde manufacturers do not adapt their systems to this new observing practice, some of the data from radiosounding at the descent will be of little use for NWP.

4

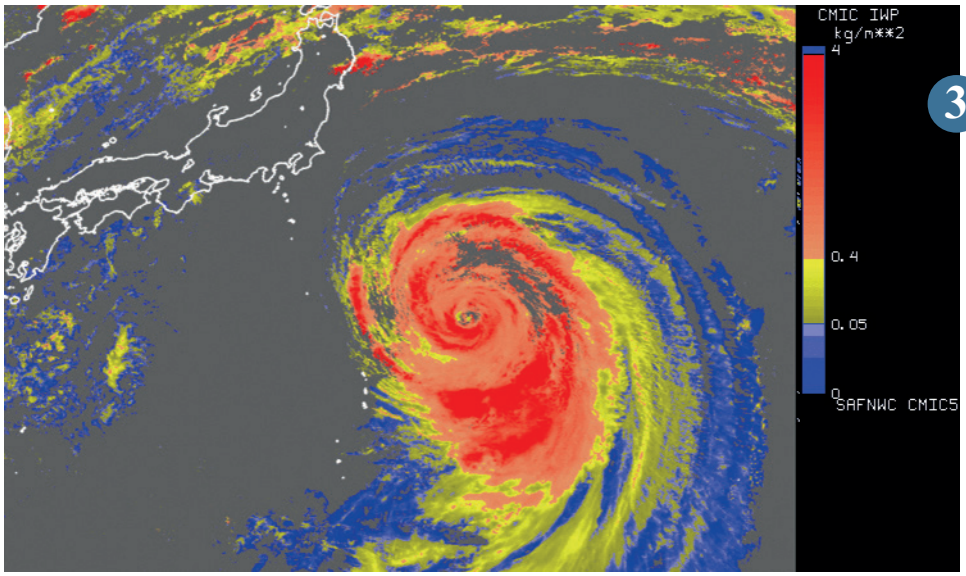

3

Example of cloud Ice Water Content using Himawari8 satellite
The Atsani typhoon near Japan coasts - 23rd August 2018 02 h UTC

The lines represent an estimate of the distance between the observations of temperature and wind and the model as a function of the atmospheric pressure. The upper part represents the stratosphere, below the troposphere.
The ascent profiles (fine and dark lines) are very similar to the descent profiles (thick and clear lines) in the troposphere. This is not the case
in the stratosphere where ascent / descent differences are marked and opposite between temperature and wind.

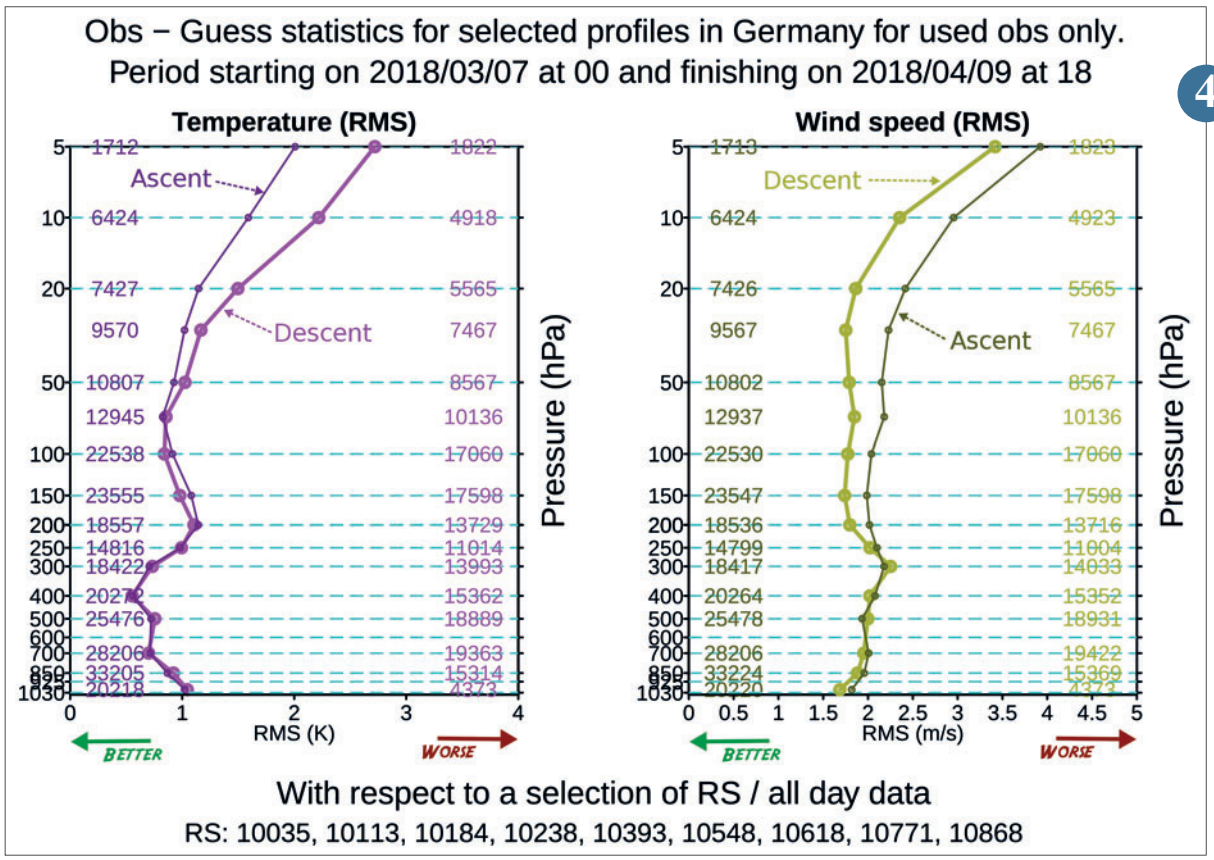

4

First wind measurements of the space-borne lidar AEOLUS

The space-borne lidar AEOLUS was launched on the 22nd of August in the frame of the Earth-Explorer programme of the European Space Agency. It is the first wind lidar ever launched in space. The development started more than 15 years ago. Many technical difficulties had to be solved. The CNRM has been involved in the development of the ground segment since 2004. It prototyped the calibration and L2A processors (retrieval of aerosol optical properties), and contributed the development of the L2B (wind) processor. The first observations arrived 10 days after the launch, during which period the satellite was carefully turned on. A first assessment of the wind data quality has been rapidly available. A comparison with ECMWF model analysis has shown a bias of the order of 1m/s and a precision of 2-3m/s on the Mie (aerosol) channel, and 4-5m/s on the Rayleigh (molecules) channel. These good results were obtained after a careful calibration of the instrument that will have to be continued in order to reduce the bias further. The assessment of the impact of wind measurements on weather forecasts is on-going at ECMWF and CNRM. The first results so far indicate a positive impact that will need to be confirmed. Studies have been carried out for the assimilation of secondary, aerosol products by air-quality models. CNRM will work on the operational maintenance of the processors during the 3-year lifetime of the mission.

5

Campaigns

A stratospheric intrusion as measured during GLAM and compared to model results and analyses

Stratospheric intrusion occurs on a tropopause folding when stratospheric air mass poor in H_2O and rich in O_3 penetrates the troposphere toward the surface. One of the criteria to detect relies on the dynamical tropopause, as used by Tyrlis in 2014 to establish a climatology and typology of intrusions according to their penetration depth, in the Mediterranean region and based on ERA-INTERIM reanalyses (1979-2012).

Here, we explore the measurements of short-lived (O_3, CO) and long-life (CH_4, CO_2) chemical species from the CHARMEX GLAM airborne campaign during which a stratospheric intrusion was identified on August 10th 2014 at 08 hTU at 300 hPa, 33°N and 28-29°E. The intrusion is characterized by positive O_3 (+50ppbv) and CO_2 (+4ppmv) anomalies associated with negative CO (-20ppbv) and CH_4 (-40ppbv) anomalies. Thus this stratospheric intrusion has not a pure stratospheric origin since CO_2 is not at its minimum (figure 1). Analyses (MERRA2 and CAMS), model (MOCAGE) and GLAM measurements are in agreement. Actually, the vertical cross section with respect to latitude from MERRA2 provides the contour of this intrusion via the dynamic tropopause (fixed at 2 PVU, figure 2a) and high O_3 gradient (figure 2b). MOCAGE with a low CO depicts the penetration of the intrusion (figure 3). Finally, CAMS suggests a deeper penetration characterized by a depletion in CH_4 (figure 4a) whilst CO_2 is not depleted (figure 4b). The intrusion is formed close to the jet stream, and its penetration is favoured here by the descending branches of the Hadley (African Monsoon) and Walker (Asian Monsoon) cells. These intrusions are essential to be taken into account in chemical assessments and trend studies because of their frequency and persistence in the Mediterranean area and the anomalies induced.

6

The STORM project (Sea Turtles for Ocean Research and Monitoring)

STORM is an exploratory program initiated in 2018 from LACy and Reunion Island CEDTM (Centre d'Etude et de Découverte des Tortues Marines) under the frame of the EU INTERREG-V research program "ReNovRisk-Cyclones and Climate Change". It aims to use bio-logging for the first time in tropical areas to investigate the ocean mixed layer (OML) properties using sea turtles (ST) equipped with specifically designed environmental sensors.

Starting in January 2019, a dozen of loggerhead sea turtles (caught in fishermen's nets or injured by boats near Reunion Island) will be equipped with Argos beacons and in-situ sensors (temperature and pressure) by CEDTM, before being released into the ocean from Reunion Island. While deploying Argos tags on ST is common among marine biologists to study migratory routes and spawning grounds of various ST species all over the world, the originality and unicity of STORM lies in the capability to simultaneously monitor ocean temperature, salinity and pressure (depth) down to several hundred meters below the surface. As ST can travel several thousand kilometres per year (see figure below), spatially explicit patterns of sea surface temperature (SST) and hydrographic profiles will be obtained over large portion of the ocean without any human intervention, and transmitted in real-time through satellite telemetry. Collected data will be used to assess the performance of coupled atmospheric-ocean models (oceanic component and OA interactions) at various time and space scales as well as to evaluate the benefit of assimilating ST-borne ocean data in regional oceanic models to improve both the description of the OML and air-sea interactions in coupled systems. STORM will also contribute to the promotion of scientific culture to raise public awareness on climate change through collaborations with tens of primary schools in Reunion Island ("adopt a turtle program").

7

EOLUS satellite ready
to be encapsulated
in the Vega rocket fairing.
© ESA

5

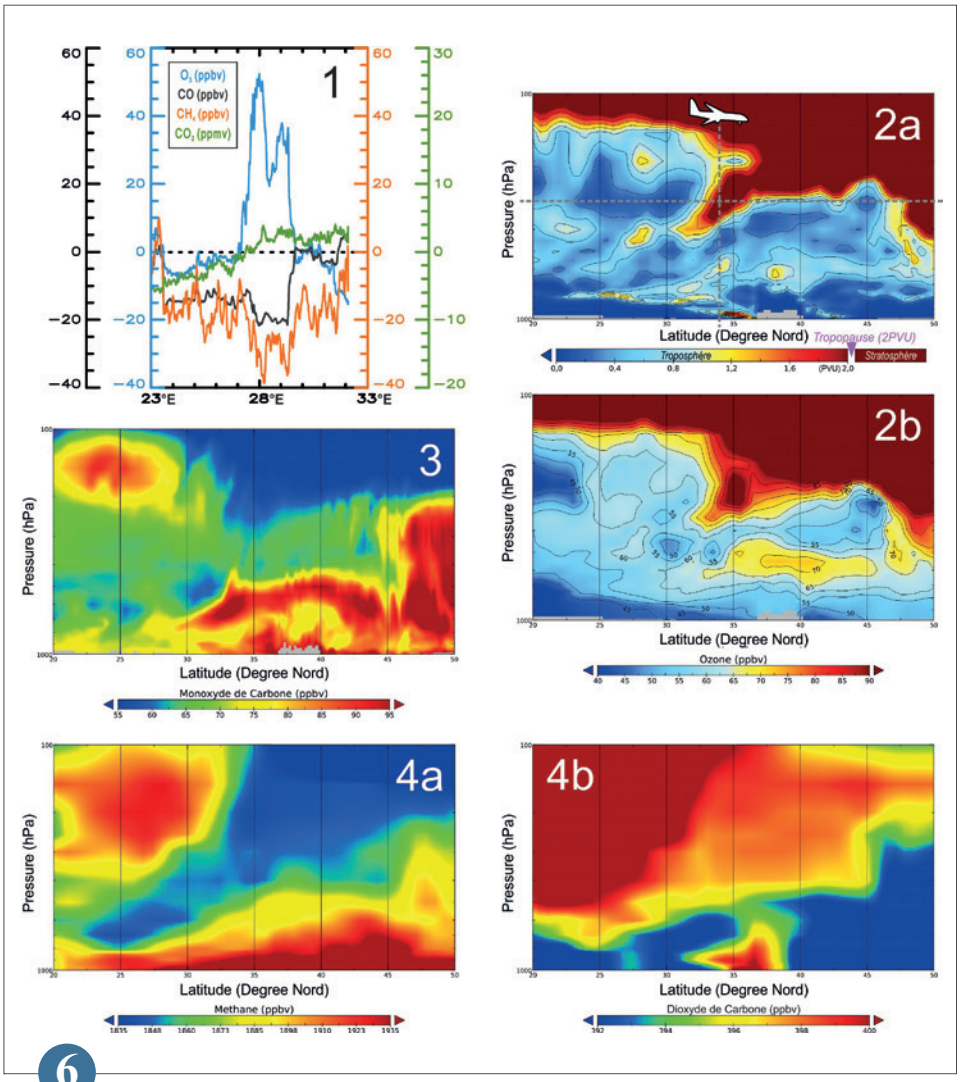

6

O_3, CO, CH_4 and CO_2 anomalies measured at 300hPa during the GLAM airborne campaign (1).
Vertical cross section with respect to latitude at 28-29°E (including the instantaneous position of aircraft measurements) of the dynamic tropopause fixed at 2 PVU (MERRA2, 2a) and concentrations of O_3, (MERRA2, 2b), CO (MOCAGE, 3), CH_4 and CO_2 (CAMS, 4a and 4b).

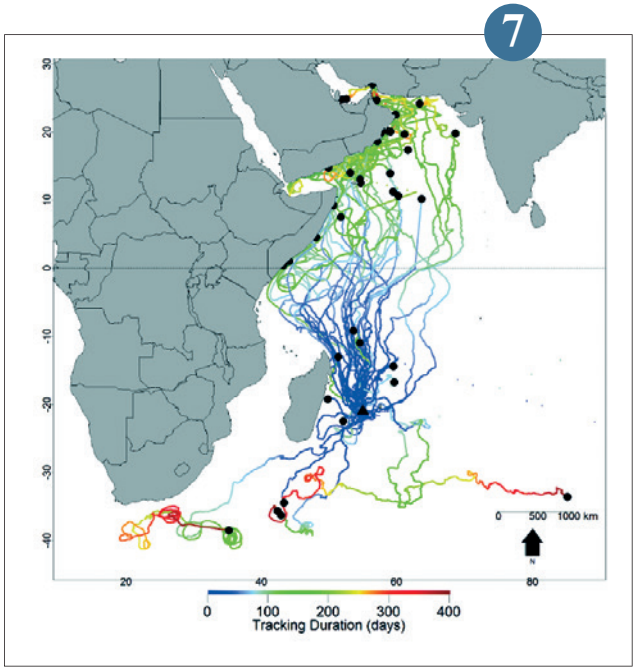

7

Spatial and temporal monitoring map of about twenty loggerhead turtles equipped with Argos beacons released from Reunion Island during the COCA-LOCA project (from Mayeul et al. 2014: The spatial ecology of juvenile loggerhead turtles (Caretta caretta) in the Indian Ocean sheds light on the "lost years" mystery. Tue. Biol. 161, 1835-1849).

Tracking greenhouse gases by aircraft and balloon to prepare forthcoming scientific space missions

Carbon dioxide (CO_2) and methane (CH_4) are the two main greenhouse gases modified by human activity. In 2018, the initiative called MAGIC (Monitoring of Atmospheric composition and Greenhouse gases through multi-Instruments Campaigns) began. It aimed at better understanding the concentration of greenhouse effect gases and their distribution in the atmosphere. MAGIC relies on SAFIRE Falcon 20 aircraft that allows scientists to measure in-situ gases concentrations, air temperature, humidity and wind as well as particles at altitudes between 0 and 11 km. MAGIC also relies on the expertise of CNES and CNRS in deploying meteorological balloons in the French areas of Landes and Loiret. During two campaigns in January and May 2018, two research aircrafts, 19 launches of meteorological balloons, 4 instrumented sites from the ICOS network and ten ground-based remote sensing instruments were deployed for this original experiment to measure the concentrations of greenhouse gases.
MAGIC will provide an improved knowledge on greenhouse gases, especially in high-troposphere and in the stratosphere since most existing networks only make measurements at the surface of Earth. It also prepares forthcoming space missions for the monitoring of greenhouse effect gases, as announced during the Paris COP21: Merlin to measure Methane, MicroCarb to measure carbon dioxide and IASI-NG to measure atmospheric composition and to monitor climate variables.
In May 2018, a narrow cooperation with the German center for aeronautics (DLR) allowed to fly together SAFIRE Falcon 20 and the HALO operated by DLR, in an attempt to benefit from the complementarity between the instruments flown onboard each aircraft.
En mai 2018, une coopération étroite avec le Centre allemand pour l'aéronautique et l'astronautique (DLR) a permis un vol conjoint entre le Falcon 20 de SAFIRE et l'avion HALO du DLR et de bénéficier de la complémentarité entre les instruments de mesure embarqués dans les deux vecteurs.

8

b) Flight plan.
© SAFIRE

a) The SAFIRE Falcon 20 just before take-off for the measurement flight.
© SAFIRE / Jean-Christophe Canonici

8

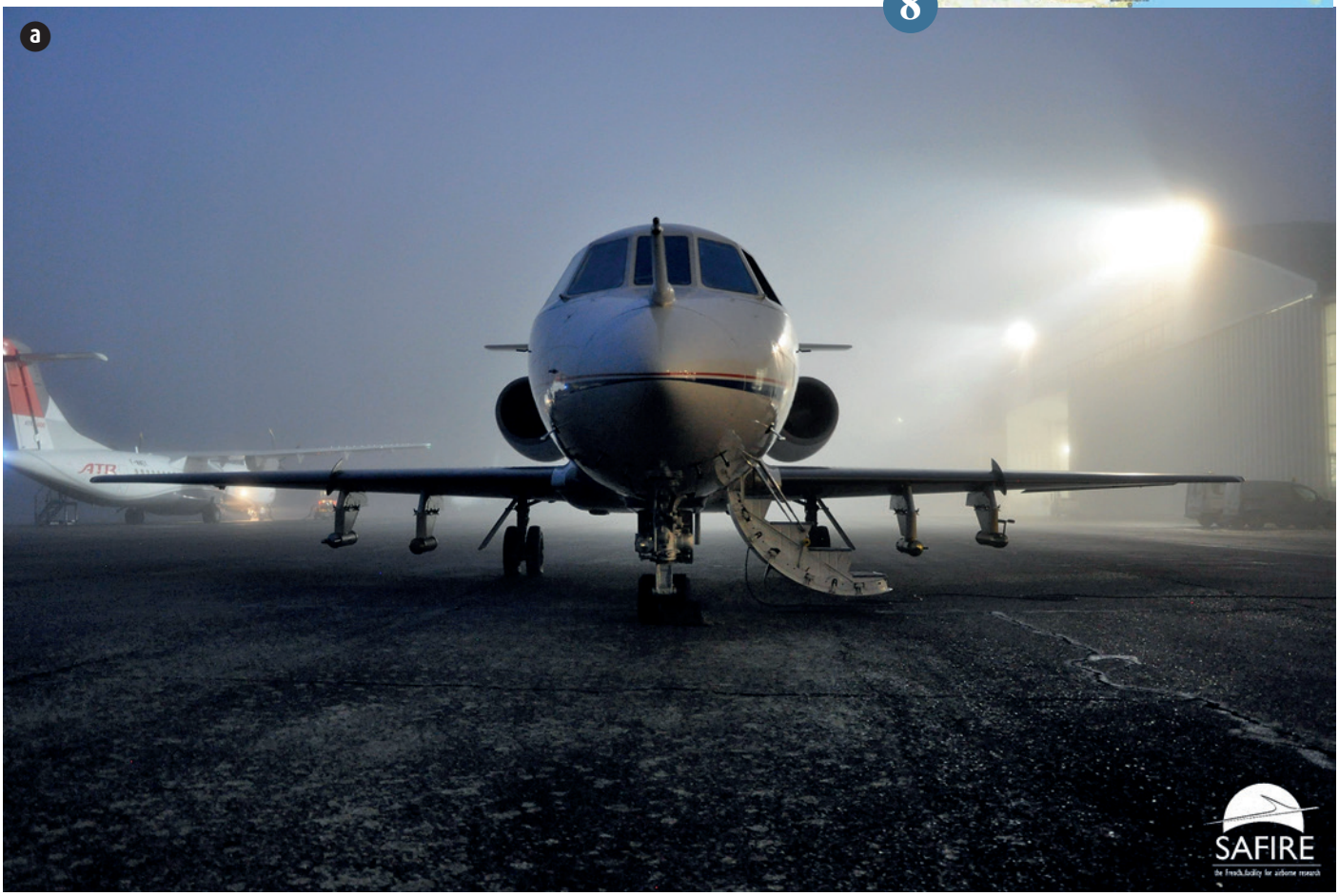

SAFIRE to the pursuit of thunderstorms in the Mediterranean sky

Scientists are still far from understanding all to the physical processes of natural lightning flashes. The ANR-16-CE04-0005 EXAEDRE project (EXploiting new Atmospheric Electricity Data for Research and the Environment coordinated by the Laboratoire d'Aérologie, CNRS/Université Toulouse III – Paul Sabatier) aims at enhancing the knowledge of the links between the various microphysical, dynamical and electrical processes occurring within any thunderstorm. The EXAEDRE project also aims at quantifying the benefit of the "lightning" information for better monitoring of thunderstorms and for improving weather forecasts by assimilating the "lightning" data in numerical weather prediction models.
The observational strategy of the EXAEDRE project relies on observations already collected during the HyMeX program, on measurements of electrical activity collected since 2014 through the SAETTA tridimensional lightning locating network operated within the framework of the CORSiCA facility and on records of Météorage operational lightning locating network ; it also includes the development of new lightning detection sensors, and finally a dedicated field campaign in Corsica including airborne measurements. During one month, the Falcon 20 of Safire has accumulated unique in situ measurements as the result of the collaboration between academics, aeronautics and space development laboratories as well as industries.

9

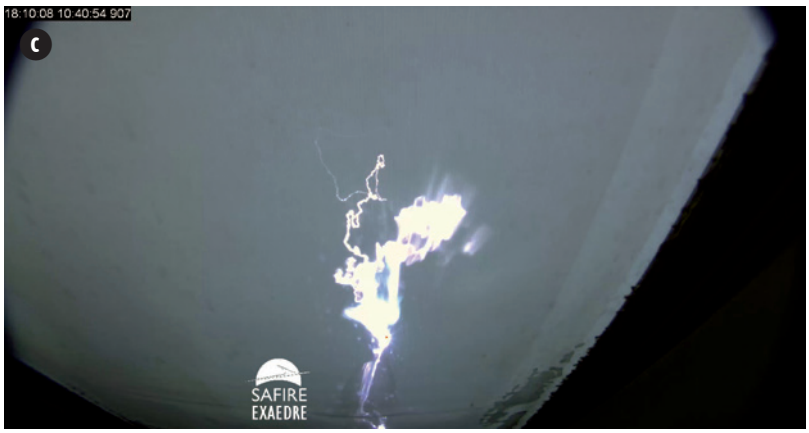

a) Rainy landing for the SAFIRE Falcon 20 after its mission between the flashes. © CNRS / C. Fresillon
b) View at the front of the SAFIRE Falcon 20 near the "anvil" of a Cumulonimbus. © SAFIRE / D. Duchanoy
c) The camera located at the front of the SAFIRE Falcon 20 captured the flash hitting its anemometric boom. © SAFIRE

Research and aeronautics

As part of its continuous involvement on research and development meteorological phenomena with impact on aviation, Météo-France carried on its activities for the modelling of ground (airport) and air phenomena.
Improving fog and low ceilings forecast remains topical, in order to fulfil airport operators' needs, for instance for the triggering of Low Visibility Procedures. Météo-France's project called IniTAF aims at providing TAF messages guess. In 2018, a new methodology for the generation of these guesses has been successfully tested. Moreover, this project and consequently the draft TAF messages it will produce will benefit the improvement of airport phenomena forecasting.
In the altitude, turbulence and convection hazards have been given a high focus this year, including within the frame of one of SESAR deployment projects. As aviation operations run on the three spatial dimensions, convective cloud top altitude is a piece of information very useful to them. In addition, aviation users would intend to anticipate impacts on their operations of hazardous phenomena such as thunderstorms. Thus, activities for the estimation of probability of convection initiation will have a certain outlet.
Météo-France also continued to be involved in other parts of the SESAR programme, including deployment projects or SESAR2020 activities. The design and conception of the future system for meteorological information exchange in compliance with SWIM have been an intense activity conducted in 2018. The organization also contributed to the development of the future European harmonized products and services.

1

Processing AROME Vertical Profiles with Machine Learning Methods to Diagnose Aeronautical Ceiling in TAF messages

As part of the IniTAF project which aims at automatically providing draft TAFs (aerodrome forecasts), work on the cloud ceiling forecast has been carried out. This work uses machine learning methods to determine the height of the cloud ceiling.
The learning and validation data are composed of METARs (hourly airport observation messages) issued from the Météo-France network from January 2016 to mid-2017 at 66 airports (10^5 records). Each METAR is related to the outputs of the AROME numerical prediction model, over a 20km × 20km domain centered on each airport. For each point of the horizontal grid, vertical profiles of several meteorological parameters (temperature, wind, humidity, cloud water content, etc...) are extracted for 24 levels from 10m to 3000m.
Thus, machine learning methods allow statistical models to be established for ceiling forecasting by using these profiles as predictors. These models are evaluated according to several criteria: accuracy, false alarms, and the ability to handle a large number of predictors. Relevant scores are calculated for each model. They are compared to the ceiling forecast scores from persistence and a diagnosis directly computed from the AROME cloudiness field. This validation is complemented by the analysis of several case studies.

2

Convection forecast allows to anticipate avoidance operations of convective clouds (at night on picture).© JPC VAN HEIJST

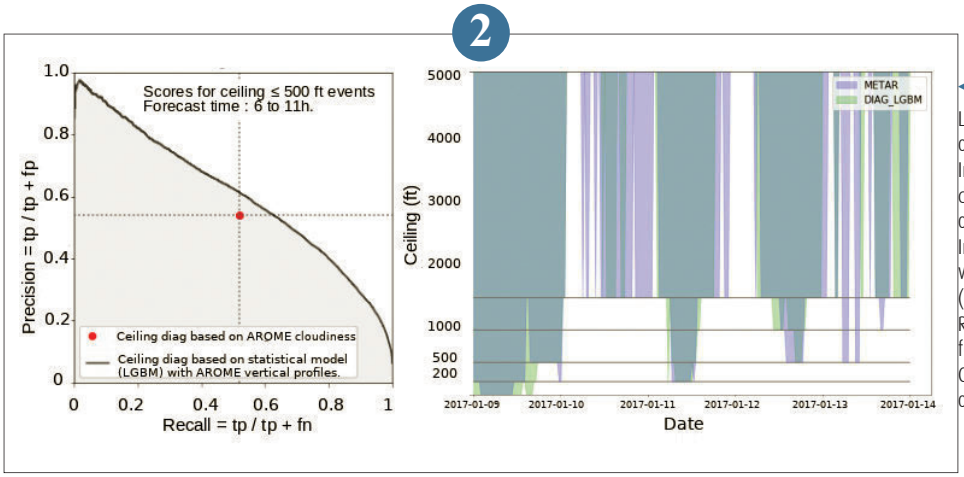

Left figure: Recall / precision scores for detection of aeronautical ceiling events – 500 ft.
In red: scores obtained for a standard aeronautical ceiling diagnosis based on the 3D cloudiness parameter of the AROME model.
In black: curve of the recall / precision pairs obtained with a tree based learning algorithm (LGBM - Light Gradient Boosting Method).
Right figure: 5 days-time series in January 2017 for Paris CDG airport
Comparison of the METAR data with the results of the diagnosis obtained by LGBM statistical model.

The IniTAF Project: a TAF initialisation methodology

Within the framework of its statutory mission of air traffic meteorological support, Météo-France provides TAF (aerodrome forecast) regulatory messages made by forecasters. The IniTAF project (TAF Initialization) aims to provide TAF initialization. This should allow aviation forecasters to focus on supporting the end users, particularly in critical weather situations (fog formation, snow, etc...) and to help the decision-making process.
Météo-France's mesoscale AROME model provides the necessary parameters for initializing TAFs. The work focused on developing an algorithm capable of establishing a TAF based on hourly sampled meteorological parameters. The technical complexity of TAF drafting stems from the need to represent variations in the meteorological situation over time with a limited number of evolution groups. A global multi-parameter approach is therefore necessary.
Thus, a new TAF generation methodology based on the analysis of stable and transient states is designed. TAF initialization is evaluated against METARs.

3

Improvement of aviation turbulence forecasts with indices combination

For safety reasons and passenger comfort, pilots seek to avoid turbulent areas. The use of Electronic Flight Bag systems (EFB) on board commercial aircraft enables the overlay of the aircraft flight trajectory and forecasts of turbulence areas, thus raising the pilot expectations of the accuracy of the turbulence areas contours.
Several turbulence diagnoses exist in literature identifying different components of the turbulence, but none of them is perfect. The combination of different diagnoses has shown to provide better results. The work consists in selecting and combining diagnoses as best as possible. For this purpose, the individual diagnoses calculated on ARPEGE (horizontal resolution of 0.25° - native vertical resolution) are firstly scaled to EDR (Eddy Dissipation Rate) by using climatology of in-situ EDR values (aircraft measurements). Several methods of selecting and combining indices are then explored among them logistic regression and random forests. Initial work is being done in the United States where observations from pilot reports and in-flight EDR measurements are available. The methodology is then applied over Europe.
The scores show an improvement in the performance when the diagnoses are calculated in the native vertical resolution of the model. Further improvement is also shown when combining individual diagnoses.

4

Diagnostic of deep convective cloud top

In the meteorological aeronautical sector, thunderstorm forecasting remains a major issue for human forecasters as well as for provision of innovative products to external users (AeroCom project, SESAR2020, etc.).
To ensure security of flights, pilots must avoid these Cumulonimbus, sources of hail, icing by ice crystals (Rio-Paris crash in 2009), etc. With increasing air traffic, these route changes could lead to overcapacities of traffic control centres and delays that generate over-costs. So it is important to provide relevant information to users both in time (present and future) and 3D space. Although tools can already provide quality information in near real time (with RDT for example), forecasting the precise localisation of thunderstorms in the next hours around the world remains a challenge.
Global numerical weather forecasting is not able to simulate thunderstorms because of their poor spatial resolution. However, parametrisations, named « convective schemes », allows to simulate the induced effects like precipitations and nebulosity. This parametrisation in the French model ARPEGE make it possible to know the height of well-developed convective clouds and to produce a new diagnostic from it.
As thunderstorms forecasting is sensitive to modelling errors, probabilistic forecasts using several members of the model should improve the previsibility of this new diagnostic.

5

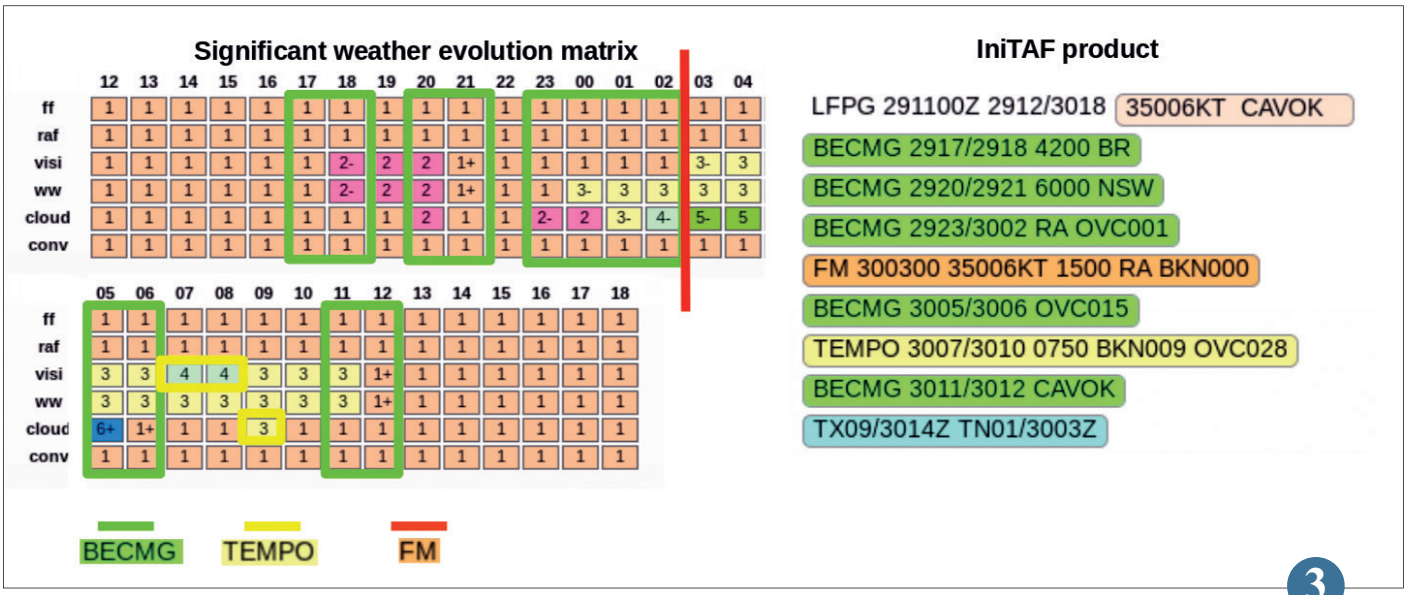

3

State transition matrix for several TAF meteorological parameters (left).
The analysis of the transient and stable states of this matrix leads to an initialized TAF (right).
BECMG, TEMPO and FROM evolutions are represented in green, yellow and orange, respectively.

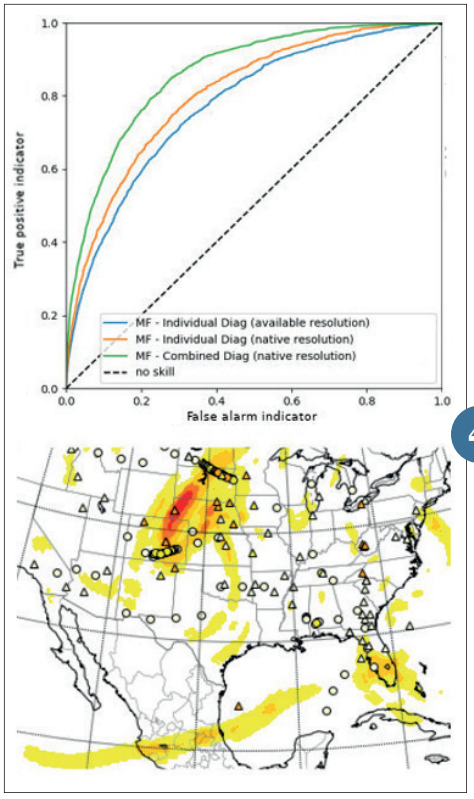

4

On the left figure: ROC curves
for moderate or severe turbulence events detection computed with several diagnoses
(NWP model: ARPEGE 0.25° - year: 2017 – validity time: 00UTC – forecast times: 12-15-18 – Observations: EDR in-situ).
Several diagnosis are compared: Météo-France operational diagnosis (blue), Météo-France diagnosis computed on the native vertical resolution (orange), and combined diagnosis computed on the native vertical resolution (green).
On the right figure: Combined diagnosis computed on a US domain is shown for 30th April 2017 at 15UTC – Flight Level 340. Filled contours show turbulence intensity. Symbols show observations (triangles/pilot reports, circles/ in-situ EDR).
Color bar: white → none/insignificant turbulence events, yellow to red → moderate to severe turbulence events).

Pressure of the top of convective clouds (in hPa) – Model ARPEGE

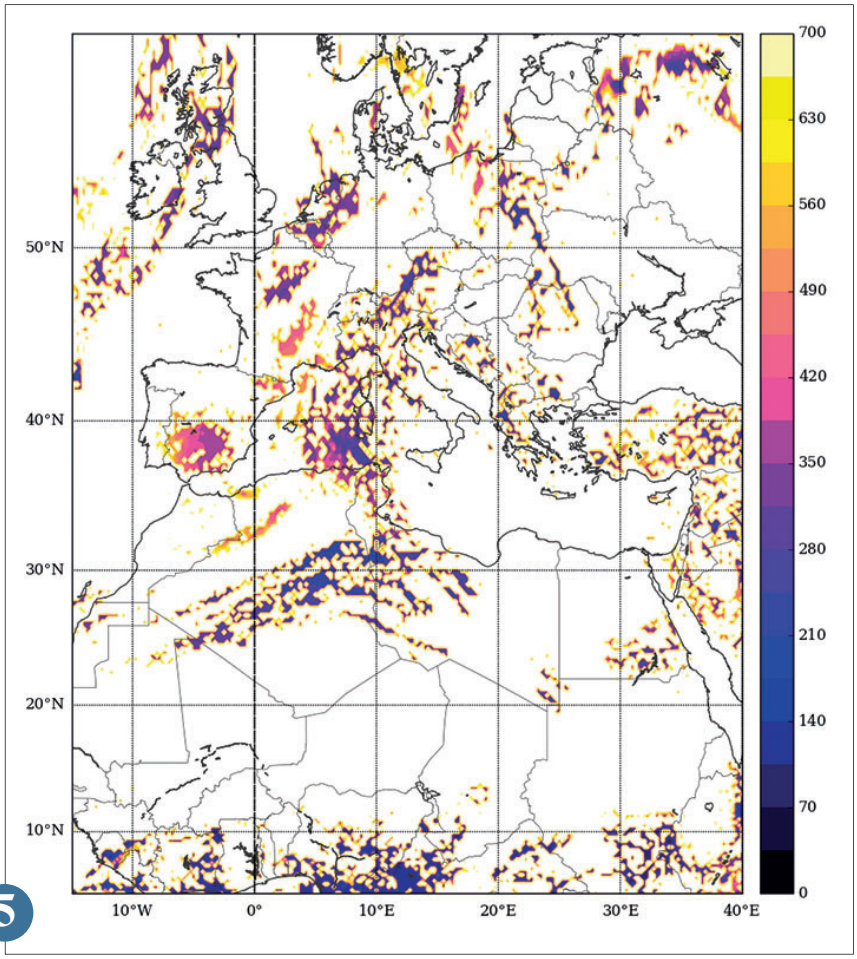

5

CI (Convection Initiation), a satellite-based product of convection initiation probability

The product is developed by Météo-France as part of the SAF Nowcasting. The objective of the product is to determine the probability of a cloudy pixel to develop into a thunderstorm within the range 0-30', 0-60' or 0-90'. The version 2018 of the software was delivered at the end of 2018 and will complement another Météo-France product developed in the framework of SAF Nowcasting: the RDT which describes the systems already developed.
The 2018 version of the CI is greatly improved compared to the previous one (v2016): better tuning of the input data (brightness temperature, brightness temperature difference and their trends), use of cloud microphysics, better pixel propagation affected by a potential convection activity.
The criteria of interest are classified in three categories: the vertical extension of the cloud, the time spent under 0°C by a part of the cloud, the growth of the top of the cloud.
The end product is useful for forecasters and aviation, even if it has false alarms and no detections when compared to a radar-like terrain truth. These false alarms and non-detection are sometimes geographically very close, which illustrates the problem of double penalty in verification.
This product will extend the tactical horizon of the convection phenomenon, very dangerous for aviation.

6

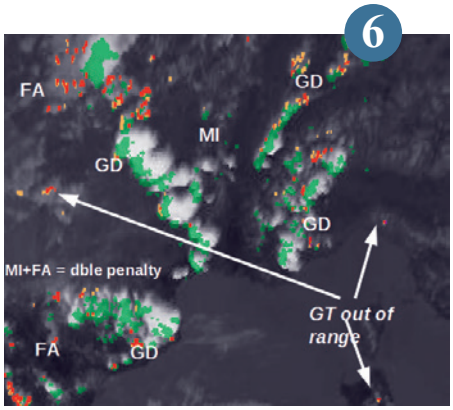

▲
MSG satellite (10.8µm channel) and cumulative convective radar echoes (in green) for half an hour (thresholds of 30 dBZ)
CI pixels for the next 30 minutes associated with probabilities of 0-25% (orange), 25-50% (dark orange), 50-75% (red) and 75-100% (magenta). FA = false alarm, GD = Good Detection, MI = miss (no detection).
FA and MI side by side illustrate the problem of double penalty in verification. Areas with GT (Ground Truth) out of range indicate that there is a radar signal but that convection has not developed completely in the 30' interval.

European Harmonised Forecast of Convection in the framework of SESAR deployment phase

The number of passengers on commercial flights in Europe is expected to double between 2012 and 2035, from 0.7 billion to 1.4 billion. The European Union initiated the SESAR project in 2004. The top-objective was to respond to technological needs in the context of the development of the Single European Sky. Météo-France has participated in several SESAR projects, 3 of which are ongoing. The current phase, "SESAR Deployment", has operational aims. Météo-France contributes on several points: the portal for access to meteorological services for aeronautical users (MET-GATE), the production of two harmonized convection products (immediate and probabilistic forecasts), the contribution to other harmonized products (turbulence, icing and winter phenomena), as well as the realization of a European composite of radar mosaics.
For convection, the harmonized product is used to report the highest severity level over a given location, regardless of the number of contributors, in order to maximize the detection of small, highly convective structures. The following figure illustrates for the nowcasting part a seamless forecast from three different contributions. An estimate of cloud top height is also produced.
This convection product is designed to give airlines, airports and ANSPs a better understanding of convection near airports in TMAs. This will facilitate tactical decision-making, safety and improve the airspace-management.

7

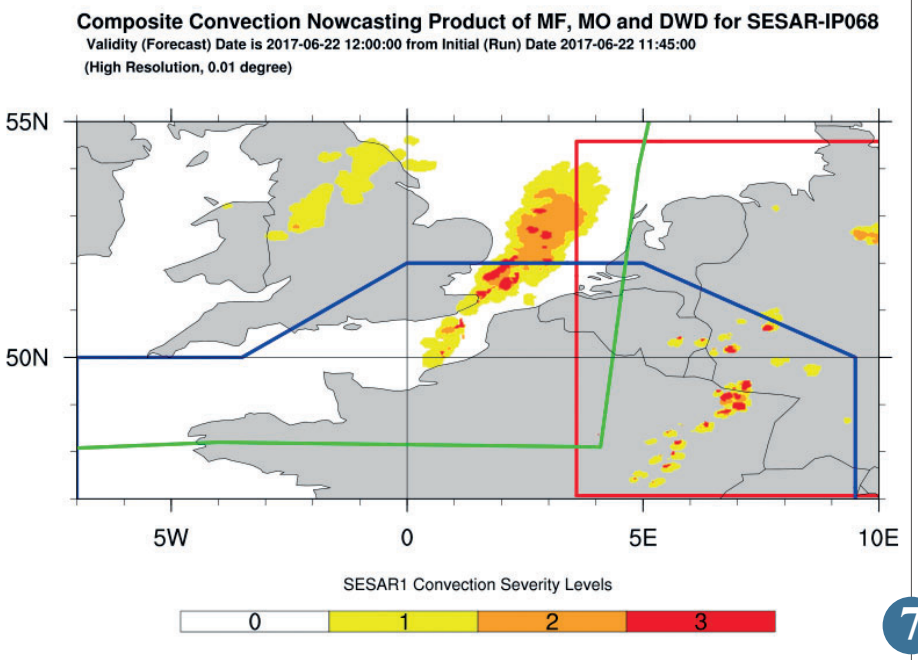

◀
Zoom on the intersection domains of the contributions of the English, German and French meteorological services for the harmonized nowcasting of convection (step +15 minutes from the 11:45 network of 22/6/2017). The severity levels used for harmonized convection range from 0 (no convection) to 3 (severe convection). The blue, red and green features are the limits of English, German and French productions.

Appendix

2018 Scientific papers list

Papers published in peer-reviewed journals (impact factor > 1)

Adam, O., F. Brient et al., 2017 : Regional and seasonal variations of the double-ITCZ bias in CMIP5 models: Climate Dynamics, Volume: 51, Issue: 1-2, Pages: 101-117, Doi : 10.1007/s00382-017-3909-1. Published: JUL 2018.

Adam, O., T. Schneider and F. Brient (2017). Regional and seasonal variations of the double-ITCZ bias in CMIP5 models. Climate Dynamics, Volume: 51, Issue: 1-2, Pages: 101-117, DOI: 10.1007/s00382-017-3909-1. Published: JUL 2018.

Akritidis, D., Katragkou, E., Zanis, P., Pytharoulis, I., Melas, D., Flemming, J., Inness, A., Clark, H., Plu, M., and Eskes, H., 2018: A deep stratosphere-totroposphere ozone transport event over Europe simulated in CAMS global and regional forecast systems: analysis and evaluation. Atmospheric Chemistry and Physics, Volume: 18, Issue: 20, Pages: 15515-15534, Doi: 10.5194/acp-18-15515-2018. Published: OCT 29 2018.

Albergel, C., Dutra, E., Munier, S., Calvet, J.-C., Munoz-Sabater, J., de Rosnay, P., and Balsamo, G., 2018 : ERA-5 and ERA-Interim driven ISBA land surface model simulations: which one performs better? Hydrology and Earth System Sciences, Volume: 22, Issue: 6, Pages: 3515-3532, Doi: 10.5194/hess-22-3515-2018. Published: JUN 28 2018.

Alonso-González, E., J. López-Moreno, J., S. Gascoin, M. García-Valdecasas Ojeda, A. Sanmiguel-Vallelado, F. Navarro-Serrano, J. Revuelto, A. Ceballos, M. J. Esteban-Parra and R. Essery, 2018: Daily gridded datasets of snow depth and snow water equivalent for the Iberian Peninsula from 1980 to 2014. Earth System Science Data, Volume: 10, Issue: 1, Pages: 303-315, Doi: 10.5194/essd-10-303-2018, Published: FEB 2018.

Andrey-Andrés J., N. Fourrié, V. Guidard, R. Armante, P. Brunel, C. Crevoisier, B. Tournier : A simulated observation database to assess the impact of the IASI-NG hyperspectral infrared sounder. Atmospheric Measurement Techniques, Volume: 11, Issue: 2, Pages: 803-818, Doi: 10.5194/amt-11-803-2018. Published: FEB 9 2018.

Antic, J. and A. Ribes, 2018 : Hurricanes Albert and Esteban: statistical analysis of a perfect 3-year return period event, Quarterly Journal of Royal Maternity Society, in press.

Auguste, F., G. Réa, R. Paoli, C. Lac, V. Masson and D. Cariolle, 2018: Implementation of an Immersed Boundary Method in the Meso-NH model: Applications to an idealized urban-like environment. See here.

Bador, M., M. Donat, O. Geoffroy, L. Alexander, 2018: ‘‘Assessing the robustness of future extreme precipitation intensification in the CMIP5 ensemble’’. Bulletin of the American Meteorological Society, Journal of Climaten, Volume: 31, Issue: 16, Pages: 6505-6525, Doi: 10.1175/JCLI-D-17-0683.1. Published: AUG 2018.

Balsamo, G., A. August-Panareda, C. Albergel, G. Arduini, A. Beljaars, J. Bidlot, N. Bousserez, S. Bousseta, A. Brown, R. Buizza, C. Buountempo, F. Chevallier, M. Choulga, H. Clo e, M. Cronin, M. Dahoui, P. de Rosnay, P. Dirmeyer, E. Dutra, M. B. E , P. Gentne, H. Hewit, S. Keeley, Y. Kerr, S. Kumar, C. Lupu, J.-F. Mahfouf, J. McNorton, S. Mec elenburg, K. Mogensen, J. Munoz-Sabater, R. Orth, F. Rabier, R. Reichle, B. Ruston, F. Pappenberger, I. Sandu, S. I. Seneviratne, S. Teitshe, I. F. Trigo, R. Uijlenhoet, N. Wedi, R. Iestyn Woolway, & X. Zreng (2018): Satellite and in-situ observatons for advancing global Earth surface modelling: a review. Remote Sensing, Volume : 10, Issue: 12, Article Number: 2038, Doi: 10.3390/rs10122038. Published: DEC 2018.

Barbier, J., F. Guichard, F. Couvreux, D. Bouniol, R. Roehrig, 2017: Detection of intraseasonal large-scale heat waves: Characteristics and historical trends during the Sahelian Spring: Journal of Climate, Volume: 31, Issue: 1, Pages: 61-80, Doi: 10.1175/JCLI-D-17-0244.1. Published: JAN 2018.

Batté, L., C. Ardilouze and M. Déqué, 2018 : Forecasting West African Heat Waves atSubseasonal and Seasonal Time Scales. Monthly Weather Review, Volume: 146, Issue: 3, Pages: 889-907, Doi: 10.1175/MWR-D-17-0211.1. Published: MAR 2018.

Behera, A. K., E. D. Rivière, V. Marécal, J.-F. Rysman, C. Claud, G. Seze, N. Amarouche, M. Ghysels, S. Khaykin, J.-P. Pommereau, G. Held, J. Burgalat and G. Durry, Modelling the TTl at the continental scale for a wet season: An evaluation of the BRAMS mesoscale model using TRO-Pico campaign and measurements from airborne and spaceborne sensors. Journal of Geophysical Research-Atmospheres, Volume: 123, Issue: 5, Pages: 2491-2508, Doi: 10.1002/2017JD027969. Published: MAR 16 2018.

Benedetto R., Girolamo, P., Suma, D., Flamant, C., Bousquet, O., Cacciani, M., Stelitano, D.,: Two-year operation of the lidar 1200: from fine-scale tropospheric structures to lower stratospheric water vapor detection. EPJ Web of Conferences, EDP Sciences, 2018, The 28th International Laser Radar Conference (ILRC 28), Bucharest 2017, 176, pp.08010. Doi: 10.1051/epjconf/201817608010.

Beniston, M., D. Farinotti, M. Stoffel, L. M. Andreassen, E. Coppola, N. Eckert, A. Fantini, F. Giacona, C. Hauck, M. Huss, H. Huwald, M. Lehning, J.-I. López-Moreno, J. Magnusson, C. Marty, E. Morán-Tejéda, S. Morin, M. Naaim, A. Provenzale, A. Rabatel, D. Six, J. Stötter, U. Strasser, S. Terzago and C. Vincent, 2018: The European mountain cryosphere: a review of its current state, trends, and future challenges. The Cryosphere, Volume: 12, Pages: 759-794, https://doi.org/10.5194/tc-12-759-2018, Published: MAR 2018.

Berre; L.,: Simulation and diagnosis of observation, model and background error contributions in data assimilation cycling. Quarterly Journal of the Royal Meteorological Society, Volume: Pages: Doi: 10.1002/qj.3454. Published : 27 November 2018.

Berthou, S., Mailler, S., Drobinski, P., Arsouze, T., Bastin, S., Béranger, K., C. Lebeaupin Brossier, 2018: Lagged effects of the Mistral wind on heavy precipitation through ocean-atmosphere coupling in the region of Valencia. Climate Dynamics, Volume: 51, Issue: 3, Special Issue: SI, Pages: 969-983, Doi: 10.1007/s00382-016-3153-0. Published: AUG 2018.

Bittencourt, GD., Bresciani, C., Pinheiro, DK., Bageston, JV., Schuch, NJ., Bencherif, H., Leme, NP., Peres, LV.,: A major event of Antarctic ozone hole influence in southern Brazil in October 2016: an analysis of tropospheric and stratospheric dynamics. Annales Geophysicae, Volume: 36, Issue: 2, Pages: 415-424, Doi: 10.5194/angeo-36-415-2018. Published: MAR 16 2018.

Blechschmidt, A.-M., Arteta, J., Coman, A., Curier, L., Eskes, H., Foret, G., Gielen, C., Hendrick, F., Marécal, V., Meleux, F., Parmentier, J., Peters, E., Pinardi, G., Piters, A. J. M., Plu, M., Richter, A., Sofiev, M., Valdebenito, Á. M., Van Roozendael, M., Vira, J., Vlemmix, T., and Burrows, J. P.: Comparison of tropospheric NO2 columns from MAX-DOAS retrievals and regional air quality model simulations, Atmos. Chem. Phys. Discuss., https://doi.org/10.5194/acp-2016-1003, in review, 2017.

Borderies M., O. Caumont, C. Augros, É. Bresson, J. Delanoë, V. Ducrocq, N. Fourrié, T. Le Bastard and M. Nuret: Simulation of W-band radar reflectivity for model validation and data assimilation. Quarterly Journal of the Royal Meteorological Society, Volume: 144, Issue: 711, Pages: 391-403, Part: B. Doi: 10.1002/qj.3210. Published: JAN 2018.

Boukachaba, N.,V. Guidard and N. Fourrie: Toward an improved assimilation of IASI over continents in the convective scale AROME France Model. Tellus.

Bourgeois, D. Bouniol, F. Couvreux, F. Guichard, J. Marsham, L. Garcia-Carreras, C. Birch and D. Parker, 2018: Characteristics of mid-level clouds over West Africa. Quartely Journal of the Royal Meteorological Society, Volume: 144, Issue: 711, Pages:426-442, Part: B, Doi: 10.1002/qj.3215. Published: JAN 2018.

Bouttier, F. et L. Raynaud, 2018: Clustering and selection of boundary conditions for limited area

ensemble prediction. Quaterly journal of the Royal Meteorological Society, Volume: 144, Issue: 717, Pages: 2381-2391, Part: B, Doi: 10.1002/qj.3304. Published: OCT 2018.

Bresciani, C., Bittencourt, GD., Bageston, JV., Pinheiro, DK., Schuch, NJ., Bencherif, H., Leme, NP., Peres, LV.,: Report of a large depletion in the ozone layer over southern Brazil and Uruguay by using multi-instrumental data. Annales Geophysicae, Volume: 36, Issue: 2, Pages: 405-413, Doi: 10.5194/angeo-36-405-2018. Published: MAR 16 2018.

Bresson, E., Arbogast, P., Aouf, L., Paradis, D., Kortcheva, A., Bogatchev, A., Galabov, V., Dimitrova, M., Morvan, G., Ohl, P., al.... On the improvement of wave and storm surge hindcasts by downscaled atmospheric forcing: application to historical storms. Natural Hazard And Earth System Sciences, Volumes: 18, Issue: 4, Pages : 997-1012, Doi: 10.5194/nhess-18-997-2018. Published: APR 4 2018.

Brocchi, V., Krysztofiak, G., Catoire, V., Guth, J., Marécal, V., Zbinden, R., El Amraoui, L., Dulac, F., and Ricaud, P.: Intercontinental transport of biomass burning pollutants over the Mediterranean Basin during the summer 2014 ChArMEx-GLAM airborne campaign. Atmospheric Chemistry and Physics, Volume: 18, Issue: 9, Pages: 6887-6906, Doi: 10.5194/acp-18-6887-2018. Published: MAY 16 2018.

Carrer, D., Pique, G., Ferlicoq, M., Ceamanos, X., Ceschia, E., 2018: What is the potential of cropland albedo management in the fight against global warming? A case study based on the use of cover crops. Environmental Research Letters, Volume: 13, Issue: 4, Article Number: 044030, Doi: 10.1088/1748-9326/aab650. Published: APR 2018 .

Cattiaux, J. and A. Ribes, 2018: Defining single extreme weather events in a climate perspective, Bulletin of the American Meteorological Society, Volume: 99, Issue: 8, Pages: 1557-1568, Doi: 10.1175/BAMS-D-17-0281.1. Published: AUG 2018.

Chan, S. K., R. Bindlish, P. O'Neill, T. Jackson, E. Njoku, S. Dunbar, J. Chaubell, J. Piepmeier, S. Yueh, D. Entekhabi, A. Colliander, F. Chen, M. H. Cosh, T. Caldwell, J. Walker, A. Berg, H. McNairn, M. Thibeault, J. Martínez-Fernández, F. Uldall, M. Seyfried, D. Bosch, P. Starks, C. Holifield Collins, J. Prueger, R. van der Velde, J. Asanuma, M. Palecki, E. E. Small, M. Zreda, J.-C. Calvet, W. T. Crow, and Y. Kerr: Development and assessment of the SMAP enhanced passive soil moisture product, Remote Sensing of Environment, Volume: 204, Pages: 931-941, Doi: 10.1016/j.rse.2017.08.025. Published: JAN 2018.

Cohen, Y., Petetin, H., Thouret, V., Marécal, V., Josse, B., Clark, H., Sauvage, B., Fontaine, A., Athier, G., Blot, R., Boulanger, D., Cousin, J.-M., and Nédélec, P.: Climatology and long-term evolution of ozone and carbon monoxide in the upper troposphere–lower stratosphere (UTLS) at northern midlatitudes, as seen by IAGOS from 1995 to 2013. Atmospheric Chemistry and Physics, Volume: 18, Issue: 8, Pages: 5415-5453, Doi: 10.5194/acp-18-5415-2018. Published: APR 20 2018.

Condom, T., M. Dumont, L. Mourre, J. E. Sicart, A. Rabatel, A. Viani and A. Soruco, 2018: Technical note: A low-cost albedometer for snow and ice measurements - theoretical results and application on a tropical mountain in Bolivia. Geoscientific Instrumentation, Methods and Data Systems, Volume: 7, Issue: 2, Pages: 169-178, Doi: https://doi.org/10.5194/gi-7-169-2018, Published: JUN 2018.

Coopmann, O., V. Guidard, N. Fourrié, M. Plu. "Assimilation of IASI ozone-sensitive channels in preparation for an enhanced coupling between Numerical Weather Prediction and Chemistry Transport Models". Journal of Geophysical Research – Atmosphere, Volume: 123, Issue: 21, Pages: 12452-12473, Doi: 10.1029/2017JD027901. Published : NOV 16 2018.

Crispel, P. and G. Roberts, 2018: All-sky photogrammetry techniques to georeference a cloud field. Atmospheric Measurement Techniques, Volume: 11, Issue: 1, Pages: 593-609, Doi: 10.5194/amt-11-593-2018. Published: JAN 31 2018.

Dahman, I., Arbogast, P., Jeannin, N., et Benammar, B.,: Rain attenuation prediction model for satellite communications based on the Meteo-France ensemble prediction system PEARP. NATURAL HAZARDS AND EARTH SYSTEM SCIENCES, Volume: 8, Issue : 12, Pages: 3327-3341. Published: DEC 18 2018.

Daniel, M., A. Lemonsu, V. Viguié, 2018: ''Role of watering practices in large-scale urban planning strategies to face the heat-wave risk in future climate''. Urban Climate, Volume: 23, Special Issue: SI, Pages: 287-308, Doi: 10.1016/j.uclim.2016.11.001. Published: MAR 2018.

Davaze, L., A. Rabatel, Y. Arnaud, P. Sirguey, D. Six, A. Letreguilly and M. Dumont, 2018: Monitoring glacier albedo as a proxy to derive summer and annual surface mass balances from optical remote-sensing data. The Cryosphere, Volume: 12, Issue: 1, Pages: 271-286, Doi: 10.5194/tc-12-271-2018, Published: JAN 2018.

De Munck, C., Lemonsu A., Masson V., Le Bras J., and Bonhomme M., 2018: Evaluating the impacts of greening scenarios on thermal comfort and energy and water consumptions for adapting Paris city to climate change. Urban Climate, Volume: 23, Special Issue: SI, Pages: 260-286, Doi: 10.1016/j.uclim.2017.01.003. Published: MAR 2018 23.

Dixit V.V., O. Geoffroy, and S. Sherwood, 2018: Control of ITCZ width by lowlevel radiative heating from upper level clouds – in aquaplanet simulations. Geophysical Research Letters, Volume: 45, Issue: 11, Pages: 5788-5797, Doi: 10.1029/2018GL078292. Published: JUN 16 2018.

Domine, F., G. Gauthier, V. Vionnet, D. Fauteux, M. Dumont and M. Barrere, 2018: Snow physical properties may be a significant determinant of lemming population dynamics in the high Arctic. Arctic Science, Doi: https://doi.org/10.1139/AS-2018-0008, Published: SEP 2018.

Duffourg F., K.-O. Lee, V. Ducrocq, C. Flamant, P. Chazette and P. Di Girolamo, 2018: Role of moisture patterns in the backbuilding formation of HyMeX IOP13 heavy precipitation systems. Quarterly Journal of the Royal Meteorological Society, Volume: 144, Issue: 710, Pages: 291-303, Part: A, Doi: 10.1002/qj.3201. Published: JAN 2018.

Duruisseau, F, Chambon P, Wattrelot E, Barreyat M, Mahfouf JF. Assimilating cloudy and rainy observations from SAPHIR on-board Megha-Tropiques within the ARPEGE global model. Quarterly Journal of the Royal Meteorological Society.

Edouard, S., Vincendon, Beatrice., Ducrocq, V., 2018 : Ensemble-based flash-flood modelling: Taking into account hydrodynamic parameters and initial soil moisture uncertainties. Journal of Hydrology, Volume : 560, Pages : 480-494, Doi : 10.1016/j.jhydrol.2017.04.048. Published : MAY 2018.

El Hajj, M., Baghdadi, N., Zribi, M., Rodríguez-Fernández, N., Wigneron, J.P., Al-Yaari, A., Al Bitar, A., Albergel, C. and Calvet, J.-C, 2018 : Evaluation of SMOS, SMAP, ASCAT and Sentinel-1 Soil Moisture Products at Sites in Southwestern France. Remote Sensing, Volume : 10, Issue : 4, Article Number : 569, Doi : 10.3390/rs10040569. Published : APR 2018.

Emery, C. M., A. Paris, S. Biancamaria, A. Boone, S. Calmant, P.-A. Garambois, and J. Santos da Silva, 2018 : Large-scale hydrological model river storage and discharge correction using a satellite altimetry-based discharge. Hydrology And Earth System Sciences, Volume : 22, Issue : 4, Pages : 2135-2162, Doi : 10.5194/hess-22-2135-2018. Published : APR 6 2018.

Federico S., R. Claudia Torcasio, E. Avolio, O. Caumont, M. Montopoli, L. Baldini, G. Vulpiani, and S. Dietrich, 2018 : The impact of lightning and radar data assimilation on the performance of very short term rainfall forecast for two case studies in Italy, NHESS.

Filippi, J.-B., Bosseur, F., Mari, C., et Lac, C. : Simulation of a Large Wildfire in a Coupled Fire-Atmosphere Model. Atmosphere, Volume: 9, Issue: 6, Article Number: 218, Doi : 10.3390/atmos9060218. Published: JUN 2018.

Flamant, C., P. Knippertz, A. Fink, A. Akpo, B. Brooks, C. Chiu, H. Coe, S. Danuor, M. Evans, G. Jegede, N. Kalthoff, A. Konare, C. Liousse, F. Lohou, C. Mari, H. Schlager, A. Schwarzenboeck, B. Adler, L. Amekudzi, J. Ayree, M. Ayoola, A. Batenburg, G. Bessardon, S. Borrmann, J. Brito, K. Bower, F. Burnet, V. Catoire, A. Colomb, C. Denjean, K. Fosu-Amankwah, P. Hill, J. Lee, M. Lothon, M. Maranan, J. Marsham, R. Meynadier, J. Ngamini, P. Rosenberg, D. Sauer, V. Smith, G. Stratmann, J. Taylor, C. Voigt, and V. Yoboue, 2017 : The Dynamics-Aerosol-Chemistry-Cloud Interactions in West Africa field campaign : Overview and research highlights. Bull. Amer. Meteor. Soc., doi : 10.1175/BAMSD-16-0256.1, 2018.

Foucart, B., Sellegri, K., Tulet, P., Rose, C., Metzger, JM., Picard, D., : High occurrence of new particle formation events at the Maido high-altitude observatory (2150 m), Reunion (Indian Ocean). Atmospheric Chemistry And Physics, Volume : 18, Issue : 13, Pages : 9243-9261, Doi : 10.5194/acp-18-9243-2018. Published : JUL 3 2018.

Freney, E., K. Sellegri, M. Chrit, K..Adachi, J. Brito, A. Waked, A. Borbon, A. Colomb, R. Dupuy, J.-M. Pichon, L. Bouvier, C. Delon, C. Jambert, P. Durand, T. Bourianne, C. Gaimoz, S. Triquet, A. Féron, M. Beekmann, F. Dulac and K. Sartelet, 2017 : Aerosol composition and the contribution of SOA formation over Mediterranean forests. Atmospheric Chemistry and Physics, Volume: 18, Issue: 10, Pages: 7041-7056, DOI: 10.5194/acp-18-7041-2018. Published: MAY 23 2018 .

Gaillardet, J., I. Braud, F. Hankard, S. Anquetin, O. Bour, N. Dorfliger, J.R. de Dreuzy, S. Galle, C. Galy, S. Gogo, L. Gourcy, F. Habets, F. Laggoun, L. Longuevergne, T. Le Borgne, F. Naaim-Bouvet, G. Nord, V. Simonneaux, D. Six, T. Tallec, C. Valentin, G. Abril, P. Allemand, A. Arènes, B. Arfib, L. Arnaud, N.

Arnaud, P. Arnaud, S. Audry, V. B. Comte, C. Batiot, A. Battais, H. Bellot, E. Bernard, C. Bertrand, H. Bessière, S. Binet, J. Bodin, X. Bodin, L. Boithias, J. Bouchez, B. Boudevillain, I. B. Moussa, F. Branger, J. J. Braun, P. Brunet, B. Caceres, D. Calmels, B. Cappelaere, H. Celle-Jeanton, F. Chabaux, K. Chalikakis, C. Champollion, Y. Copard, C. Cotel, P. Davy, P. Deline, G. Delrieu, J. Demarty, C. Dessert, M. Dumont, C. Emblanch, J. Ezzahar, M. Estèves, V. Favier, M. Faucheux, N. Filizola, P. Flammarion, P. Floury, O. Fovet, M. Fournier, A. J. Francez, L. Gandois, C. Gascuel, E. Gayer, C. Genthon, M. F. Gérard, D. Gilbert, I. Gouttevin, M. Grippa, G. Gruau, A. Jardani, L. Jeanneau, J. L. Join, H. Jourde, F. Karbou, D. Labat, Y. Lagadeuc, E. Lajeunesse, R. Lastennet, W. Lavado, E. Lawin, T. Lebel, C. Le Bouteiller, C. Legout, Y. Lejeune, E. Le Meur, N. Le Moigne, J. Lions, A. Lucas, J. P. Malet, C. Marais-Sicre, J. C. Maréchal, C. Marlin, P. Martin, J. Martins, J. M. Martinez, N. Massei, A. Mauclerc, N. Mazzilli, J. Molénat, P. Moreira-Turcq, E. Mougin, S. Morin, J. N. Ngoupayou, G. Panthou, C. Peugeot, G. Picard, M. C. Pierret, G. Porel, A. Probst, J. L. Probst, A. Rabatel, D. Raclot, L. Ravanel, F. Rejiba, P. René, O. Ribolzi, J. Riotte, A. Rivière, H. Robain, L. Ruiz, J. M. Sanchez-Perez, W. Santini, S. Sauvage, P. Schoeneich, J. L. Seidel, M. Sekhar, O. Sengtaheuanghoung, N. Silvera, M. Steinmann, A. Soruco, G. Tallec, E. Thibert, D. V. Lao, C. Vincent, D. Viville, P. Wagnon and R. Zitouna, 2018. OZCAR: The French Network of Critical Zone Observatories, Vadose Zone Journal, Volume: 17, Number:1, Doi: https://doi.org/10.2136/vzj2018.04.0067.

Gao, Z., Bresson R., Qu Y., Milliez M., de Munck C. and Carissimo B., 2018: High resolution unsteady RANS simulation of wind, thermal effects and pollution dispersion for studying urban renewal scenarios in a neighborhood of Toulouse. Urban Climate, Volume: 23, Special Issue: SI,Pages: 114-130, Doi: 10.1016/j.uclim.2016.11.002. Published: MAR 2018 3.

Garrigues, S., A. Boone, B. Decharme, A. Olioso, C. Albergel, J. Calvet, S. Moulin, S. Buis, and E. Martin, 2018: Impacts of the Soil Water Transfer Parametrization on the Simulation of Evapotranspiration over a 14-Year Mediterranean Crop Succession. Journal of Hydrometeorology, Volume: 19, Issue: 1, Pages: 3-25, Doi: 10.1175/JHM-D-17-0058.1. Published: JAN 2018.

Gelati, E., Decharme, B., Calvet, J.-C., Minvielle, M., Polcher, J., Fairbairn, D., and Weedon, G. P., 2018: Hydrological assessment of atmospheric forcing uncertainty in the Euro-Mediterranean area using a land surface model. Hydrological and Earth System Sciences, Volume: 22, Issue: 4, Pages: 2091-2115, Doi: 10.5194/hess-22-2091-2018. Published: APR 5 2018.

Gilet, J-B., Plu, M., Joly, A., et Arbogast, P.: The occurrence density of tracked tropopause coherent structures around intensifying mid-latitude surface cyclones. Journal of Atmospheric Sciences. 74, Issue 10, 451-3471.

Gustafsson, N. , Janjić, T. , Schraff, C. , Leuenberger, D. , Weissmann, M. , Reich, H. , Brousseau, P., Montmerle, T. , Wattrelot, E. , Bučánek, A. , Mile, M., Hamdi, R. , Lindskog, M. , Barkmeijer, J. , Dahlbom, M. , Macpherson, B. , Ballard, S. , Inverarity, G. , Carley, J. , Alexander, C. , Dowell, D. , Liu, S. , Ikuta, Y. and Fujita, T. (2018), Survey of data assimilation methods for convective-scale numerical weather prediction at operational centres. Quarterly Journal of the Royal Meteorological Society, Volume: 144 Issue: 713 Pages: 1218-1256 Part: B. Published: APR 2018 Doi: 10.1002/qj.3179.

Guth, J., Marécal, V., Josse, B., Arteta, J., and Hamer, P.: Primary aerosol and secondary inorganic aerosol budget over the Mediterranean Basin during 2012 and 2013. Atmospheric Chemistry and Physics, Volume: 18, Issue: 7, Pages: 4911-4934, Doi: 10.5194/acp-18-4911-2018. Published: APR 11 2018.

Hadad, D., Baray, JL., Montoux, N., Van Baelen, J., Freville, P., Pichon, JM., Bosser, P., Ramonet, M., Kwok, CY., Begue, N., al... Surface and Tropospheric Water Vapor Variability and Decadal Trends at Two Supersites of CO-PDD (Cézeaux and Puy de Dôme) in Central France. Atmosphere, Volume: 9, Issue: 8, Article Number: 302, Doi: 10.3390/atmos9080302. Published: AUG 2018.

Hagenmuller, P., A. van Herwijnen, C. Pielmeier and H.-P. Marshall, 2018: Evaluation of the snow penetrometer Avatech SP2. Cold Regions Science and Technology, Volume: 149, Pages: 83–94, Doi: 10.1016/J.COLDREGIONS.2018.02.006, Published: MAY 2018.

Hall, S. R., Ullmann, K., Prather, M. J., Flynn, C. M., Murray, L. T., Fiore, A. M., Correa, G., Strode, S. A., Steenrod, S. D., Lamarque, J.-F., Guth, J., Josse, B., Flemming, J., Huijnen, V., Abraham, N. L., and Archibald, A. T.: Cloud impacts on photochemistry: building a climatology of photolysis rates from the Atmospheric Tomography mission. Atmospheric Chemistry and Physics, Volume: 18, Issue: 22, Pages: 16809-16828, Doi: 10.5194/acp-18-16809-2018. Published: NOV 28 2018.

Hoarau, T., Barthe, C., Tulet, P., Claeys, M., Pinty, JP., Bousquet, O., Delanoe, J., Vie, B., Impact of the Generation and Activation of Sea Salt Aerosols on the Evolution of Tropical Cyclone Dumile, Journal of Geophysical Research-Atmospheres, Volume: 123, Issue: 16, Pages: 8813-8831, DOI: 10.1029/2017JD028125. Published: AUG 27 2018.

Hoarau, T., J-P Pinty and C Barthe, 2018: A representation of the collisional ice break-up process in the two-moment microphysics LIMA v1.0 scheme of Meso-NH. See here.

Illingworth, A. J., Bataglia A., Bradford J., Forsythe M., Joe P., Kollias P., Lean K., Lori M., Mahfouf J.-F., Mello S., Midthassel R., Munro Y., Nicol J., Pothast R., Rennie M., Stein T. H., M., Tanelli S., Tridon F., Walden C. J., & M. Wolde (2018): WIVERN: A new satellite concept to provide global in-cloud winds, precipitaton and cloud propertes, Bulletin of American Meteorology Society, Volume: 99, Issue: 8, Pages: 1669-1687, Doi: 10.1175/BAMS-D-16-0047.1. Published: AUG 2018.

Jaidan, N., El Amraoui, L., Attié, J.-L., Ricaud, P., and Dulac, F., 2018: Future changes in surface ozone over the Mediterranean Basin in the framework of the Chemistry-Aerosol Mediterranean Experiment (ChArMEx). Atmospheric Chemistry and Physics, Volume: 18, Issue: 13, Pages: 9351-9373, Doi: 10.5194/acp-18-9351-2018. Published: JUL 4 2018.

Kazadzis, S., Founda, D., Psiloglou, B., Kambezidis, H., Mihalopoulos, N., Sanchez-Lorenzo, A., Meleti, C., Raptis, P. I., Pierros, F. and Nabat, P., 2018 : Long-term series of surface solar radiation at Athens, Greece. Atmospheric Chemistry and Physicshem, Volume: 18, Issue: 4, Pages: 2395-2411, Doi: 10.5194/acp-18-2395-2018. Published: FEB 19 2018.

Kévin, L., Portafaix, T., Brogniez, C., Godin-Beekmann, S., Bencherif, H., Morel, B., Pazmino, A., Metzger, JM., Auriol, F., Deroo, C., Duflot, V., Goloub, P., and Charles, N. Long, CN. : Ultraviolet radiation modelling from ground-based and satellite measurements on Reunion Island, southern tropics. Atmospheric Chemistry And Physics, Volume : 18, Issue : 1, Pages: 227-246, Doi: 10.5194/acp-18-227-2018. Published: JAN 9 2018.

Kohno, N., Dube, SK., Entel, M., Fakhruddin, SHM., Greenslade, D., Leroux, MD., Rhome, J., Thuy, NB.,: RECENT PROGRESS IN STORM SURGE FORECASTING. Tropical Cyclone Research and Review, Volume: 7, Issue: 2, Pages : 128-139, Doi: 10.6057/2018TCRR02.04. Published: MAY 15 2018.

Kokhanovsky, A., M. Lamare, B. Di Mauro, G. Picard, L. Arnaud, M. Dumont, F. Tuzet, C. Brockmann and J. E. Box, 2018: On the reflectance spectroscopy of snow. The Cryosphere,Volume: 12, Pages: 2371-2382, Doi: 10.5194/tc-12-2371-2018, Published: JUL 2018.

Krinner, G., Derksen, C., Essery, R., Flanner, M., Hagemann, S., Clark, M., Hall, A., Rott, H., Brutel-Vuilmet, C., Kim, H., Ménard, C. B., Mudryk, L., Thackeray, C., Wang, L., Arduini, G., Balsamo, G., Bartlett, P., Boike, J., Boone, A., Chéruy, F., Colin, J., Cuntz, M., Dai, Y., Decharme, B., Derry, J., Ducharne, A., Dutra, E., Fang, X., Fierz, C., Ghattas, J., Gusev, Y., Haverd, V., Kontu, A., Lafaysse, M., Law, R., Lawrence, D., Li, W., Marke, T., Marks, D., Ménégoz, M., Nasonova, O., Nitta, T., Niwano, M., Pomeroy, J., Raleigh, M. S., Schaedler, G., Semenov, V., Smirnova, T. G., Stacke, T., Strasser, U., Svenson, S., Turkov, D., Wang, T., Wever, N., Yuan, H., Zhou, W. and Zhu, D., 2018: ESM-SnowMIP: assessing snow models and quantifying snow-related climate feedbacks. Geoscience Model Developement, Volume: 11, Issue: 12, Pages: 5027-5049, Doi: https://doi.org/10.5194/gmd-11-5027-2018.

Krysztofiak, G., V. Catoire, P. D. Hamer, V. Marécal, C. Robert, A. Engel, H. Bönisch, K. Grossman, B. Quack, E. Atlas and K. Pfeilsticker, 2018: Evidence of convective transport in tropical West Pacific region during SHIVA experiment. Atmospheric Science Letters, Volume: 19, Issue: 1, Article Number: UNSP e798, Doi: 10/1002/asl.798. Published: JAN 2018.

Kurzrock, F., Cros, S., Chane-Ming, F., Otkin, J., Hutt, A., Linguet, L., Lajoie, G., Potthast, R., .A Review of the Use of Geostationary Satellite Observations in Regional-Scale Models for Short-term Cloud Forecasting. Meteorologische Zeitschrift, Berlin, Volume: 27, Issue: 4, Pages: 277-298, Doi: 10.1127/metz/2018/0904. Published: 2018.

Lac, C., Chaboureau, J.-P., Masson, V., Pinty, J.-P., Tulet, P., Escobar, J., Leriche, M., Barthe, C., Aouizerats, B., Augros, C., Aumond, P., Auguste, F., Bechtold, P., Berthet, S., Bielli, S., Bosseur, F., Caumont, O., Cohard, J.-M., Colin, J., Couvreux, F., Cuxart, J., Delautier, G., Dauhut, T., Ducrocq, V., Filippi, J.-B., Gazen, D., Geoffroy, O., Gheusi, F., Honnert, R., Lafore, J.-P., Lebeaupin Brossier, C., Libois, Q., Lunet, T., Mari, C., Maric, T., Mascart, P., Mogé, M., Molinié, G., Nuissier, O., Pantillon, F., Peyrillé, P., Pergaud, J., Perraud, E., Pianezze, J., Redelsperger, J.-L., Ricard, D., Richard, E., Riette, S., Rodier, Q., Schoetter, R., Seyfried, L., Stein, J., Suhre, K., Taufour, M., Thouron, O., Turner, S., Verrelle, A., Vié, B., Visentin, F., Vionnet, V., and Wautelet, P., 2018: Overview of the Meso-NH model version 5.4 and its applications. Geoscientific Model Development, Volume : 11, Issue : 5, Pages: 1929-1969, Doi : Published: MAY 29 2018 .

Lac, C., Chaboureau, P., Masson, V., Pinty, P., Tulet, P., Escobar, J., Leriche, M., Barthe, C., Aouizerats, B., Augros, C., Aumond, P., Auguste, F., Bechtold, P., Berthet, S., al.... : Temperature inter-comparison effort in the framework of Hydrological Cycle in the Mediterranean Experiment – Special Observation Period (HyMeX-SOP1). Geoscientific Model Development, Copernicus Publ, 2018, pp.1929-1969. Doi: 10.5194/gmd-2017-297.

Lac, C., J.-P. Chaboureau, V. Masson, P. Tulet, J. Escobar, C. Augros, S. Bieilli, O. Caumont, J. Colin, F. Couvreux, G. Delautier, V. Ducrocq, R. Honnert, J.-P. Lafore, C. Lebeaupin Brossier, Q. Libois, O. Nuissier, P. Peyrillé, J. Perraud, J.-L. Redelsperger, D. Ricard, S. Riette, Q. Rodier, R. Schoetter, O.Pergaud, E. Thouron, S. Turner, A. Verrelle, B. Vié, V. Vionnet and al. 2018: Overview of the Meso-NH model version 5.4 and its applications. Geoscientific Model Development, Volume: 11, Issue: 5, Pages: 1929-1969, Doi: 10.5194/gmd-11-1929-2018. Published: MAY 29 2018.

Lamy, K., Portafaix, T., Josse, B., Brogniez, C., Godin-Beekmann, S., Benchérif, H., Revell, L., Akiyoshi, H., Bekki, S., Hegglin, M., Jöckel, P., Kirner, O., Marecal, V., Morgenstern, O., Stenke, A., al... : Ultraviolet Radiation modelling using output from the Chemistry Climate Model Initiative. Atmospheric Chemistry and Physics Discussions, European Geosciences Union, In press, Doi: 10.5194/acp-2018-525.

Lancz, D., Balázs Szintai, Rachel Honnert : Modification of shallow convection parametrization in the gray zone in a mesoscale model, Boundary-layer Meteorology, Volume: 169, Issue: 3, Pages: 483-503, Doi: 10.1007/s10546-018-0375-1. Published: DEC 2018.

Langford, AO., Alvarez, RJ., Brioude, J., Evan, S., Iraci, LT., Kirgis, G., Kuang, S., Leblanc, T., Newchurch, MJ., Pierce, RB., al... Coordinated profiling of stratospheric intrusions and transported pollution by the Tropospheric Ozone Lidar Network (TOLNet) and NASA Alpha Jet experiment (AJAX): Observations and comparison to HYSPLIT, RAQMS, and FLEXPART. Atmospheric Environment, Volume: 174, Pages: 1-14, Doi: Published: FEB 2018.

Larroza, EG., Keckhut, ., Baray, JL., Nakaema, WM., Veremes, H., Landulfo, E., Dionisi, D., Khaykin, S., Ravetta, F.,: Long-Range Transport of Water Channelized through the Southern Subtropical Jet: Atmosphere, Volume: 9, Issue: 10, Article Number: 374, Doi : 10.3390/atmos9100374. Published: OCT 2018.

Larue, F., A. Royer, D. De Sève, A. Roy, G. Picard, V. Vionnet and E. Cosme, 2018 : Simulation and assimilation of passive microwave data using a snowpack model coupled to a calibrated radiative transfer model over North–Eastern Canada. Water Resources Research, Volume: 54, Pages: ??, Doi: 10.1029/2017WR022132, Published: JUN 2018.

Le Quéré, C., Andrew, R. M., Friedlingstein, P., Sitch, S., Pongratz, J., Manning, A. C., Korsbakken, J. I., Peters, G. P., Canadell, J. G., Jackson, R. B., Boden, T. A., Tans, P. P., Andrews, O. D., Arora, V. K., Bakker, D. C. E., Barbero, L., Becker, M., Betts, R. A., Bopp, L., Chevallier, F., Chini, L. P., Ciais, P., Cosca, C. E., Cross, J., Currie, K., Gasser, T., Harris, I., Hauck, J., Haverd, V., Houghton, R. A., Hunt, C. W., Hurtt, G., Ilyina, T., Jain, A. K., Kato, E., Kautz, M., Keeling, R. F., Klein Goldewijk, K., Körtzinger, A., Landschützer, P., Lefèvre, N., Lenton, A., Lienert, S., Lima, I., Lombardozzi, D., Metzl, N., Millero, F., Monteiro, P. M. S., Munro, D. R., Nabel, J. E. M. S., Nakaoka, S.-I., Nojiri, Y., Padin, X. A., Peregon, A., Pfeil, B., Pierrot, D., Poulter, B., Rehder, G., Reimer, J., Rödenbeck, C., Schwinger, J., Séférian, R., Skjelvan, I., Stocker, B. D., Tian, H., Tilbrook, B., Tubiello, F. N., van der Laan-Luijkx, I. T., van der Werf, G. R., van Heuven, S., Viovy, N., Vuichard, N., Walker, A. P., Watson, A. J., Wiltshire, A. J., Zaehle, S., and Zhu, D., 2018: Global Carbon Budget 2017. Earth System Science Data, Volume: 10, Issue: 1, Pages: 405-448, Doi: 10.5194/essd-10-405-2018. Published: MAR 12 2018.

Leroux, D.J., Calvet, J.C., Munier, S., Albergel, C., 2018: Using Satellite-Derived Vegetation Products to Evaluate LDAS-Monde over the Euro-Mediterranean Area. REMOTE SENSING Volume: 10. Issue: 8. Article Number: 1199. Published: AUG 2018.

Leroux, MD., Meister, J., Mekies, D., Dorla, AL., Caroff, P.,: A Climatology of Southwest Indian Ocean Tropical Systems : Their Number, Tracks, Impacts, Sizes, Empirical Maximum Potential Intensity, and Intensity Changes. Journal of Applied Meteorology and Climatology, Volume: 5, Issue: 4, Pages: 1021-1041, Doi: 10.1175/JAMC-D-17-0094.1. Published: APR 2018.

Leroux, MD., Wood, K., Elsberry, RL., Cayanan, EO., Es Hendricks, E., Kucas, M., Otto, P., Rogers, R., Sampson, B., Yu, ZF. Tropical Cyclone Research and Review Volume: 7 Issue: 2 Pages: 85-105, Doi: 10.6057/2018TCRR02.02. Published: MAY 15 2018.

López-Moreno, J. I., F. Navarro-Serrano, C. Azorín-Molina, P. Sánchez-Navarrete, E. Alonso-González, I. Rico, E. Morán-Tejeda, S. Buisan, J. Revuelto, M. Pons, and S.M. Vicente-Serrano, 2018: Air and wet bulb temperature lapse rates and their impact on snowmaking in a Pyrenean ski resort. Theoretical and Applied Climatology, Volume: 132, Pages: 1-13, Doi: 10.1007/s00704-018-2448-y, Published: MAR 2018.

Mallet, PE., Pujol, O., Brioude, J., Evan, S., Jensen, A.,: Marine aerosol distribution and variability over the pristine Southern Indian Ocean. Atmospheric Environment, Volume: 182, Pages: 17-30, Doi: 10.1016/j.atmosenv.2018.03.016. Published: JUN 2018.

Marquet, P. and Th. Dauhut, 2018: Reply to "Comments on 'A Third-Law Isentropic Analysis of a Simulated Hurricane". Journal of the Atmospheric Sciences, Volume: 75, Issue: 10, Pages : 3735-3747, Doi: 10.1175/JAS-D-18-0126.1. Published: OCT 2018. Vol.75, N°10, p.3735-3747.

Marquet, P., J.-F. Mahfouf and D. Holdaway (2018): Defniton of the moist-air available enthalpy (exergy) norm: a comparision with existng "moist energy norms". Quarterly Journal of the Royal Meteorological Society (soumis).

Masson, T., M. Dumont, M. D. Mura, P. Sirguey, S. Gascoin, J.-P. Dedieu and J. Chanussot, 2018: An Assessment of Existing Methodologies to Retrieve Snow Cover Fraction from MODIS Data. Remote Sensing, Volume: 10, Issue: 4, Pages: 619, Doi: 10.3390/rs10040619, Published: APR 2018.

Masson, T., M. Dumont, M. D. Mura, P. Sirguey, S. Gascoin, J.-P. Dedieu and J. Chanussot, 2018: An Assessment of Existing Methodologies to Retrieve Snow Cover Fraction from MODIS Data. Remote Sensing, Volume: 10, Issue: 4, Pages: 619, Doi: 10.3390/rs10040619, Published: APR 2018.

Masson, V., Lemonsu A. and Voogt J., 2018: The 9th International Conference on Urban Climate. Urban Climate, Volume: 23, Special Issue: SI, Pages: 1-7, Doi: 10.1016/j.uclim.2017.07.007. Published: MAR 2018 23.

Mede, T., Chambon, G., Hagenmuller, P., & Nicot, F. (2018). A medial axis based method for irregular grain shape representation in DEM simulations. Granular Matter, Volume: 20, Doi: https://doi.org/10.1007/s10035-017-0785-7, Published: APR 2018.

Meloni, D., di Sarra, A., Brogniez, G., Denjean, C., De Silvestri, L., Di Iorio, T., Formenti, P., Gómez-Amo, J. L., Gröbner, J., Kouremeti, N., Liuzzi, G., Mallet, M., Pace, G., and Sferlazzo, D. M.: Determining the infrared radiative effects of Saharan dust: a radiative transfer modelling study based on vertically resolved measurements at Lampedusa. Atmospheric Chemistry And Physics, Volume: 18, Issue: 6, Pages: 4377-4401, Doi : 10.5194/acp-18-4377-2018. Published: MAR 29 2018.

Meloni, D., di Sarra, A., Brogniez, G., Denjean, C., De Silvestri, L., Di Iorio, T., Formenti, P., Gómez-Amo, J. L., Gröbner, J., Kouremeti, N., Liuzzi, G., Mallet, M., Pace, G., and Sferlazzo, D. M.: Determining the infrared radiative Saharan dust: a radiative transfer modelling study based on vertically resolvedeffects of measurements at Lampedusa. Atmospheric Chemistry And Physics, Volume: 18, Issue: 6, Pages: 4377-4401, Doi: 10.5194/acp-18-4377-2018. Published: MAR 29 2018.

Mercier F., Gürol S., Jolivet P., Michel Y. and Montmerle T : 2018a: Block Krylov methods for accelerating ensembles of variational data assimilations. Quarterly Journal of the Royal Meteorological Society, TY Volume: 144, Issue : 717, Pages: 2463-2480, Part: B, Doi: 10.1002/qj.3329. Published: OCT 2018.

Mercier, F., Michel, Y., Montmerle, T , Gürol S. and P. Jolivet : 2018b : Speeding up the ensemble data assimilation system of the limited area model of Météo France using a Block Krylov algorithm. Accepted for publication in Quarterly Journal of the Royal Meteorological Society.

Michel, Y.: Revisiting Fisher's approach to the handling of horizontal spatial correlations of the observation errors in a variational framework. Quarterly Journal of the Royal Meteorological Society, AL Volume: 144, Issue : 716, Pages: 2011-2025, Part : A, Doi: 10.1002/qj.3249. Published: OCT 2018.

Michel, Y. and S. Guedj: Correlated observation errors in a variational framework, Quarterly Journal of the Royal Meteorological Society.

Montmerle, T., Michel Y. , Arbogast E., Ménétrier B. and P. Brousseau, 2018: A 3D Ensemble Variational Data Assimilation Scheme for the limited area AROME model: formulation and preliminary results. Quarterly Journal of the Royal Meteorological Society, Volume: 144, Issue: 716 , Pages: 2196-2215, Part: A, Doi: 10.1002/qj.3334. Published: OCT 2018.

Mudryk, L. R., C. Derksen, S. Howell, F. Laliberté, C. Thackeray, R. Sospedra-Alfonso, V. Vionnet, P.J. Kushner and R. Brown, 2018: Canadian snow and sea ice: historical trends and projections. The Cryosphere, Volume: 12, Pages: 1157-1176, Doi: 10.5194/tc-12-1157-2018, Published: MAR 2018.

Munier, S., D. Carrer, C. Planque, F. Camacho, C. Albergel, and J.-C. Calvet : Satellite Leaf Area Index: global scale analysis of the tendencies per vegetation type over the last 17 years. Remote

Sensing, Volume: 10, Issue: 3, Article Number: 424, Doi: 10.3390/rs10030424. Published: MAR 2018 10.

Muñoz-Sabater, J.; de Rosnay, P.; Albergel, C.; Isaksen, L. , 2018: Sensitivity of Soil Moisture Analyses to Contrasting Background and Observation Error Scenarios. Water, Volume: 10, Issue: 7, Article Number: 890, Doi: 10.3390/w10070890. Published: JUL 2018.

Nicolet, G., N. Eckert, S. Morin and J. Blanchet, 2018: Assessing climate change impact on the spatial dependence of extreme snow depth maxima in the French Alps. Water Resources Research, Volume: 54, Doi: https://doi.org/10.1029/2018WR022763, Published: OCT. 2018.

Obermann-Hellhund A., D. Conte, S. Somot, C.Z. Torma, B. Ahrens B., 2017 : Mistral and Tramontane wind systems in regional and global climate simulations from 1950 to 2100. Climate Dynamics, Volume: 50, Issue : 1-2, Pages: 693-703, Doi: 10.1007/s00382-017-3635-8, pp.1-11. Published: JAN 2018.

Orbe, C., D. H. Yang, W. Waugh, G. Zeng, O. Morgenstern, D. E. Kinnison, J.-F. Lamarque, S. Tilmes, D. A. Plummer, J. F. Scinnoca, B Josse,V. Marécal, P. Jockel, L. D. Oman, S. E. Strahan, M. Deushi, T. Y. Tanaka, K. Yoshida, H. Akiyoshi, Y. Yamashita, A. Stenke, L. Revell, T. Sukhodolov, E. Rozanov, G. Pitari, D. Visioni, K. A. Stone, and R. Schofield, Large-scale tropospheric transport in the Chemistry-Climate-Initiative (CCMI) simulations, Atmospheric Chemistry and Physics, Volume: 18, Issue: 10, Pages: 7217-7235, Doi: 10.5194/acp-18-7217-2018. Published: MAY 25 2018.

Osinski, R. and F. Bouttier, 2017: Short-range probabilistic forecasting of convective risks for aviation based on a LAF-ensemble approach. Meteorological Applications, Volume: 25, Issue: 1, Pages: 105-118, Doi: 10.1002/met.1674. Published : JAN 2018.

Pianezze, J., Barthe, C., Bielli, S., Tulet, P., Jullien, S., Cambon, G., Bousquet, O., Claeys, M., Cordier, E., A New Coupled Ocean-Waves-Atmosphere Model Designed for Tropical Storm Studies: Example of Tropical Cyclone Bejisa (2013-2014) in the South-West Indian Ocean. Journal of Advances in Modeling Earth Systems, Volume: 10, Issue: 3, Pages: 801-825, Doi: 10.1002/2017MS001177. Published: MAR 2018.

Pineau-Guillou, L., F. Ardhuin, M.-N. Bouin, J.-L. Redelsperger, B. Chapron, J.R. Bidlot and Y. Quilfen, 2018: Strong winds in a coupled waveatmosphere model during a North Atlantic storm event: evaluation against observations. Quarterly Journal of the Royal Meteorological Society, Volume: 144, Issue: 711, Pages: 317-332, Part: B, Doi : 10.1002/qj.3205. Published: JAN 2018.

Planton, Y., A. Voldoire, H. Giordani, G. Caniaux, Main processes of interannual variability of the atlantic cold tongue, Climate Dynamics, Volume: 50, Issue: 5-6, Pages: 1495-1512, Doi: 10.1007/s00382-017-3701-2. Published: MAR 2018.

Price, J. D. , S. Lane, I. A. Boutle, D. K. E. Smith, T. Bergot, C. Lac, L. Duconge, J. McGregor, A. Kerr-Munslow, M. Pickering, and R. Clark, 2018: LANFEX: A Field and Modeling Study to Improve Our Understanding and Forecasting of Radiation Fog. Bulletin of American Meteorology Society, vol 99.

Queno, L., V. Vionnet, F. Cabot, D. Vrecourt and I. Dombrowski-Etchevers, 2018: Forecasting and modelling ice layer formation on the snowpack due to freezing precipitation in the Pyrenees. Cold Regions Science and Technology, Volume: 146, Pages: 19-31, Doi: 10.1016/j.coldregions.2017.11.007, Published: FEB 2018.

Raynaud, L., Touze, B., et Arbogast, P.,Detection of Severe Weather Events in a High-Resolution Ensemble Prediction System Using the Extreme Forecast Index (EFI) and Shift of Tails (SOT). Weather And Forecasting, Volume: 33, Issue: 4, Pages : 901-908, Doi: 10.1175/WAF-D-17-0183.1. Published: AUG 2018.

Renard J-B, F. Dulac, P. Durand, Q. Bourgeois, C. Denjean, D. Vignelles, B. Couté, M. Jeannot, N. Verdier, and M. Malle, 2018: In situ measurements of desert dust particles above the western Mediterranean Sea with the balloonborne Light Optical Aerosol Counter/sizer (LOAC) during the ChArMEx campaign of summer 2013. Atmospheric Chemistry And Physics, Volume: 18, Issue: 5, Pages: 3677-3699, Doi : 10.5194/acp-18-3677-2018. Published: MAR 13 2018.

Réveillet, M., D. Six, C. Vincent, A. Rabatel, M. Dumont, M. Lafaysse, S. Morin, V. Vionnet and M. Litt, 2018: Relative performance of empirical and physical models in assessing the seasonal and annual glacier surface mass balance of Saint-Sorlin Glacier (French Alps). The Cryosphere,Volume: 12, Pages: 1367-1386, Doi: https://doi.org/10.5194/tc-12-1367-2018, Published: APR 2018.

Revuelto, J., G. Lecourt, M. Lafaysse, I. Zin, L. Charrois, V. Vionnet, M. Dumont, A. Rabatel, D. Six, T. Condom, S. Morin, A. Viani and P. Sirguey, 2018: Multi-Criteria Evaluation of Snowpack Simulations in Complex Alpine Terrain Using Satellite and In Situ Observations. Remote Sensing, Volume:10, Issue: 8, Page: 1171, Doi: http://www.mdpi.com/2072-4292/10/8/1171, Published: JUL 2018.

Ricaud, P., R. Zbinden, V. Catoire, V. Brocchi, F. Dulac, E. Hamonou, J.-C. Canonici, L. El Amraoui, S. Massart, B. Piguet, U. Dayan, P. Nabat, J. Sciare, M. Ramonet, M. Delmotte, A. di Sarra, D. Sferlazzo, T. Di Iorio, S. Piacentino, P. Cristofanelli, N. Mihalopoulos, G. Kouvarakis, M. Pikridas, C. Savvides, R. Mamouri, A. Nisantzi, D. Hadjimitsis, J.-L. Attié, H. Ferré, P. Theron, Y. Kangah, N. Jaidan, J. Guth, P. Jacquet, S. Chevrier, C. Robert, A. Bourdon, J.-F. Bourdinot, J.-C. Etienne, G. Krysztofiak, P. Theron, 2018: The GLAM Airborne Campaign over the Mediterranean Basin. Bulletin of the American Meteorological Society, Volume: 99, Issue: 2, Pages: 361-380, Doi: 10.1175/BAMS-D-16-0226.1. Published: FEB 2018.

Richon, C., Dutay, J.-C., Dulac, F., Wang, R., Balkanski, Y., Nabat, P., Aumont, O., Desboeufs, K., Laurent, B., Guieu, C., Raimbault, P., Beuvier, J., 2017: Modeling the impacts of atmospheric deposition of nitrogen and desert dust–derived phosphorus on nutrients and biological budgets of the Mediterranean Sea : Progress in Oceanography, Volume: 163, Special Issue: SI, Pages: 21-39, Doi: 10.1016/j.pocean.2017.04.009. Published: APR 2018.

Roca, R., Dejus, M., Chambon, P., Cloché, S., Capderou, M., 2018: The Megha-Tropiques mission after 7 years in space. Soumis pour publication dans le livre "Satellite Precipitation Measurement" aux éditions Springer.

Roca, R., Guérou, A., Junca R., Chambon, P., Gosset, M., Cloché, S., Schröder, M., 2018: Merging the infrared fleet and the microwave constellation for Tropical Hydrometeorology (TAPEER) and global climate monitoring (GIRAFE) applications. Soumis pour publication dans le livre "Satellite Precipitation Measurement" aux éditions Springer.

Roca, R., Taburet, N., Lorant, E., Chambon, P., Alcoba, M., Brogniez, H., Cloché, S., Dufour, C., Gosset, M., Guilloteau, C., 2017: Quantifying the contribution of the Megha-Tropiques mission to the estimation of daily accumulated rainfall in the Tropics. Quarterly Journal of the Royal Meteorological Society, Volume: 144, Issue: S1, Pages 49-63, Doi: 10.1002/qj.3327. Published: 29 juin 2018.

Rogers, R., Cheung, K., Russel, R., Elsberry, Kohno, N., Leroux, MD., Otto, P.: The World Meteorological Organization's Fourth International Workshop on Tropical Cyclone Landfall Processes (IWTCLP-IV): A Summary. Tropical Cyclone Research and Review, Volume: 7, Issue: 2, Pages: 77-84, Doi: 10.6057/2018TCRR02.01. Published: MAY 15 2018.

Schafler, A., Craig, G., Wernli, H., Arbogast, P. Doyle, J.D., James. D., McTaggart-Cowan, R. Methven, J., Riviere, G., Ament, F., Boettcher, M., Al... . The North Atlantic Wave guide and Downsream Impac Experiment. Bulletin of the American Meteorology Society, Volume: 99, Issue: 8, Pages: 1607-1637, Doi: 10.1175/BAMS-D-17-0003.1. Published: AUG 2018.

Schön, P., F. Naaim-Bouvet, V. Vionnet and A. Prokop, 2018: Merging a terrain-based parameter with blowing snow fluxes for assessing snow redistribution in alpine terrain. Cold Regions Science and Technology, Volume: 155, Pages: 161-173, Doi: https://doi.org/10.1016/j.coldregions.2018.08.002, Published: NOV 2018.

Séférian R., M. Rocher, C. Guivarch, J. Colin, 2018: Constraints on biomass energy deployment in mitigation pathways : the case of water scarcity. Environmental Research Letters, Volume: 13, Issue: 5, Article Number: 054011, Doi: 10.1088/1748-9326/aabcd7. Published: MAY 2018.

Séférian, R., Berthet, S. & Chevallier, M., 2018: Assessing the decadal predictability of land and ocean carbon uptake. Environmental Research Letters, Volume: 45, Issue: 5, Pages: 2455-2466, Doi: 10.1002/2017GL076092. Published: MAR 16 2018.

Séférian, R., S. Baek, O. Boucher, J.-L. Dufresne, B. Decharme, D. Saint-Martin and R. Roehrig, 2017: An interactive ocean surface albedo scheme (OSAv1.0): formulation and evaluation in ARPEGE-Climat (V6.1) and LMDZ (V5A) : Geoscientific Model Development, Volume: 11, Issue: 1, Pages: 321-338, Doi : 10.5194/gmd-11-321-2018. Published: JAN 23 2018.

Seneviratne S., J. Rogelj, R. Séférian and al., 2018: The many possible climates from the Paris Agreement's aim of 1.5 °C warming. Nature, Volume: 558, Issue: 7708, Pages: 41-49, Doi: 10.1038/s41586-018-0181-4.Published: JUN 7 2018.

Skiles, S. M., M. Flanner, J. M. Cook, M. Dumont and T. H. Painter, 2018: Radiative forcing by light-absorbing particles in snow. Nature Climate Change, Doi: https://doi.org/10.1038/s41558-018-0296-5.

Somot, S; Houpert, Loic; Sevault, Florence; Testor, P. ; Bosse, A.; Taupier-Letage, I; Bouin, MN ; Waldman, R ; Cassou, C ; Sanchez-Gomez, E, 2018: Characterizing, modelling and understanding the climate variability of the deep water formation in

the North-Western Mediterranean Sea. Climate Dynamics, Volume: 51, Issue: 3, Special Issue: SI, Pages: 1179-1210, Published: AUG 2018.

Stavropulos-Laffaille X., K. Chancibault, J.-M. Brun, A. Lemonsu, V. Masson, A. Boone and H. Andrieu, 2018: Improvements to the hydrological processes of the Town Energy Balance model (TEB-Veg, SURFEX v7.3) for urban modelling and impact assessment - Geoscientific Model Development, 11, 4175-4194.

Su, Z., W. Timmermans, Y. Zeng, J. Schulz, V. O. John, R. A. Roebeling, P. Poli, D. Tan, F. Kaspar, A. Kaiser-Weiss, E. Swinnen, C. Toté, H. Gregow, T. Manninen, A. Riihelä, J.-C. Calvet, Y. Ma, and J. Wen: An overview of European efforts in generating climate data records. Bulletin of American Meteorology Society, Volume: 99, Issue: 2, Pages: 349-359, Doi: 10.1175/BAMS-D-16-0074.1. Published: FEB 2018.

Taufour, M., Vie, B., Augros, C., Boudevillain, B. Delanoe, J. Delautier, G. Ducrocq, V. Lac, C. Pinty, JP. Et Schwarzenbock, A. : Evaluation of the two-moment scheme LIMA based on microphysical observations from the HyMeX campaign Quaterly Journal of the Royal Meteorological Volume: 144 Issue: 714 Pages: 1398-1414 Part: A DOI: 10.1002/qj.3283 Published: JUL 2018.

Techel, F., C. Mitterer, E. Ceaglio, C. Coléou, S. Morin, F. Rastelli and R. S. Purves, 2018 : Spatial consistency and bias in avalanche forecasts – a case study in the European Alps. Natural Hazards and Earth System Sciences, Volume: 18, Issue: 10, Pages: 2697-2716, Doi: https://doi.org/10.5194/nhess-18-2697-2018, Published: OCT 2018.

Termonia, P., C. Fischer, E. Bazile, F. Bouyssel, R. Brožková, Pierre Bénard, B. Bochenek, D. Degrauwe, M. Derkova, R. El Khatib, R. Hamdi, J. Mašek, P. Pottier, N. Pristov, Y. Seity, P. Smolíková, O. Spaniel, M. Tudor, Y. Wang, C. Wittmann and A. Joly, 2017: The ALADIN System and its Canonical Model Configurations AROME CY41T1 and ALARO CY40T1. Geoscientific Model Development, Volume: 11, Pages: 257-281, Doi: 10.5194/gmd-11-257-2018. Published: 18 Jan 2018.

Testor P., Bosse A., Houpert L., Margirier F., Mortier L., Lego H., Dausse D., Labaste M., Karstensen J., Hayes D., Olita A., Ribotti A., Schroeder K., Chiggiato J., Onken R., Heslop E., Mourre B., D'Ortenzio F., Mayot N., Lavigne H., de Fommervault O., Coppola L., Prieur L., Taillandier V., Durrieu de Madron X., Bourrin F., Many G., Damien P., Estournel C., Marsaleix P., Taupier-Letage I., Raimbault P. Waldman R., Bouin M.-N., Giordani H., Caniaux G., Somot S., Ducrocq V., Conan P. (2017) Multiscale observations of deep convection in the northwestern Mediterranean Sea during winter 2012-2013 using multiple platforms: Journal of Geophysical Research-Oceans, Volume: 123, Issue: 3, Pages: 1745-1776, Doi: 10.1002/2016JC012671. Published: MAR 2018.

Thibert, E., P. Dkengne Sielenou, V. Vionnet, N. Eckert and C. Vincent, 2018: Causes of glacier melt extremes in the Alps since 1949. Geophysical Research Letters, Volume: 45, Doi: 10.1002/2017GL076333, Published: JAN 2018.

Toihir, AM., Portafaix, T., Sivakumar, V., Bencherif, H., Pazmino, A., Begue, N.,: Variability and trend in ozone over the southern tropics and subtropics. Annales Geophysicae, Volume : 36, Issue: 2, Pages: 381-404, Doi: 10.5194/angeo-36-381-2018. Published: MAR 16 2018.

Touzeau, A., A. Landais, S. Morin, L. Arnaud and G. Picard, 2018: Numerical experiments on vapor diffusion in polar snow and firn and its impact on isotopes using the multi-layer energy balance model Crocus in SURFEX v8.0. Geoscientific Model Development, Volume: 11, Issue: 6, Pages: 2393-2418, Doi: https://doi.org/10.5194/gmd-11-2393-2018, Published: JUN 2018.

Tramblay, Y., Jarlan L., Hanich L., Somot S. (2017) Future scenarios for surface water resources availability in North African dams: Water Resources Management, Volume: 32, Issue: 4, Pages: 1291-1306, Doi:10.1007/s11269-017-1870-8. Published: MAR 2018.

Van Weverberg, K., C. J. Morcrette, J. Petch, S. A. Klein, H.-Y. Ma, C. Zhang, S. Xie, Q. Tang, W. I. Gustafson Jr, Y. Qian, L. K. Berg, Y. Liu, M. Huang, M. Ahlgrimm, R. Forbes, E. Bazile, R. Roehrig, J. Cole, W. Merryfield, W.-S. Lee, F. Cheruy, L. Mellul, Y.-C. Wang, K. Johnson, M. M. Thieman. CAUSES: Attribution of Surface Radiation Biases in NWP and Climate Models near the U.S. Southern Great Plains. Journal of Geophysical Research-Atmospheres, Volume: 123 Issue: 7 Pages: 3612-3644. Doi: 10.1002/2017JD027188 Published: APR 16 2018.

Venturini, MS., Bageston, JV., Caetano, NR., Peres, LV., Bencherif, H., Schuch, NJ.,: Mesopause region temperature variability and its trend in southern Brazil: Annales Geophysicae, Volume: 36, Issue: 2, Pages: 301-310, Doi: 10.5194/angeo-36-301-2018. Published: MAR 5 2018.

Vérèmes, H., Payen, G., Keckhut, P., Duflot, V., Baray, JL., Cammas, JP., Leclair de Bellevue, J., Posny, F., Evan, S., Metzger, JM., Marquestaut, N., al... : Ultraviolet Radiation modelling using output from the Chemistry Climate Model Initiative. EPJ Web of Conferences, EDP Sciences, 2018, The 28th International Laser Radar Conference (ILRC 28), Bucharest 2017, 176, pp.05015. Doi: 10.1051/epjconf/201817605015.

Verfaillie, D., M. Lafaysse, M. Déqué, N. Eckert, Y. Lejeune and S. Morin, 2018: Multi-components ensembles of future meteorological and natural snow conditions in the Northern French Alps. The Cryosphere, Volume: 12, Pages: 1249-1271, Doi: 10.5194/tc-12-1249-2018, Published: APR 2018.

Viani, A., T. Condom, C. Vincent, A. Rabatel, B. Bacchi, J. E. Sicart, J. Revuelto, D.Six and I.Zin, 2018. Glacier-wide summer surface mass balance reconstruction: hydrological balance applied on Argentière and Mer de Glace drainage basins (Mont Blanc, France). Journal of Glaciology, Volume: 64, Issue: 243, Pages: 119-131, Doi: https://doi.org/10.1017/jog.2018.7, Published: FEB 2018.

Vidot, J., Brunel P., Dumont M., Carmagnola C., Hocking J., 2018: The VIS/NIR Land and Snow BRDF Atlas for RTTOV: Comparison between MODIS MCD43C1 C5 and C6. Remote Sensing, Volume: 10, Issue: 1, Article Number: 21, Doi: 10.3390/rs10010021. Published: JAN 2018.

Vincent C., M. Dumont, D. Six, F. Brun, G. Picard and L. Arnaud, 2018 : Why do the dark and light ogives of Forbes bands have similar surface mass balances ? Journal of Glaciology, Volume: 64, Pages: 1-11. Doi: https://doi.org/10.1017/jog.2018.12, Published: APR 2018.

Vionnet, V., G. Guyomarc'h, M. Lafaysse, F. Naaim-Bouvet, G. Giraud and Y. Deliot, 2018: Operational implementation and evaluation of a blowing snow scheme for avalanche hazard forecasting. Cold Regions Science and Technology, Volume: 147, Pages: 1-10, Doi: 10.1016/j.coldregions.2017.12.006, Published: MAR 2018.

Xueref, R., I., Dieudonne, E., Vuillemin, C., et al.: Diurnal, synoptic and seasonal variability of atmospheric CO_2 in the Paris megacity area : Atmospheric Chemistry and Physics, Volume: 18, Issue: 5, Pages: 3335-3362, Doi : 10.5194/acp-18-3335-2018. Published: MAR 7 2018.

Yano J.-I., M. Z. Ziemian´ski, M. Cullen, P. Termonia, J. Onvlee, L. Bengtsson, A. Carrassi, R. Davy, A. Deluca, S. L. Gray, V. Homar, M. Köhler, S. Krichak, S. Michaelides, V. T. J. Phillips, P. M. M. Soares, and A. Wyszogrodzki, 2018: Scientific Challenges of Convective-Scale Numerical Weather Prediction, Bulletin of the American Meteorological Society, Volume: 99, Issue: 4, Pages: 699-710, Doi: 10.1175/BAMS-D-17-0125.1. Published: APR 2018.

Yano, J-I, Andrew J. Heymsfield, and A. Bansemer, 2018: Determination of the Ice Particle Size Distributions Using Observations as the Integrated Constraints, Journal of the Atmospheric Sciences - Volume: 75, Number: 3 (March 2018).

Zhang, S., Calvet, J.-C., Darrozes, J., Roussel, N., Frappart, F., Bouhours, G.: Deriving surface soil moisture from reflected GNSS signal observations over a grassland site in southwestern France. Hydrology and Earth System Sciences, Volume: 22, Issue: 3, Pages: 1931-1946. Doi: 10.5194/hess-22-1931-2018. Published: MAR 20 2018.

Zhu, YQ., Toon, OB., Kinnison, D., Harvey, VL., Mills, MJ., Bardeen, CG., Pitts, M., Begue, N., Renard, JB., Berthet, G., al... : Stratospheric Aerosols, Polar Stratospheric Clouds, and Polar Ozone Depletion After the Mount Calbuco Eruption in 2015. Journal of Journal of Geophysical Research-Atmospheres, Volume: 123, Issue: 21, Pages: 12308-12331, Doi: 10.1029/2018JD028974. Published: NOV 16 2018.

2018 Papers published in peer-reviewed journals (outside DR)

Andrey-Andres, J., Fourrié, N., Guidard, V., Armante, R., Brunel, P., Crevoisier, C., Tournier, B., 2018: A simulated observation database to assess the impact of the IASI-NG hyperspectral infrared sounder, Atmospheric Measurement Techniques 11(2), 803-818.

Aouf, L., A. Dalphinet, S. Law-Chune, Y. Drillet, The upgraded CMEMS global wave system: improvements and efficiency for ocean/waves coupling, General Assembly EGU, Avril 2018, Vienna, Austral.

Aouf, L., A. Dalphinet, R. Husson, S. Law-Chune, The assimilation of Sentinel-1A and 1B SAR wave spectra in the CMEMS global wave system. Workshop ESA SEASAR, Frascati, 7-10 Mai 2018.

Aouf, L., A. Dalphinet, Toward a more and more accurate wave forecasting system: Thanks to Altimetry. symposium 25 years of progress in radar altimetry, Ponta Delgada, 24-29 september 2018.

Aouf, L., D. Hauser, C. Tison, B. Chapron : On the assimilation of multi-source of directional wave spectra from Sentinel-1A and 1B, and CFOSAT in the wave model MFWAM: Toward an operational use in CMEMS-MFC. Proceedings IGARSS 2018, Valencia, Spain.

Aumann, H. H.; Chen, X.; Fishbein, E.; Geer, A.; Havemann, S.; Huang, X.; Liu, X.; Liuzzi, G.; DeSouza-Machado, S.; Manning, E. M.; Masiello, G.; Matricardi, M.; Moradi, I.; Natraj, V.; Serio, C.; Strow, L.; Vidot, J.; Wilson, R. C.; Wu, W.; Yang, Q. & Yung, Y. L. (2018), ''Evaluation of Radiative Transfer Models With Clouds'', Journal of Geophysical Research: Atmospheres 123(11), 6142-6157.

Augros, C. , Caumont, O. , Ducrocq, V. and Gaussiat, N. (2018), Assimilation of radar dual-polarization observations in AROME model. Q.J.R. Meteorol. Soc. 2018;144:1352-1368. doi:10.1002/qj.3269.

Bresson, E., Philippe Arbogast, Lotfi Aouf, Denis Paradis, Anna Kortcheva, Andrey Bogatchev, Vasko Galabov, Marieta Dimitrova, Guillaume Morvan, Patrick Ohl, Boryana Tsenova, and Florence Rabier: On the improvement of wave and storm surge hindcasts by downscaled atmospheric forcing: application to historical storms, Natural Hazards Earth System Sciences, 18, 997-1012, 2018.

Brönnimann, S., Allan, R., Atkinson, C., Buizza, R., Bulygina, O., Dahlgren, P., Dee, D., Dunn, R., Gomes, P., John, V.O., Jourdain, S., Haimberger, L., Hersbach, H., Kennedy, J., Poli, P., Pulliainen, J., Rayner, N., Saunders, R., Schulz, J., Sterin, A., Stickler, A., Titchner, H., Valente, M.A., Ventura, C. and Wilkinson, C. (2018), ''Observations for Reanalyses''. Bull. Amer. Meteor. Soc., 99, 1851-1866. doi:10.1175/BAMS-D-17-0229.1.

Buizza, R., Poli, P., Rixen, M., Alonso-Balmaseda, M., Bosilovich, M.G., Brönnimann, S., Compo, G.P., Dee, D.P., Desiato, F., Doutriaux-Boucher, M., Fujiwara, M., Kaiser-Weiss, A.K., Kobayashi, S., Liu, Z., Masina, S., Mathieu, P., Rayner, N., Richter, C., Seneviratne, S.I., Simmons, A.J., Thépaut, J., Auger, J.D., Bechtold, M., Berntell, E., Dong, B., Kozubek, M., Sharif, K., Thomas, C., Schimanke, S., Storto, A., Tuma, M., Välisuo, I, and Vaselali, A. (2018), ''Advancing Global and Regional Reanalyses''. Bull. Amer. Meteor. Soc., 99, ES139-ES144. doi: 10.1175/BAMS-D-17-0312.1.

Dalphinet A. , Aouf L., Husson R., Michaud H.: Impact of the SAR wind in regional wave model on the french Mediterranean sea, Workshop ESA SEASAR, Frascati, 7-10 Mai 2018.

Dalphinet A., Aouf, L., Osinski R., Michaud H.: High resolution coastal wave model for the West Indies under major hurricanes of 2017, symposium 25 years of progress in radar altimetry, Ponta Delgada, 24-29 sept 2018.

Krien, Y.; Arnaud, G.; Cécé, R.; Ruf, C.; Belmadani, A.; Khan, J.; Bernard, D.; Islam, A. K. M. S.; Durand, F.; Testut, L.; Palany, P. & Zahibo, N. (2018), 'Can we improve parametric cyclonic wind fields using recent satellite remote sensing data?', Remote Sensing 2018(10), 1963.

Laloyaux, P., de Boisseson, E., Balmaseda, M., Bidlot, J., Broennimann, S., Buizza, R., Dalhgren, P., Dee, D., Haimberger, L., Hersbach, H., Kosaka, Y., Martin, M., Poli, P., Rayner, N., Rustemeier, E. and Schepers, D. (2018), ''CERA-20C: A coupled reanalysis of the twentieth century''. J. Adv. Model. Earth Syst., 10, 1172-1195. doi: 10.1029/2018MS001273.

Law-Chune, S., L. Aouf: Wave effects in global ocean modelling : parametrizations vs forcing from wave model. Ocean Dynamics, Topical collection, December 2018, Volume 68, Issue 12, pp 1739-1758.

Legrand, S., P; de la Vallée, L.R. Hole, K.-F. Dagestad and P. Daniel, 2018: Towards NOOS-Drift, a multi-models ensemble system to assess and improve drift forecast accuracy, 4th GEO Blue Planet Symposium, Toulouse, France, 4-6 July 2018.

Leroux, M., J. Meister, D. Mekies, A. Dorla, and P. Caroff, 2018: A Climatology of Southwest Indian Ocean Tropical Systems: Their Number, Tracks, Impacts, Sizes, Empirical Maximum Potential Intensity, and Intensity Changes. J. Appl. Meteor. Climatol., 57, 1021–1041, doi: 10.1175/JAMC-D-17-0094.1.

Osinski, R.; Dalphinet, A.; Aouf, L. & Palany, P. (2018), 'Estimation of the hundred year return level of the significant wave height for the French Guiana coast', Brazilian Journal of Oceanography 66(4), 325-334.

Patou, M.; Vidot, J.; Riédi, J.; Penide, G. & Garrett, T. J. (2018), 'Prediction of the Onset of Heavy Rain Using SEVIRI Cloud Observations', Journal of Applied Meteorology and Climatology 57(10), 2343--2361.

Picart, S. S.; Tandeo, P.; Autret, E. & Gausset, B. (2018), ''Exploring Machine Learning to Correct Satellite-Derived Sea Surface Temperatures'', Remote Sensing 10(2), 224.

Poli, P. & Brunel, P. (2018), ''Assessing reanalysis quality with early sounders Nimbus-4 IRIS (1970) and Nimbus-6 HIRS (1975)'', Advances in Space Research 62(2), 245-264. doi:10.1016/j.asr.2018.04.022.

Saunders, R.; Hocking, J.; Turner, E.; Rayer, P.; Rundle, D.; Brunel, P.; Vidot, J.; Roquet, P.; Matricardi, M.; Geer, A.; Bormann, N. & Lupu, C. (2018), ''An update on the RTTOV fast radiative transfer model (currently at version~12)'', Geoscientific Model Development 11(7), 2717--2737.

Sauvage, C.; Brossier, C. L.; Ducrocq, V.; Bouin, M.-N.; Vincendon, B.; Verdecchia, M.; Taupier-Letage, I. & Orain, F. (2018), ''Impact of the representation of the freshwater river input in the Western Mediterranean Sea'', Ocean Modelling 131, 115-131.

Su, Z., Timmermans, W., Zeng, Y., Schulz, J., John, V.O., Roebeling, R.A., Poli, P., Tan, D., Kaspar, F., Kaiser-Weiss, A.K., Swinnen, E., Toté, C., Gregow, H., Manninen, T., Riihelä, A., Calvet, J., Ma, Y. and Wen, J. (2018), ''An Overview of European Efforts in Generating Climate Data Records''. Bull. Amer. Meteor. Soc., 99, 349-359. doi: 10.1175/BAMS-D-16-0074.1.

Verron, J., P. Bonnefond, L. Aouf, et al : The Benefits of the Ka-Band as Evidenced from the SARAL/AltiKa Altimetric Mission: Scientific Applications. Remote Sensing 2018, 10, 163; doi: 10.3390/rs10020163.

Yu, N., N. Gaussiat and P. Tabary, 2018, Polarimetric X-band weather radars for quantitative precipitation estimation in mountainous regions. Q J R Meteorol Soc. 2018; 144: 2603-2619. DOI: 10.1002/qj.3366.

PHD defended in 2018

Abdel-Lathif, A., 2018 : Représentation de la convection par CNRM-CM6 dans le cadre de la campagne CINDY2011/DYNAMO, le 6 février 2018

Borderies, M., 2018 : Assimilation de données de radar à nuages aéroporté pendant la campagne de mesures HyMeX, le 7 décembre 2018.

Calmer, R., 2018: Vertical wind measurements using a 5-hole Probe with Remotely Piloted Aircraft for studying aerosol-cloud interactions, le 20 mars 2018.

Cohen, Y., 2018 : Climatologies et tendances de l'ozone et du monoxyde de carbone dans l'UTLS, vues par les mesures IAGOS et le modèle MOCAGE, le 30 novembre 2018.

Descheemaecker, M., 2018 : Capacité du capteur géostationnaire MTG-FCI à améliorer la prévision de la concentration des aérosols dans un modèle de chimie-transport, le 25 octobre 2018.

Farouk, I, 2018 : Quelles approches pour l'assimilation des radiances nuageuses IASI en prévision numérique du temps ?, le 19 décembre 2018.

Jaidan, D., 2018 : Étude des processus d'import et d'export de la pollution gazeuse et particulaire au-dessus du Bassin Méditerranéen dans le cadre du projet ChArMEx, le 5 février 2018.

Léger, J., 2018 : Un modèle d'ascendance convective simple prenant en compte explicitement le terme de pression non-hydrostatique, le 6 décembre 2018.

Morel, X., 2018 : Observations et modélisation in-situ du carbone des sols boréaux et des émissions de méthane associées, le 28 juin 2018.

Planque, C., 2018 : Observation satellitaire et modélisation de l'albédo des forêts sur le territoire français métropolitain : dynamiques temporelles et impacts radiatifs, le 7 février 2018.

Plazzota, M., 2018 : Impacts de la gestion du rayonnement solaire sur le système Terre : rôle des boucles de rétroaction liées aux cycles du carbone et hydrologique, le 3 décembre 2018.

Sabatier, T., 2018 : Circulations à fine échelle et qualité de l'air hivernal dans une vallée alpine urbanisée, le 28 novembre 2018.

Taufour, M., 2018 : Validation et amélioration du schéma microphysique à deux moments LIMA à partir des observations de la campagne de mesures HyMeX, le 20 décembre 2018.

« Habilitations à diriger des recherches » defended in 2018

Lemonsu, A., 2018 : Étude du climat urbain pour l'amélioration du cadre de vie et l'adaptation au changement climatique, le 19 mars 2018.

Glossary

Organisms

ADEME	Agence de l'Environnement et de la Maîtrise de l'Energie
AIEA	Agence Internationale de l'Energie Atomique
ANAM	National Agency of Agro-Meteorology of Burkina Faso
ANELFA	Association Nationale d'Etude et de Lutte contre les Fléaux Atmosphériques
ANR	Agence Nationale de la Recherche
BEC	Bureau d'Etudes et de Consultance
CDM	Centre Départemental de la Météorologie
CDMA	Cellule de développement Météo-Air
CEH	Centre for Ecology and Hydrology
CEMAGREF	CEntre national du Machinisme Agricole, du Génie Rural, des Eaux et Forêts (Institut national de Recherche en Sciences et Technologies pour l'Environnement et l'Agriculture)
CEN	Centre d'Etudes de la Neige
CEPMMT	Centre Européen pour les Prévisions Météorologiques à Moyen Terme
CERFACS	Centre Européen de Recherche et de Formation Avancée en Calcul Scientifique
CMM	Centre de Météorologie Marine
CMRS	Centre Météorologique Régional Spécialisé
CMS	Centre de Météorologie Spatiale
CNES	Centre National d'Études Spatiales
CNP	Centre National de Prévision
DGA	Délégation générale pour l'armement
DGPR	Direction Générale de la Prévention des Risques
DGSCGC	Direction générale de la Sécurité Civile et de la Gestion de Crise
EALAT	Ecole de l'Aviation Légère de l'Armée de Terre
EASA	European Aviation Safety Agency, Agence Européenne de la Sécurité Aérienne
ECMWF	European Centre for Medium-range Weather Forecasts
EEA	Agence Environnementale Européenne
ENAC	Ecole Nationale de l'Aviation Civile
ENM	Ecole Nationale de la Météorologie
ESA	European Space Agency
ETNA	Division Ecoulements Torrentiels, Neige et Avalanches du CEMAGREF
EUFAR	Réseau européen d'infrastructures de recherche aéroportée pour les sciences environnementales et de la Terre
EUMETNET	EUropean METeorological NETwork
EUMETSAT	Organisation européenne pour l'exploitation de satellites météorologiques
FAA	Federal Aviation Agency, Agence US de la Sécurité Aérienne
FAAM	Facility for Airborne Atmospheric Measurements (United Kingdom)
FMI	Institut Finlandais de Météorologie
ICARE	International Conference on Airborne Research for the Environment
IFREMER	Institut Francais de Recherche pour l'Exploitation de la MER
INERIS	Institut National de l'Environnement et des RISques
INRIA	Institut National de Recherche en Informatique et en Automatique
INSU	Institut National des Sciences de l'Univers
IPEV	Institut Paul Emile Victor
IRD	Institut de Recherche pour le Développement
IRSTEA	Institut national de Recherche en Sciences et Technologies pour l'Environnement et l'Agriculture (anciennement CEMAGREF)
JAXA	Japan Aerospace eXploration Agency
JMA	Japan Meteorological Agency
KNMI-TNO	Royal Netherlands Meteorological Institute and Netherlands Organization for Applied Scientific Research
MEEM	Ministère de l'Environnement, de l'Energie et de la Mer
MERCATOR-OCEAN	Société Civile Française d'océanographie opérationnelle
MetOffice	United Kingdom Meteorological Office
MPI	Max Planck Institut
NASA	National Aeronautics and Space Administration
NCAR	National Center for Atmospheric Research
NEC	Nippon Electric Company
NIWA	National Institute for Water and the Atmosphere (Nouvelle-Zélande)
NOAA	National Ocean and Atmosphere Administration
OACI	Organisation de l'Aviation Civile Internationale
OMM	Organisation Météorologique Mondiale
OMP	Observatoire Midi-Pyrénées
OMS	Organisation Mondiale de la Santé
ONERA	Office national d'études et de recherches aérospatiales
RTRA-STAE	Réseau Thématique de Recherche Avancée - Sciences et Technologies pour l'Aéronautique et l'Espace
SCHAPI	Service Central d'Hydrométéorologie et d'Appui à la Prévision des Inondations
SHOM	Service Hydrographique et Océanographique de la Marine
SMHI	Swedish Meteorological and Hydrological Institute
UE	Union Européenne
UKMO	United Kingdom Meteorological Office
VAAC	Volcanic Ash Advisory Centre

Laboratories or R&D units

3SR	Laboratoire Sols – Solides – Structures – Rhéologie, UJF Grenoble / CNRS / Grenoble INP
BRGM	Bureau de Recherches Géologiques et Minières
CEREA	Centre d'Enseignement et de Recherche en Environnement Atmosphérique
CESBIO	Centre d'Etudes Spatiales de la BIOsphère
CNRM	Centre National de Recherches Météorologiques
CNRS	Centre National de Recherches Scientifiques
CRA	Centre de Recherches Atmosphériques
DSO	Direction des Systèmes d'Observation (Météo-France)
GAME	Groupe d'Etude de l'Atmosphère Météorologique
GSMA	Groupe de spectrométrie moléculaire et atmosphérique, UMR 7331 CNRS Université de Reims Champagne Ardennes
IFSTTAR	Institut Français des Sciences et Technologies des Transports, de l'Aménagement et des Réseaux
IGN	Institut Géographique National
IPSL	Institut Pierre Simon Laplace
LaMP	Laboratoire de Météorologie Physique
LATMOS	Laboratoire ATmosphères, Milieux, Observations Spatiales
LAVUE	Laboratoire Architecture, Ville, Urbanisme, Environnement
LCP	Laboratoire Chimie et Procédés
LEGI	Laboratoire des écoulements physiques et industriels
LGGE	Laboratoire de Glaciologie et de Géophysique de l'Environnement
LHSV	Laboratoire d'Hydraulique Saint-Venant
LIRIS	Laboratoire d'InfoRmatique en Image et Systèmes d'information
LISST	Laboratoire Interdisciplinaire Solidarités, Sociétés, Territoires
LMD	Laboratoire de Météorologie Dynamique
LOCEAN	Laboratoire d'Océanographie et du Climat : Expérimentations et Approches Numériques
LPCEE	Laboratoire de Physique et Chimie de l'Environnement et de l'Espace
LPED	Laboratoire Population Environnement Développement

LRA	Laboratoire de Recherche en Architecture
LSCE	Laboratoire des Sciences du Climat et de l'Environnement
RIU	Rhenish Institute for environmental research at the University of Cologne
SAFIRE	Service des Avions Français Instrumentés pour la Recherche en Environnement
WUT	Warsaw University of Technology (Politechnika Warszawska)

National or international programs or projects

BACCHUS	Impact of Biogenic versus Anthropogenic emissions on Clouds and Climate: towards a Holistic UnderStanding
BAMED	BAlloons in the MEDiterranean
C3AF	Changement Climatique et Conséquences sur les Antilles Françaises
CHFP	Climate Historical Forecasting Project
CHROME	Couplage Hydrométéorologique RégiOnal Multi-Ensemble
CIDEX	Calibration and Icing Detection EXperiment
CMIP	Coupled Model Intercomparaison Project
COPERNICUS	European Earth observation system http://www.copernicus.eu/pages-principales/services/climate-change/
CREWS	Climate Risk and Early Warning Systems
CYPRIM	projet Cyclogénèse et précipitations intenses dans la zone méditerranéenne
DYAMOND	DYnamics of the Atmospheric general circulation Modeled On Non-hydrostatic Domains
ERA-CLIM	European Reanalysis of Global Climate Observations
ERDF	European Regional Development Fund
ESURFMAR	Eumetnet SURFace MARine programme
EUFAR2	2nd projet EUFAR dans le cadre de 7e PCRD et 4e projet EUFAR depuis 2000
EUREQUA	Evaluation mUltidisciplinaire et Requalification Environnementale des QUArtiers, projet financé par l'Agence Nationale pour la Recherche, ANR-2011-VILD-006. Partenaires : GAME, IFSTTAR, CEREA, LISST, LAVUE, LPED.
EURO4M	European reanalysis and observations for monitoring http://www.euro4m.eu/
FEDER	Fonds Européen de Developpement Régional
GeoMIP	Geoengineering Model Intercomparison Project
GHRSST	International Group for High Resolution SST
GLOSCAL	GLobal Ocean Surface salinity CALibration and validation
H2020	Programme-cadre pour la recherche et l'innovation (2014-2020)
HOMONIM	Historique Observation MOdélisation des Niveaux Marins
HyMeX	Hydrological cYcle in the Mediterranean EXperiment
IMAGINES	Implementing Multi-scale Agricultural Indicators Exploiting Sentinels
IncREO	Increasing Resilience through Earth Observation
LEFE	programme national « Les Enveloppes Fluides et l'Environnement »
MACC	Monitoring Atmospheric Composition and Climate
METOP	METeorological Operational Polar satellites
MISVA	Monitoring of IntraSeasonal Variability of Africa: misva.seddo.fr
PCRD	Programme Cadre de Recherche et de Développement
PLUVAR	Variabilité sub-saisonnière des pluies sur les iles du Pacifique Sud
PNRA	Programma Nazionale di Recerche in Antartide
QUANTIFY	Programme QUANTIFYing the climate impact of global and European transport systems
RHYTMME	Risques HYdro-météorologiques en Territoires de Montagnes et MEditerranéens
SCAMPEI	Scénarios Climatiques Adaptés aux Montagnes : Phénomènes extrêmes, Enneigement et Incertitudes - projet de l'ANR coordonné par le CNRM
SESAR	Single European Sky ATM Research
SMOS	Soil Moisture and Ocean Salinity
Suomi-NPP	Programme américain de satellites météorologiques en orbite polaire
THORPEX	THe Observing system Research and Predictability EXperiment
TIREX	Transfert des apprentIssages de Retours d'EXpériences scientifiques pour le renforcement des capacités de réponse et d'adaptation individuelles et collectives dans un contexte de changement climatique
UERRA	Uncertainties in Ensembles of Regional Re-Analyses
USAP	United States Antarctic Program
VOLTIGE	Vecteur d'Observation de La Troposphère pour l'Investigation et la Gestion de l'Environnement
WCRP	World Climate Research Programme

Campaigns

AMMA	Analyses Multidisciplinaires de la Mousson Africaine
CAPITOUL	Canopy and Aerosol Particles Interactions in Toulouse Urban Layer
CORDEX	COordinated Regional climate Downscaling EXperiment
EUREQUA	Evaluation mUltidisciplinaire et Requalification Environnemental des QUArtiers
HAIC	High Altitude and Ice Crystals (www.haic.eu)
MEGAPOLI	Megacities : Emissions, urban, regional and Global Atmospheric POLlution and climate effects, and Integrated tools for assessment and mitigation
SMOSREX	Surface MOnitoring of the Soil Reservoir EXperiment

Other acronyms

AIRS	Sondeur Infrarouge avancé
ALADIN	Aire Limitée Adaptation Dynamique et développement InterNational
ALIDS	Interféromètre laser aéroporté pour mesurer la granulométrie des gouttes d'eau dans les nuages
AMSR	Advanced Microwave Scanning Radiometer
AMSU	Advanced Microwave Sounding Unit
AMSU-A	Advanced Microwave Sounding Unit-A
AMSU-B	Advanced Microwave Sounding Unit-B
AMULSE	Atmospheric Measurements by Ultra-Light SpEctrometer
ANASYG	ANAlyse Synoptique Graphique
ANSP	Air Navigation Service Provider
ANTILOPE	ANalyse par spaTIaLisation hOraire des PrEcipitations
ARAMIS	Application Radar A la Météorologie Infra-Synoptique
ARGO	Array for Real time Geostrophic Oceanography
AROME	Application de la Recherche à l'Opérationnel à Méso-Échelle
AROME-COMB	AROME - COMBinaison
AROME-PERTOBS	AROME (OBServations PERTurbées aléatoirement)
AROME-WMED	Configuration AROME sur la Méditerranée occidentale
ARPEGE	Action de Recherche Petite Échelle Grande Échelle
AS	Adaptations Statistiques
ASAR	Advanced Synthetic Arperture Radar
ASCAT	Advanced SCATterometer
ASTEX	Atlantic Stratocumulus Transition EXperiment
ATM	Air Traffic Management - Contrôle du trafic aérien
ATMS	Advanced Technology Microwave Sounder
AVHRR	Advanced Very High Resolution Radiometer
BAS	British Antarctic Survey
BLLAST	Boundary Layer Late Afternoon and Sunset Turbulence
BPCL	Ballon Pressurisé de Couche Limite
BSS	Score probabiliste « Brier Skill Score »
CALIOP	Cloud-Aerosol Lidar with Orthogonal Polarization
CALIPSO	Cloud-Aerosol Lidar and Infrared Pathfinder Satellite Observations
CANARI	Code d'Analyse Nécessaire à ARPEGE pour ses Rejets et son Initialisation
CAPE	Convective Available Potential Energy
CAPRICORNE	CAractéristiques PRIncipales de la COuveRture NuageusE
CARIBOU	Cartographie de l'Analyse du RIsque de Brume et de brOUillard
CAROLS	Combined Airborne Radio-instruments for Ocean and Land Studies
Cb	Cumulonimbus
CFMIP	Cloud Feedback Intercomparison Project
CFOSAT	Chinese-French SATellite
ChArMEx	Chemistry-Aerosol Mediterranean Experiment
C-IFS	Composition - Integrated Forecasting System
CISMF	Centre Inter-armées de Soutien Météorologique aux Forces
CLAS	Couches Limites Atmosphériques Stables
CMC	Cellule Météorologique de Crise
CMIP6	6e phase du Coupled Model Intercomparison Project

CNRM-CM5	Version 5 du Modèle de Climat du CNRM
CNRM-RCSM	Regional Climate System Model
COP	Contrat d'Objectifs et de Performances
COPAL	COmmunity heavy-PAyload Long endurance instrumented aircraft for tropospheric research in environmental and geo-sciences
CPR	Cloud Profiling Radar
CrIS	Cross-track Infra-Red Sounder
CROCUS	Modèle de simulation numérique du manteau neigeux développé par Météo-France.
CTRIP	CNRM-Total Routing Integrated Pathway
DCSC	Direction de la Climatologie et des Services Climatiques
DCT	Diffraction Contrast Tomography
DEM	Discrete Element Method
DISORT	Discrete Ordinates Radiative Transfer model
DMT	Dropplet Measurement Technologies
DOA	Département de l'Observation en Altitude
DP	Direction de la Production
DPI	Droits de Propriété Intellectuelle
DPR	Dual frequency Precipitation Radar
DPrévi	Direction de la Prévision
DSI	Direction des Systèmes d'Information (Météo-France)
DSNA	Direction des Services de la Navigation Aérienne
ECOCLIMAP	Base de données de paramètres de surface
ECUME	Exchange Coefficients from Unified Multi-campaings Estimates
EGEE	Etude du golfe de GuinEE
ENVISAT	ENVIronmental SATellite
ERA	European Re-Analysis
ESGF	Earth System Grid Federation
ESRF	European Synchrotron Radiation Facility
EUCLIPSE	European Union Cloud Intercomparison, Process Study & Evaluation
FAB	Fonctionnal Aerospace Block
FABEC	Functional Airspace Block Europe Central
FAR	Fausse AleRte
FSO	Forecast Sensitivity to Observations
FSOi	Forecast Sensitivity to Observations-based impact
GABLS4	Gewex Atmospheric Boundary Layer Study
GELATO	Global Experimental Leads and ice for ATmosphere and Ocean
GEV	Loi généralisée des valeurs extrêmes
GIEC	Groupe Intergouvernemental d'experts sur l'Evolution du Climat
GMAP	Groupe de Modélisation et d'Assimilation pour la Prévision
GMEI	Groupe de Météorologie Expérimentale et Instrumentale
GMME	Groupe de Météorologie de Moyenne Echelle
GMES	Global Monitoring for Environment and Security
GNSS-R	Global Navigation by Satellite System (Géolocalisation et Navigation par un Système de Satellites) – R pour « Réflectométrie »
GOES 16/17	American meteorological geostationary satellites
GPM	Global Precipitation Measurement
GPP	Gross Primary Production
GPS	Global Positionning System
GSMA	Groupe de Spectrométrie Moléculaire et Atmosphérique
High IWC	High Ice Water Content
Himawari8	Japanese meteorological geostationary satellite
HIRLAM	HIgh Resolution Limited Area Model
HISCRTM	HIgh Spectral resolution Cloudy-sky Radiative Transfer Model
HSS	Measurement of improvement of the forecast
HTBS	Haute Troposphère - Basse Stratosphère
HYCOM	HYbrid Coordinate Ocean Model
IAGOS	In-service Aircraft for Global Observing System
IASI	Interféromètre Atmosphérique de Sondage Infrarouge
IAU	Incremental analysis update, mise à jour incrémentale par une analyse
IFS	Integrated Forecasting System
IIR	Infrared Imaging Radiometer
INDARE	Indian Ocean Data Rescue Initiative
IPS	Indice Piézométrique Standardisé
ISBA	Interaction Sol-Biosphère-Atmosphère
ISBA-A-gs	Modèle Interactions Sol-Biosphère-Atmosphère, avec représentation de la photosynthèse et de la croissance de la végétation
ISBA - ES	Modèle numérique du CNRM représentant l'évolution du sol en surface (végétation incluse) et en profondeur, mettant particulièrement l'accent sur l'évolution de la couverture de neige
ISBA-TOP	Couplage du schéma de surface ISBA et d'une version « méditerranéenne » du modèle hydrologique TOPMODEL
ISFC	Indice de Segmentation de la Composante de Fourier
ISIS	Algorithme de suivi automatique des systèmes identifiés à partir de l'imagerie infra-rouge de Météosat
IWC	Ice Water Content
LAI	Leaf Area Index (indice foliaire)
Land-SAF	LAND Satellite Application Facilities
LAURE	Loi sur l'Air et l'Utilisation Rationnelle de l'Energie
LCCS	Land Cover Classification System
LES	Large Eddy Simulation model
LISA	LIdar SAtellite
4M	Moyens Mobiles de Mesures Météorologiques
Med-CORDEX	Mediterranean Coordinated Regional Climate Downscaling Experiment
MEDUP	MEDiterranean intense events : Uncertainties and Propagation on environment
Megha-Tropiques	Satellite franco-indien dédié à l'étude du cycle de l'eau et des échanges d'énergie dans la zone tropicale
MEPRA	Modèle Expert de Prévision du Risque d'Avalanche (modélisation)
MERSEA	Marine EnviRonment and Security for the European Area
MESCAN	Combinaison de MESAN (nom du système suédois) et de CANARI
MESO-NH	Modèle à MESO-échelle Non Hydrostatisque
MFWAM	Météo-France WAve Model
MHS	Microwave Humidity Sounder
MISR	Multi-angle Imaging SpectroRadiometer
MNPCA	Microphysique des Nuages et de Physico-Chimie de l'Atmosphère
MOCAGE	MOdélisation de la Chimie Atmosphérique de Grande Echelle (modélisation)
MODCOU	MODèle hydrologique COUplé surface-souterrain.
MODIS	MODerate-resolution Imaging Spectro-radiometer (instrument)
MoMa	Méthodes Mathématiques pour le couplage modèles et données dans les systèmes non-linéaires stochastiques à grand nombre de degrés de liberté
MOTHY	Modèle Océanique de Transport d'HYdrocarbure
MRR	Micro Rain Radars
MSG	Météosat Seconde Génération
NAO	North Atlantic Oscillation
NEMO	Nucleus for European Modelling of Ocean
NEMO-WMED36	Configuration de NEMO sur la Méditerranée occidentale
NSF	Norges StandardiseringsForbund
NWCSAF	Satellite Application Facility for Nowcasting
OASIS	Ocean Atmosphere Sea Ice Soil
OPIC	Objets pour la Prévision Immédiate de la Convection
ORACLE	Opportunités et Risques pour les Agro-ecosystèmes et les forêts en réponse aux changements CLimatiquE, socio-économiques et politiques en France
ORCHIDEE	ORganizing Carbon and Hydrology in Dynamic EcosystEms
OSCAT	OCEANSAT-2 Scatterometer
OSTIA	Operational Sea surface Temperature sea Ice Analysis
OTICE	Organisation du Traité d'Interdiction Complète des Essais nucléaires
PALM	Projet d'Assimilation par Logiciel Multi-méthodes
PDO	Pacific Decadal Oscillation
PEARO	Prévision d'Ensemble AROME
PEARP	Prévision d'Ensemble ARPège
PI	Prévision Immédiate
PN	Prévision Numérique
PNT	Prévision Numérique du Temps
POD	PrObabilité de Détection
POI	Période d'Observation Intensive
PRESYG	PREvision Synoptique Graphique
Prev'Air	Plateforme nationale de la qualité de l'air
PREVIBOSS	PREvisibilité à courte échéance de la variabilité de la VIsibilité dans le cycle de vie du Brouillard, à partir de données d'Observation Sol et Satellite.

Prévi-Prob	Projet sur les prévisions probabilistes
PSI	Pollutant Standard Index
PSR	Plan Submersions Rapides
PVM	Particulate Volume Monitor
PVs	Tourbillon potentiel de l'air humide
RADOME	Réseau d'Acquisition de Données d'Observations Météorologiques Etendu
RCP8.5	8.5 W/m² Representative Concentration Pathway corresponding to a 8.5 W/m² radiative forcing at the end of the 21st century compared to preindustrial climate
RDI	Référent Départemental Inondation
RDT	Rapid Developing Thunderstorm
RHI	Range Height Indicator (coupe verticale)
ROC	Relative Operating Characteristic curve
RRTM	Rapid Radiative Transfer Model
RTI	Recherche Technologie & Innovation
RTTOV	Radiative Transfer for TOVS
SAF NWC	Satellite Application Facility on support to Nowcasting
SAF NWP	Satellite Application Facility for Numerical Weather Prediction
SAF OSI	Satellite Application Facility for Ocean and Sea Ice
SAFRAN	Système d'Analyse Fournissant des Renseignements Atmosphériques pour la Neige
SAPHIR	Sondeur Atmosphérique du Profil d'Humidité Intertropicale par Radiométrie
SARA	Spectroscopy by Amplified Resonant Absorption
SATOB	Satellite Observation
SCM	Single-Column Model
SEVIRI	Spinning Enhanced Visible and Infra-Red Imager
SFRI	Système Français de Recherche et d'Innovation
S2M	SAFRAN - SURFEX/ISBA-Crocus – MEPRA
SIM	SAFRAN ISBA MODCOU
SIRTA	Site Instrumental de Recherche par Télédétection Atmosphérique
SMOSMANIA	Soil Moisture Observing System – Meteorological Automatic Network Integrated Application
SMT	Système Mondial de Télécommunications
SOERE/GLACIOCLIM	Système d'Observation et d'Expérimentation sur le long terme pour la Recherche en Environnement : « Les GLACIers, un Observatoire du CLIMat ».
SOP	Special Observing Period
SPC	Service de Prévision des Crues
SPI	Standardized Precipitation Index (Indice de Précipitation Standardisé)
SPIRIT	SPectromètre Infra-Rouge In situ Toute altitude
SPPT	Stochastically Perturbed Parametrization Tendencies
SSI	Solar Surface Irradiance
SSMI/S	Special Sounder Microwave Imager/Sounder
SURFEX	code de SURFace EXternalisé
SVP	Surface Velocity Program
SWI	Soil Wetness Index
SWIM	Surface Wave Investigation and Monitoring
SYMPOSIUM	SYstème Météorologique de Prévision Orienté Services, Intéressant des Usagers Multiples - découpage du territoire métropolitain en 615 zones « climatiquement » homogènes, dont la taille varie de 10 à 30 km
TACTIC	Tropospheric Aerosols for ClimaTe In CNRM
TCU	Towering Cumulus
TMA	Terminal Manoeuvring Area
TRL	Technology Readiness Level
TEB	Town Energy Balance
TRIP	Total Runoff Integrating Pathways
TSM	Températures de Surface de la Mer
UHF	Ultra-Haute Fréquence
UNIBAS	Modèle de précipitations
VARPACK	Current tool for diagnostic analysis in Meteo-France
VHF	Very High Frequency
VOS	Voluntary Observing Ships
WWLLN	World Wide Lightning Location Network
Xios	Librairie d'entrées-sorties pour modèles numériques

DR: Management structure

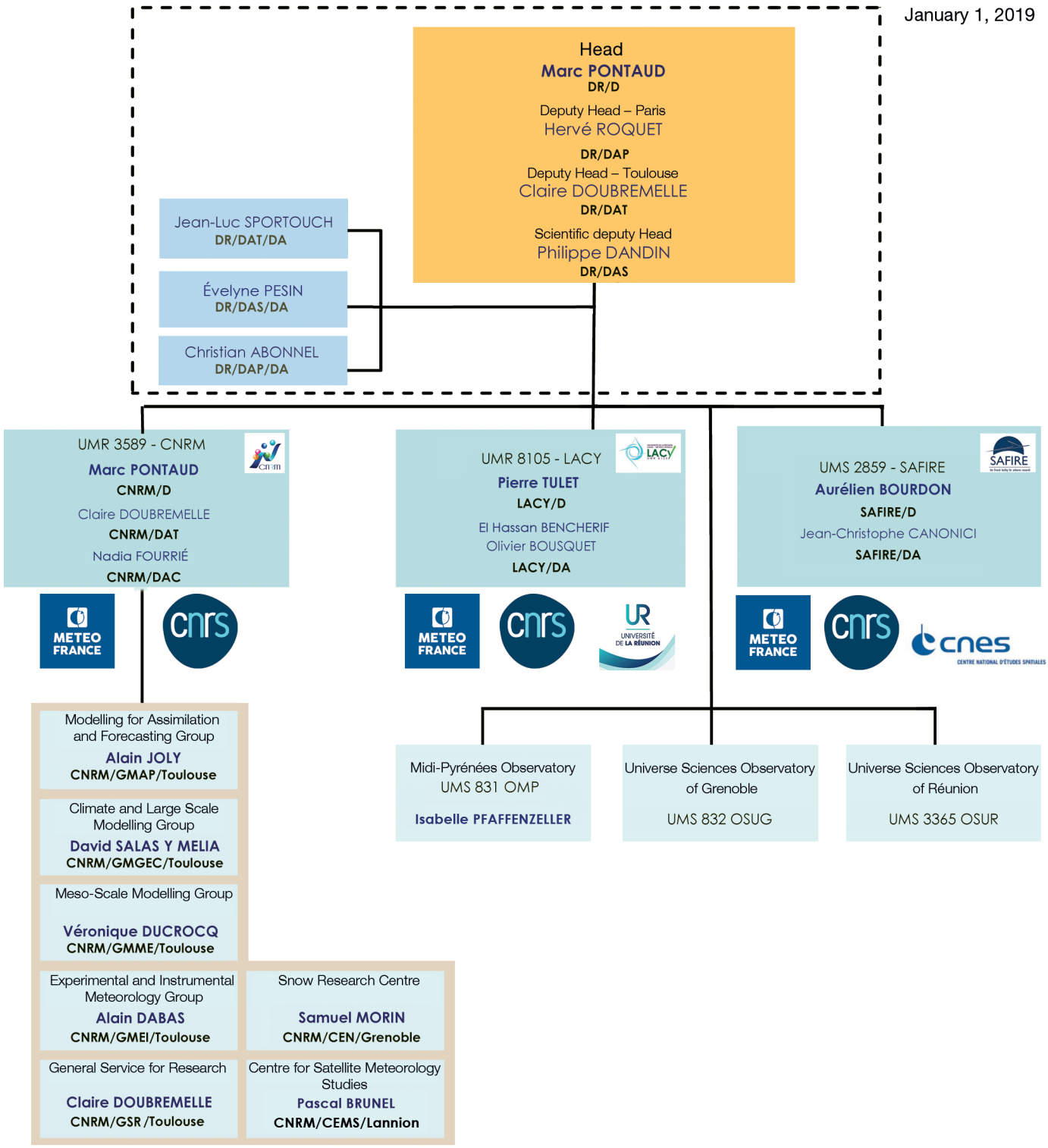

UMR: Joint Research Unit
UMS: Joint Service Unit

Météo-France
73, avenue de Paris
94165 Saint-Mandé Cedex
Phone: +33 (0) 1 77 94 77 94
Fax: +33 (0) 1 77 94 70 05
www.meteofrance.com

Research Department
42, avenue Gaspard Coriolis
31057 Toulouse Cedex 1 France
Phone: +33 (0) 5 61 07 93 70
Fax: +33 (0) 5 61 07 96 00
http://www.urm-cnrm.fr
Mail: contact@cnrm.meteo.fr

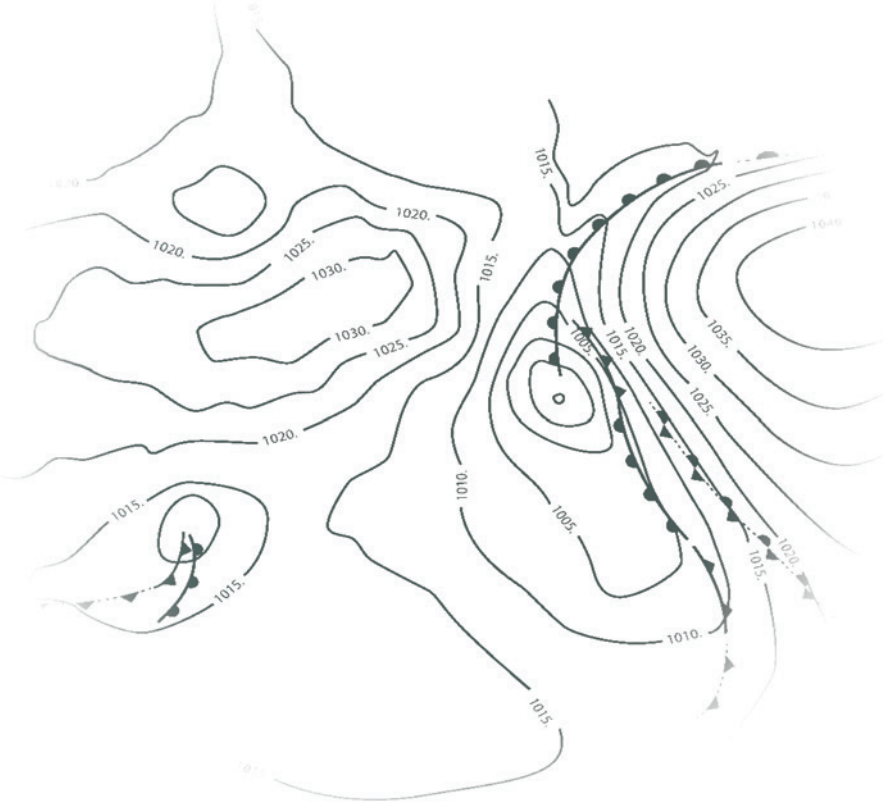

Liberté • Égalité • Fraternité
RÉPUBLIQUE FRANÇAISE

MINISTÈRE
DE LA TRANSITION
ÉCOLOGIQUE
ET SOLIDAIRE

Création DIRCOM

ISSN : 2116-4541